

Horizon 2020

Call: ERC-2016-PoC

(Call for proposals for ERC Proof of Concept Grant)

Topic: ERC-PoC-2016

Type of action: ERC-POC
(Proof of Concept Grant)

Proposal number: 727233

Proposal acronym: PACODOM

Deadline Id: ERC-2016-PoC

Table of contents

Section	Title	Action
1	General information	
2	Participants & contacts	
3	Budget	
4	Ethics	
5	Call-specific questions	

How to fill in the forms

The administrative forms must be filled in for each proposal using the templates available in the submission system. Some data fields in the administrative forms are pre-filled based on the previous steps in the submission wizard.



Proposal ID **727233**

Acronym **PACODOM**

1 - General information

Topic ERC-PoC-2016

Call Identifier ERC-2016-PoC

Type of Action ERC-POC

Deadline Id ERC-2016-PoC

Acronym PACODOM

Proposal title* Parameterising Convective Dust Storms in Operational Forecast Models

Note that for technical reasons, the following characters are not accepted in the Proposal Title and will be removed: < > " &

Duration in months*

18

Related ERC Project ID number*

257543

End date of the related ERC project(DD/MM/YYYY)

30/09/2015

Free keywords

mineral dust, moist convection, parameterisation, weather, climate, air quality

Proposal ID **727233**Acronym **PACODOM**

Abstract*

Sand and Dust Storms (SDS) are extreme weather phenomena that represent a serious hazard for life, health, property, environment and economy in many countries, particularly in some of the least developed ones. Airborne dust particles play a significant role in different aspects of weather, climate and atmospheric chemistry. In the last years, the development of global and regional SDS forecasts has intensified because of their potential to mitigate impacts upon transportation, energy production, health and agriculture. While operational forecast models are skillful when SDS are caused by synoptic-scale weather systems, they are severely limited to forecast 'haboobs' – immense walls of blowing sand and dust formed by cold outflows from deep moist convection –, which are by far the most damaging among dust storm types. One outstanding outcome of the ERC Desert Storms project is the development of a novel parameterisation for dust emission by haboobs, based on the convective outflow behaving as a density current. In PACODOM Desert Storms researchers will transfer this cutting-edge technology to two globally leading centres in operational weather, dust and climate prediction (Barcelona Supercomputing Center, European Centre for Medium-Range Weather Forecasts) to make a leap forward in our ability to forecast SDS globally, and therefore drastically improve mitigation potential. Both are partners of the Sand and Dust Storm Warning Advisory and Assessment System of the World Meteorological Organization, an initiative endorsed by more than 40 countries, whose mission is to enhance their ability to deliver timely and quality SDS forecasts, observations, information and knowledge to users. The transfer of this new technology will improve air quality and weather predictions, benefitting a wide range of commercial and non-commercial users. A full operational implementation of the new approach will give ERC Desert Storms a lasting legacy and great international visibility.

Remaining characters

6

In order to best review your application, do you agree that the above non-confidential proposal title and abstract can be used, without disclosing your identity, when contacting potential reviewers?*

☒ Yes☐ No

Has this proposal (or a very similar one) been submitted in the past 2 years in response to a call for proposals under the 7th Framework Programme, Horizon 2020 or any other EU programme(s)?

☒ Yes☐ No

Please give the proposal reference or contract number.

692752

Proposal ID **727233**

Acronym **PACODOM**

Declarations

1) The Principal Investigator declares to have the explicit consent of all applicants on their participation and on the content of this proposal.*	<input checked="" type="checkbox"/>
2) The Principal Investigator declares that the information contained in this proposal is correct and complete.	<input checked="" type="checkbox"/>
3) The Principal Investigator declares that this proposal complies with ethical principles (including the highest standards of research integrity — as set out, for instance, in the European Code of Conduct for Research Integrity — and including, in particular, avoiding fabrication, falsification, plagiarism or other research misconduct).	<input checked="" type="checkbox"/>
4) The Principal Investigator hereby declares that (<i>please select one of the three options below</i>):	
- in case of multiple participants in the proposal, the coordinator has carried out the self-check of the financial capacity of the organisation on http://ec.europa.eu/research/participants/portal/desktop/en/organisations/lfv.html or to be covered by a financial viability check in an EU project for the last closed financial year. Where the result was “weak” or “insufficient”, the Principal Investigator confirms being aware of the measures that may be imposed in accordance with the H2020 Grants Manual (Chapter on Financial capacity check) .	<input type="radio"/>
- in case of multiple participants in the proposal, the coordinator is exempt from the financial capacity check being a public body including international organisations, higher or secondary education establishment or a legal entity, whose viability is guaranteed by a Member State or associated country, as defined in the H2020 Grants Manual (Chapter on Financial capacity check) .	<input checked="" type="radio"/>
- in case of a sole participant in the proposal, the applicant is exempt from the financial capacity check.	<input type="radio"/>
5) The Principal Investigator hereby declares that each applicant has confirmed to have the financial and operational capacity to carry out the proposed action. Where the proposal is to be retained for EU funding, each beneficiary applicant will be required to present a formal declaration in this respect.	<input checked="" type="checkbox"/>
The Principal Investigator is only responsible for the correctness of the information relating to his/her own organisation. Each applicant remains responsible for the correctness of the information related to him/her and declared above. Where the proposal is to be retained for EU funding, the coordinator and each beneficiary applicant will be required to present a formal declaration in this respect.	

According to Article 131 of the Financial Regulation of 25 October 2012 on the financial rules applicable to the general budget of the Union (Official Journal L 298 of 26.10.2012, p. 1) and Article 145 of its Rules of Application (Official Journal L 362, 31.12.2012, p.1) applicants found guilty of misrepresentation may be subject to administrative and financial penalties under certain conditions.

Personal data protection

Your reply to the grant application will involve the recording and processing of personal data (such as your name, address and CV), which will be processed pursuant to Regulation (EC) No 45/2001 on the protection of individuals with regard to the processing of personal data by the Community institutions and bodies and on the free movement of such data. Unless indicated otherwise, your replies to the questions in this form and any personal data requested are required to assess your grant application in accordance with the specifications of the call for proposals and will be processed solely for that purpose. Details concerning the processing of your personal data are available on the [privacy statement](#). Applicants may lodge a complaint about the processing of their personal data with the European Data Protection Supervisor at any time.

Your personal data may be registered in the [Early Warning System \(EWS\)](#) only or both in the EWS and [Central Exclusion Database \(CED\)](#) by the Accounting Officer of the Commission, should you be in one of the situations mentioned in:

- the Commission Decision 2008/969 of 16.12.2008 on the Early Warning System (for more information see the [Privacy Statement](#)), or
- the Commission Regulation 2008/1302 of 17.12.2008 on the Central Exclusion Database (for more information see the [Privacy Statement](#)).



Proposal ID **727233**

Acronym **PACODOM**

List of participants

#	Participant Legal Name	Country
1	KARLSRUHER INSTITUT FUER TECHNOLOGIE	Germany
2	UNIVERSITY OF LEEDS	United Kingdom
3	BARCELONA SUPERCOMPUTING CENTER - CENTRO NACIONAL DE SUPERCOMPUTACION	Spain
4	EUROPEAN CENTRE FOR MEDIUM-RANGE WEATHER FORECASTS	United Kingdom



Proposal ID **727233**

Acronym **PACODOM**

Short name **KIT**

2 - Administrative data of participating organisations

Host Institution

PIC

990797674

Legal name

KARLSRUHER INSTITUT FUER TECHNOLOGIE

Short name: KIT

Address of the organisation

Street KAISERSTRASSE 12

Town KARLSRUHE

Postcode 76131

Country Germany

Webpage www.kit.edu

Legal Status of your organisation

Research and Innovation legal statuses

Public bodyyes

Legal person yes

Non-profityes

International organisation no

International organisation of European interest no

Secondary or Higher education establishmentyes

Research organisationyes

Enterprise Data

SME self-declared status.....2011 - no

SME self-assessment unknown

SME validation sme..... unknown

Based on the above details of the Beneficiary Registry the organisation is not an SME (small- and medium-sized enterprise) for the call.

NACE Code: 721 - Research and experimental development on natural sciences and engineering



Proposal ID **727233**

Acronym **PACODOM**

Short name **KIT**

Department(s) carrying out the proposed work

Department 1

Department name

☐ not applicable

☒ Same as organisation address

Street

Town

Postcode

Country



Proposal ID **727233**

Acronym **PACODOM**

Short name **KIT**

Principal Investigator

The following information of the Principal Investigator is used to personalise the communications to applicants and the evaluation reports. Please make sure that your personal information is accurate and please inform the ERC in case your e-mail address changes by using the call specific e-mail address:

For Proof-of-Concept Applicants: ERC-PoC-applicants@ec.europa.eu

The name and e-mail of contact persons including the Principal Investigator, Host Institution contact are read-only in the administrative form, only additional details can be edited here. To give access rights and contact details of contact persons, please save and close this form, then go back to Step 4 of the submission wizard and save the changes.

Researcher ID

Last Name* **KNIPPERTZ**

Last Name at Birth

First Name(s)* **Peter**

Gender* ☒ Male ☐ Female

Title

Country of residence*

Nationality*

Country of Birth*

Date of Birth* (DD/MM/YYYY)

Place of Birth*

Contact address

☒ Same as organisation address

Current organisation name

Current Department/Faculty/Institute/
Laboratory name

Street

Postcode/Cedex

Town*

Phone*

Country*

Phone2 / Mobile

E-mail*

Proposal ID **727233**Acronym **PACODOM**Short name **KIT***Contact address of the Host Institution and contact person*

The name and e-mail of Host Institution contact persons are read-only in the administrative form, only additional details can be edited here. To give access rights and contact details of Host Institution, please save and close this form, then go back to Step 4 of the submission wizard and save the changes. Please note that the submission is blocked without a contact person and e-mail address for the Host Institution.

Organisation Legal Name **KARLSRUHER INSTITUT FUER TECHNOLOGIE**First name* **Kristine**Last name* **Bentz**E-Mail* **kristine.bentz@kit.edu**Position in org. Department ☐ Same as organisation☒ Same as organisation addressStreet Town Postcode Country Phone Phone2/Mobile *Other contact persons*

First Name	Last Name	E-mail	Phone
Georgia	Wessels	georgia.wessels@kit.edu	+49 721 608 45194



Proposal ID **727233**

Acronym **PACODOM**

Short name **UNIVLEEDS**

Partner organisation

PIC

999975426

Legal name

UNIVERSITY OF LEEDS

Short name: **UNIVLEEDS**

Address of the organisation

Street **WOODHOUSE LANE**

Town **LEEDS**

Postcode **LS2 9JT**

Country **United Kingdom**

Webpage **www.leeds.ac.uk**

Legal Status of your organisation

Research and Innovation legal statuses

Public body yes

Non-profit yes

International organisation no

International organisation of European interest no

Secondary or Higher education establishment yes

Research organisation no

Legal person yes

Enterprise Data

SME self-declared status.....2011 - no

SME self-assessment unknown

SME validation sme..... unknown

Based on the above details of the Beneficiary Registry the organisation is not an SME (small- and medium-sized enterprise) for the call.

NACE Code: 853 - Higher education



Proposal ID **727233**

Acronym **PACODOM**

Short name **UNIVLEEDS**

Department(s) carrying out the proposed work

Department 1

Department name

☐ not applicable

☒ Same as organisation address

Street

Town

Postcode

Country



European Commission -
Research & Innovation - Participant Portal

Proposal Submission Forms

European Research Council Executive Agency

Proposal ID **727233**

Acronym **PACODOM**

Short name **UNIVLEEDS**

Proposal ID **727233**Acronym **PACODOM**Short name **UNIVLEEDS***Contact address of the partner organisation and contact person*

The name and e-mail of Partner Organisation contact persons are read-only in the administrative form, only additional details can be edited here. To give access rights and contact details of Partner Organisation, please save and close this form, then go back to Step 4 of the submission wizard and save the changes. The contact person needs to be added as 'Main Contact' for the Partner Organisation.

Organisation Legal Name **UNIVERSITY OF LEEDS**First name* **John H.**Last name* **Marshall**E-Mail* **j.marshall@leeds.ac.uk**Position in org. Department ☐ Same as organisation☒ Same as organisation addressStreet Town Postcode Country Phone Phone2/Mobile *Other contact persons*

First Name	Last Name	E-mail	Phone
Vicky	Jackson	v.s.jackson@leeds.ac.uk	
Denise	Nicholas	d.nicholas@leeds.ac.uk	



Proposal ID **727233**

Acronym **PACODOM**

Short name **BSC**

Partner organisation

PIC

999655520

Legal name

BARCELONA SUPERCOMPUTING CENTER - CENTRO NACIONAL DE SUPERCOMPUTACION

Short name: **BSC**

Address of the organisation

Street Calle Jordi Girona 31

Town BARCELONA

Postcode 08034

Country Spain

Webpage www.bsc.es

Legal Status of your organisation

Research and Innovation legal statuses

Public body yes

Legal person yes

Non-profit yes

International organisation no

International organisation of European interest no

Secondary or Higher education establishment no

Research organisation yes

Enterprise Data

SME self-declared status.....2011 - no

SME self-assessment unknown

SME validation sme..... unknown

Based on the above details of the Beneficiary Registry the organisation is not an SME (small- and medium-sized enterprise) for the call.

NACE Code: 72 - Scientific research and development



Proposal ID **727233**

Acronym **PACODOM**

Short name **BSC**

Department(s) carrying out the proposed work

Department 1

Department name

Earth Science

☐ not applicable

☐ Same as organisation address

Street

Calle Jordi Girona 29

Town

Barcelona

Postcode

08034

Country

Spain



European Commission -
Research & Innovation - Participant Portal

Proposal Submission Forms

European Research Council Executive Agency

Proposal ID **727233**

Acronym **PACODOM**

Short name **BSC**

Proposal ID **727233**Acronym **PACODOM**Short name **BSC***Contact address of the partner organisation and contact person*

The name and e-mail of Partner Organisation contact persons are read-only in the administrative form, only additional details can be edited here. To give access rights and contact details of Partner Organisation, please save and close this form, then go back to Step 4 of the submission wizard and save the changes. The contact person needs to be added as 'Main Contact' for the Partner Organisation.

Organisation Legal Name **BARCELONA SUPERCOMPUTING CENTER - CENTRO NACIONAL DE SUPERCOMPUTAC**First name* **Carlos**Last name* **Pérez García-Pando**E-Mail* **carlos.perezga@nasa.gov**Position in org. Department ☐ Same as organisation☐ Same as organisation addressStreet Town Postcode Country Phone Phone2/Mobile *Other contact persons*

First Name	Last Name	E-mail	Phone
Marina	Azor	marina.azor@bsc.es	+34934134082



Proposal ID **727233**

Acronym **PACODOM**

Short name **ECMWF**

Partner organisation

PIC

999916741

Legal name

EUROPEAN CENTRE FOR MEDIUM-RANGE WEATHER FORECASTS

Short name: *ECMWF*

Address of the organisation

Street SHINFIELD PARK

Town READING

Postcode RG2 9AX

Country United Kingdom

Webpage www.ecmwf.int

Legal Status of your organisation

Research and Innovation legal statuses

Public body yes

Non-profit yes

International organisation yes

International organisation of European interest yes

Secondary or Higher education establishment no

Research organisation yes

Legal person yes

Enterprise Data

SME self-declared status..... unknown

SME self-assessment unknown

SME validation sme..... unknown

Based on the above details of the Beneficiary Registry the organisation is not an SME (small- and medium-sized enterprise) for the call.

NACE Code: - - Not applicable



Proposal Submission Forms

European Research Council Executive Agency

Proposal ID **727233**

Acronym **PACODOM**

Short name **ECMWF**

Department(s) carrying out the proposed work

Department 1

Department name Copernicus Atmosphere Monitoring Service

☐ not applicable

☒ Same as organisation address

Street SHINFIELD PARK

Town READING

Postcode RG2 9AX

Country United Kingdom



European Commission -
Research & Innovation - Participant Portal

Proposal Submission Forms

European Research Council Executive Agency

Proposal ID **727233**

Acronym **PACODOM**

Short name **ECMWF**

Proposal ID **727233**Acronym **PACODOM**Short name **ECMWF***Contact address of the partner organisation and contact person*

The name and e-mail of Partner Organisation contact persons are read-only in the administrative form, only additional details can be edited here. To give access rights and contact details of Partner Organisation, please save and close this form, then go back to Step 4 of the submission wizard and save the changes. The contact person needs to be added as 'Main Contact' for the Partner Organisation.

Organisation Legal Name **EUROPEAN CENTRE FOR MEDIUM-RANGE WEATHER FORECASTS**First name* **Angela**Last name* **Benedetti**E-Mail* **angela.benedetti@ecmwf.int**Position in org. Department ☐ Same as organisation☒ Same as organisation addressStreet Town Postcode Country Phone Phone2/Mobile *Other contact persons*

First Name	Last Name	E-mail	Phone
Hilary	Mepham	hilary.mepham@ecmwf.int	+44 1189499210

Proposal ID **727233**

Acronym **PACODOM**

3 - Budget

Participant Number in this proposal	Organisation Short Name	Organisation Country	Total eligible costs/€ (including 25% indirect costs) ?	Requested grant/€
1	KIT	DE	13 750	13 750
2	UNIVLEEDS	UK	78 152	78 152
3	BSC	ES	54 763	54 763
4	ECMWF	UK	2 375	2 375
Total			149 040	149 040

Proposal ID **727233**

Acronym **PACODOM**

4 - Ethics issues table

1. HUMAN EMBRYOS/FOETUSES		Page
Does your research involve Human Embryonic Stem Cells (hESCs) ?	<input type="radio"/> Yes <input checked="" type="radio"/> No	
Does your research involve the use of human embryos?	<input type="radio"/> Yes <input checked="" type="radio"/> No	
Does your research involve the use of human foetal tissues / cells?	<input type="radio"/> Yes <input checked="" type="radio"/> No	
2. HUMANS		Page
Does your research involve human participants?	<input type="radio"/> Yes <input checked="" type="radio"/> No	
Does your research involve physical interventions on the study participants?	<input type="radio"/> Yes <input checked="" type="radio"/> No	
3. HUMAN CELLS / TISSUES		Page
Does your research involve human cells or tissues (other than from Human Embryos/ Foetuses, i.e. section 1)?	<input type="radio"/> Yes <input checked="" type="radio"/> No	
4. PERSONAL DATA		Page
Does your research involve personal data collection and/or processing?	<input type="radio"/> Yes <input checked="" type="radio"/> No	
Does your research involve further processing of previously collected personal data (secondary use)?	<input type="radio"/> Yes <input checked="" type="radio"/> No	
5. ANIMALS		Page
Does your research involve animals?	<input type="radio"/> Yes <input checked="" type="radio"/> No	
6. THIRD COUNTRIES		Page
In case non-EU countries are involved, do the research related activities undertaken in these countries raise potential ethics issues?	<input type="radio"/> Yes <input checked="" type="radio"/> No	
Do you plan to use local resources (e.g. animal and/or human tissue samples, genetic material, live animals, human remains, materials of historical value, endangered fauna or flora samples, etc.)?	<input type="radio"/> Yes <input checked="" type="radio"/> No	
Do you plan to import any material - including personal data - from non-EU countries into the EU? <i>For data imports, please fill in also section 4.</i> <i>For imports concerning human cells or tissues, fill in also section 3.</i>	<input type="radio"/> Yes <input checked="" type="radio"/> No	
Do you plan to export any material - including personal data - from the EU to non-EU countries? <i>For data exports, please fill in also section 4.</i> <i>For exports concerning human cells or tissues, fill in also section 3.</i>	<input type="radio"/> Yes <input checked="" type="radio"/> No	

Proposal ID **727233**

Acronym **PACODOM**

If your research involves low and/or lower middle income countries, are benefits-sharing actions planned?	<input type="radio"/> Yes <input checked="" type="radio"/> No	
Could the situation in the country put the individuals taking part in the research at risk?	<input type="radio"/> Yes <input checked="" type="radio"/> No	
7. ENVIRONMENT & HEALTH and SAFETY		Page
Does your research involve the use of elements that may cause harm to the environment, to animals or plants? <i>For research involving animal experiments, please fill in also section 5.</i>	<input type="radio"/> Yes <input checked="" type="radio"/> No	
Does your research deal with endangered fauna and/or flora and/or protected areas?	<input type="radio"/> Yes <input checked="" type="radio"/> No	
Does your research involve the use of elements that may cause harm to humans, including research staff? <i>For research involving human participants, please fill in also section 2.</i>	<input type="radio"/> Yes <input checked="" type="radio"/> No	
8. DUAL USE		Page
Does your research have the potential for military applications?	<input type="radio"/> Yes <input checked="" type="radio"/> No	
9. MISUSE		Page
Does your research have the potential for malevolent/criminal/terrorist abuse?	<input type="radio"/> Yes <input checked="" type="radio"/> No	
10. OTHER ETHICS ISSUES		Page
Are there any other ethics issues that should be taken into consideration? Please specify	<input type="radio"/> Yes <input checked="" type="radio"/> No	

I confirm that I have taken into account all ethics issues described above and that, if any ethics issues apply, I will complete the ethics self-assessment and attach the required documents. ☒

[How to Complete your Ethics Self-Assessment](#)

Proposal ID **727233**

Acronym **PACODOM**

5 - Call specific questions

Eligibility	
I acknowledge that I am aware of the eligibility requirements for applying for this ERC call as specified in the ERC Work Programme 2016, and certify that, to the best of my knowledge my application is in compliance with all these requirements. I understand that my proposal may be declared ineligible at any point during the evaluation or granting process if it is found not to be compliant with these eligibility criteria.*	<input checked="" type="checkbox"/>
I confirm that the proposal that I am about to submit draws substantially on an existing or recently finished ERC funded frontier research grant.	<input checked="" type="checkbox"/>
<p>The PACODOM project aims to implement a new parameterisation for convective dust storms developed as part of the ERC Starting Grant "Desert Storms" into the operational forecast models run by the European Centre for Medium-Range Weather Forecasts and Barcelona Supercomputing Center. The parameterisation is a direct outcome of Desert Storms and has been published in the Journal of Atmospheric Sciences (Pantillon et al. 2015). The scheme has further been developed and tested with new model data (Pantillon et al. 2016, Journal of Geophysical Research, accepted subject to minor revisions). Thus, so far the new parameterisation has only been used in a research environment. Developing it towards operational usage is an important next step that can only be achieved through direct collaboration with operational services.</p>	
Data-Related Questions and Data Protection	
(Consent to any question below is entirely voluntary. A positive or negative answer will not affect the evaluation of your project proposal in any form and will not be communicated to the evaluators of your project.)	
For communication purposes only, the ERC asks for your permission to publish your name, the proposal title, the proposal acronym, the panel, and host institution, should your proposal be retained for funding.	<input checked="" type="radio"/> Yes <input type="radio"/> No
Some national and regional public research funding authorities run schemes to fund ERC applicants that score highly in the ERC's evaluation but which can not be funded by the ERC due to its limited budget. In case your proposal could not be selected for funding by the ERC do you consent to allow the ERC to disclose the results of your evaluation (score and ranking range) together with your name, non-confidential proposal title and abstract, proposal acronym, host institution and your contact details to such authorities? This consent is entirely voluntary and refusal to give it will in no way affect the evaluation of your proposal.	<input checked="" type="radio"/> Yes <input type="radio"/> No
The ERC is sometimes contacted for lists of ERC funded researchers by institutions that are awarding prizes to excellent researchers. Do you consent to allow the ERC to disclose your name, non-confidential proposal title and abstract, proposal acronym, host institution and your contact details to such institutions? This consent is entirely voluntary and refusal to give it will in no way affect the evaluation of your proposal.	<input checked="" type="radio"/> Yes <input type="radio"/> No
The Scientific Council of the ERC has developed a monitoring and evaluation strategy in order to help it fulfil its obligations to establish the ERC's overall strategy and to monitor and quality control the programme's implementation from the scientific perspective. As provided by section 3.10 of the ERC Rules for Submission , a range of projects and studies may be initiated for purposes related to monitoring, study and evaluating implementation of ERC actions. Do you consent to allow the third parties carrying out these projects and studies to process the content of your proposal including your personal data? The privacy statement on grants explains further how your personal data is secured. This consent is entirely voluntary and refusal to give it will in no way affect the outcome of the evaluation of your proposal.	<input checked="" type="radio"/> Yes <input type="radio"/> No

ERC Proof of Concept Grant 2016 Part B

Section 1: The idea - Innovation potential

a. Succinct description of the idea to be taken to proof of concept

Sand and Dust Storms (SDS) are extreme weather phenomena that represent a serious hazard for life, health, property, environment and economy in many countries, particularly in some of the least developed ones. Moreover, airborne dust particles play a significant role in different aspects of weather, climate and atmospheric chemistry. In the last years, the development of global and regional SDS forecasts has intensified because of their potential to mitigate impacts upon transportation, energy production, health and agriculture. While operational forecast models are skillful when SDS are caused by synoptic-scale weather systems, they are severely limited to forecast ‘haboobs’ – immense walls of blowing sand and dust formed by cold outflows from deep moist convection – which are by far the most damaging among dust storm types. One outstanding outcome of the ERC Desert Storms project is the development of a novel parameterisation for dust emission by haboobs, based on the convective outflow behaving as a density current. In PACODOM Desert Storms researchers will transfer this cutting-edge technology to two globally leading centres in operational weather, dust and climate prediction (Barcelona Supercomputing Center, BSC; European Centre for Medium-Range Weather Forecasts, ECMWF) to make a leap forward in our ability to forecast SDS globally, and therefore drastically improve mitigation potential. Both are partners of the Sand and Dust Storm Warning Advisory and Assessment System (SDS-WAS) under the framework of the World Meteorological Organization (WMO), an initiative endorsed by more than 40 countries, whose mission is to enhance their ability to deliver timely and quality SDS forecasts, observations, information and knowledge to users. The transfer of this new technology will improve air quality and weather predictions, benefitting a wide range of commercial and non-commercial users in Europe and beyond. A full operational implementation of the new approach will give ERC Desert Storms a lasting legacy and great international visibility.

b. Demonstration of Innovation Potential

SDS severely compromise air quality, disrupt ground and air transportation due to poor visibility, affect commercial solar energy production systems by reducing solar insolation, and damage croplands and livestock. Two recent examples illustrate the magnitude and effects of this hazard. In September 2015 a dust storm in Syria/Iraq (entitled “Dustpocalypse” by the Washington Post) that also affected Israel, caused five deaths and 3580 cases of asphyxia, dyspnea, breathlessness and asthma. Earlier in the season, Tehran (Iran) experienced a dust storm that caused chaos across the city, with at least four people reported dead, 30 injured and flights from the international airport cancelled. Dust storms in the so-called “dust belt” have always been a regular occurrence but there is evidence that they are happening much more frequently as a result of changes in land and water use and also climate change. For example, between 2000 and 2009 the frequency of dust storms increased by 70 to 170% in the western provinces of Iran, when compared with the preceding 30 years [1]. In addition, airborne dust particles significantly affect weather and climate through their influences on thermal and solar radiation, cloud microphysics, atmospheric chemistry and the carbon cycle via the fertilization of ecosystems through iron and other nutrients contained in dust.

Such significant effects of dust and the potential for mitigation have motivated researchers and operational services to include dust in weather models with increasing sophistication [2]. The global dust cycle involves the lifting of particles by strong near-surface winds, vertical transport through mixing in the planetary boundary layer or deeper convective or frontal motions, horizontal transport through synoptic- to planetary-scale wind systems and finally removal by gravitational settling, turbulence or precipitation on land and into oceans. All these processes are parameterised in global or regional atmospheric models that represent dust effects dynamically. Dust-lifting winds remain a key uncertainty in dust predictions [3,4]. This is largely due to the strongly nonlinear dependence of emissions on peak winds, which are often underestimated in models and even analysis data. Dust-lifting winds can be generated by a range of meteorological processes, spanning scales from few meters to thousands of kilometres. While emission caused by synoptic scale high- and low-pressure systems and their fronts are usually satisfactorily represented in numerical weather prediction (NWP) models, at least qualitatively, uncertainties are substantial at smaller scales, e.g. in relation to dry and moist convection.

The ERC-funded Desert Storms project (ended September 2015) at the Karlsruhe Institute of Technology (KIT) and University of Leeds (UoL) substantially advanced our understanding of crucial meteorological uncertainties in dust emission and developed concepts to improve the way emission is treated in numerical models (see 31 publications in Appendix). A particular focus of the project was on daytime downward mixing of momentum from nocturnal low-level jets, convective cold pools and small-scale dust devils and plumes. To achieve this, Desert Storms undertook: (a) a detailed analysis of observations including station data, measurements from recent field campaigns, analysis data and novel satellite products, (b) a comprehensive comparison between output from a wide range of global and regional dust models, and (c) extensive sensitivity studies with regional and large-eddy simulation models in realistic and idealized set-ups to explore effects of resolution and model physics. In contrast to previous studies, all evaluations were made on a process level concentrating on specific meteorological phenomena. Amongst the outstanding results from Desert Storms are works on the climatological relevance, the physical understanding and the modelling of haboobs in the Sahel and Sahara, the world's largest dust source. Haboobs are caused by downdrafts from deep moist convection that spread at the surface as a cold pool with a sharp leading edge. The abrupt increase in wind speed often creates a dramatic, fast moving “wall of dust” (Fig. 1 left). Desert Storms research showed that haboobs: (a) cause at least a third of summertime dust emission in the Sahel / southern Sahara (consistent with observations [5]); (b) are difficult to observe from space due to cloud contamination; and (c) are lacking in models using convective parameterisations (all global and most regional models), as those do not resolve cold pools. Both the catastrophic Syrian/Iraqi and Iranian SDS events mentioned above were related to haboobs and were completely missed by operational models across the board, demonstrating the urgent need to improve the representation of such storms.

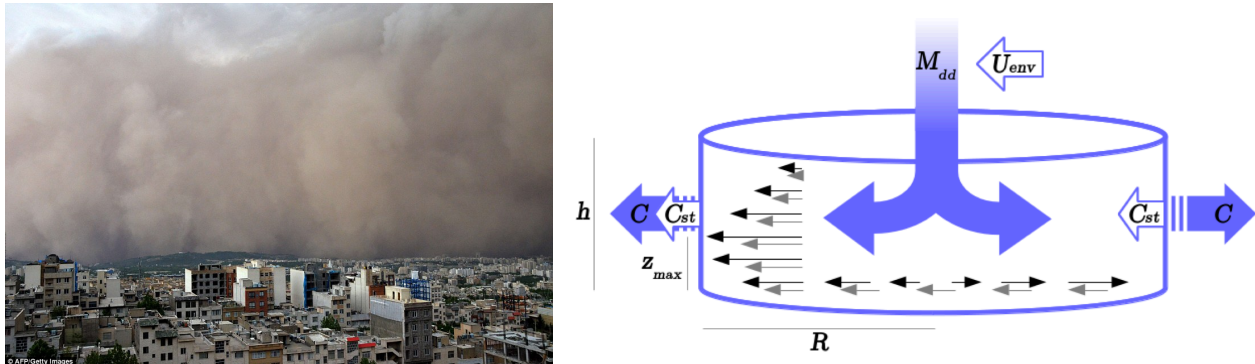


FIG. 1: Left: Haboob approaching Tehran. Right: Conceptual model developed by [6], which uses the downdraft mass flux from the convection scheme, M_{dd} , and the environmental steering wind, U_{env} , to derive a distribution of near surface winds.

As a response, Desert Storms researchers developed a novel parameterisation that links grid-scale quantities with probabilities of winds exceeding a given threshold within a gridbox, which can be used to drive a dust emission scheme [6]. The parameterisation is based on the assumption that the downdraft mass flux from the convection scheme spreads out radially in a cylindrical cold pool (Fig. 1 right). The winds from the parameterisation were tested “offline” (no impact of soil moisture) using the UK Met Office’s Unified Model and the German Weather Service’s COSMO model [7]. The parameterisation is calibrated with convection-permitting runs and applied to convection-parameterised runs, and successfully produces the extensive area of dust-generating winds from cold pool outflows over the Sahara. Location and timing of dust-generating winds are only weakly sensitive to the parameters of the conceptual model. Biases are related directly to biases caused by the convection scheme (e.g. geographical distribution, diurnal cycle). Overall, the results demonstrate that a simple parameterisation corrects a major and long-standing limitation in dust models and arguably one of the largest sources of error in dust forecasting. In PACODOM, the parameterisation of [6] will be integrated into two world-leading state-of-the-art operational forecast models used to predict dust concentrations and standard weather parameters, i.e. those operated by BSC and ECMWF. Something like this has never been attempted before and the resulting model will have unique capabilities. As the forecast products generated by BSC and ECMWF are used by a wide range of commercial and non-commercial users in Europe and beyond, the potential economic and societal benefits are enormous. Haboobs have been observed over all major dust source areas worldwide [8] and the produced dust can be transported over long distances, such that forecast improvements can be expected to go well beyond Africa and the Middle East. Moreover, since dust affects the atmosphere through radiation and other processes, improvements of global weather and climate prediction can also be expected.

a. Economic and/or societal benefits

PACODOM will significantly improve the skills of forecasts at two of the world's leading providers of global and regional dust and weather information [2,9]. At ECMWF, the EU-funded “Global and regional Earth-system (Atmosphere) Monitoring using Satellite and in-situ data” (GEMS) and “Monitoring Atmospheric Composition and Climate” (MACC) projects were the first European attempts at establishing an integrated analysis and forecasting system for atmospheric composition and paved the way for the current “Copernicus Atmospheric Monitoring Service” (CAMS). The CAMS system includes sophisticated online chemistry and aerosol schemes including dust and utilizes satellite data for optimal initialization with a 4D-Var assimilation system. The global modelling system is also used to provide the boundary conditions for an ensemble of regional models that produce 4-day forecasts of air quality for Europe. The BSC develops and provides operational regional and global dust forecasts with the NMMB/BSC-CTM, a multi-scale atmospheric chemistry and weather prediction system (see e.g. Fig. 2). In addition, the BSC hosts (together with the Spanish Weather Service, AEMET) the World Meteorological Organization (WMO) Sand and Dust Storm Warning Advisory and Assessment System (SDS-WAS) Regional Center for Northern Africa, Middle East and Europe (NA-ME-E, <http://sds-was.aemet.es>), which coordinates research and operational communities to enhance the ability of countries to deliver timely and quality SDS forecasts, observations, information and knowledge to users. The SDS-WAS was established in 2007 as a federation of partners in response to the intention of 40 WMO member countries to improve capabilities for more reliable SDS forecasts that contribute to risk reduction in many areas and benefit society. In addition to NA-ME-E, there is an Asian Node (hosted by China). More than 15 organizations currently provide daily dust forecasts in different geographic regions. Both the NMMB/BSC-CTM and CAMS systems contribute to multi-model ensemble dust prediction for the WMO SDS-WAS and the International Cooperative for Aerosol Prediction (<http://icap.atmos.und.edu>). Europe is therefore in a unique position to provide services related to dust prediction thanks to national and European initiatives and international collaboration.

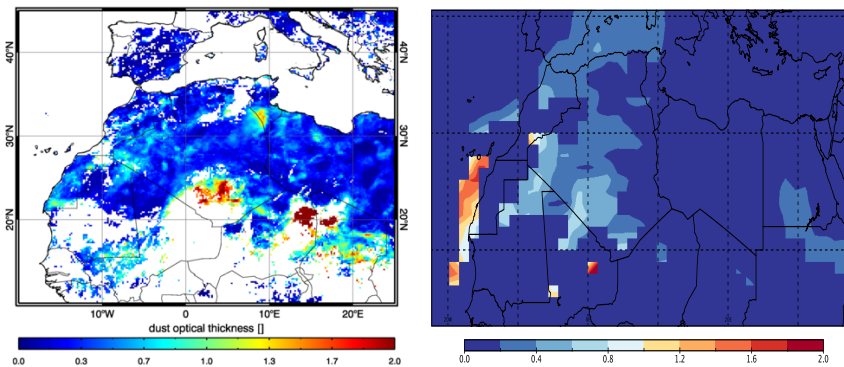


FIG. 2: Left: Satellite-based estimate of aerosol optical depth (AOD) over the Sahara at 09 UTC 29 June 2012 showing remnants of a haboob over Algeria, Niger and Chad. Right: 9-hour forecast of clear-sky dust optical depth by the NMMB/BSC-Dust system for the same time.

However, despite the enormous recent efforts and substantial progress, models like those run by the BSC and ECMWF still struggle to reliably reproduce many aspects of the dust cycle, particularly convective dust storms as demonstrated in Desert Storms and illustrated by the example shown in Fig. 2 and the Syrian/Iraqi case mentioned above. Similarly, the Tehran case of June 2015 was the subject of a coordinated modelling effort by the contributors to the NA-ME-E mode: no operational model was able to capture the magnitude and exact location of the event. Models tend to have better skills at synoptic scales due to resolution and parameterizations. However, for the Tehran haboob not even a high resolution run of the ECMWF model at 16km resolution was able to provide a skillful synopsis of the event. This study shows the need for further improvements of dust forecasting at the mesoscales, when dust storms are the strongest and have the biggest impact on society, especially when they happen close to cities. By capturing an emission process missing in global models, the new parameterisation should improve the forecast of SDS and the seasonal and geographical distribution of dust in source regions, Europe and indeed globally. These improvements will immediately create economic and societal benefit in the following areas:

- **Air pollution:** SDS frequently cause unhealthful levels of dust particles in (semi-)arid environments but also far from sources through long-range transport [10]. According to the World Health Organisation, air pollution is now the world's single biggest environmental health risk, linked to ~7M premature deaths a year (~1 in 8 in 2012). Saharan dust contributes significantly to PM10 exceedances in southern Europe [11,12] and sometimes even as far as the UK [13]. Through EU regulations these have substantial financial

implications for the countries affected. Dust has also been associated to Meningitis outbreaks [14] that, in some West African countries, are responsible for more infant deaths than malaria [15].

- **Severe weather:** Intense dust storms with high winds and low visibility are a natural hazard and dust forecasts are being increasingly used to issue warnings. Europe has many interests and infrastructure in dust regions (e.g. oil and gas, civil aviation, military and increasingly solar power).
- **Agriculture:** SDS cause loss of crop and livestock. Sandblasting results loss of plant tissue, which reduces photosynthetic activity and therefore growth, reproduction and development of grain, fibre or fruit [16]. Improved SDS forecasts could help mitigation and adaptation actions to be taken in advance, including harvesting of maturing crops, sheltering livestock and changing the time of planting.
- **Photovoltaic energy production:** Dust reduces the output of solar panels, especially systems relying on direct solar radiation [17]. The solar energy industry requires insolation forecasts to help predict optimal hours of operations and contributions to the power grid. Respective products from the ECMWF have over 400,000 users, mostly commercial companies. The massive increase in solar-generated power expected in the dust-rich Middle East/North Africa region will increase the need for such information massively, providing an economic opportunity for information providers.
- **Weather prediction:** Incorporating radiative effects of dust in models can improve weather forecasts in directly affected and remote regions [18–22]. Therefore better dust forecasts can be expected to create measurable improvements in weather variables such as temperature, wind and precipitation.
- **Climate projections:** Dust affects climate through radiation, cloud impacts and by coupling with the carbon cycle. Particularly monsoon systems, on which millions rely for their annual rains, are sensitive to changes in dust. As stressed by the IPCC, however, dust projections and their impacts remain highly uncertain [23]. Operational centres are increasingly using 'seamless' model frameworks with weather forecast evaluation feeding into climate model assessment [24]. A new parameterisation automatically becomes part of the standard scientific configuration for the next model upgrades. For example, the CAMS systems feeds into the ECMWF's Numerical Weather Prediction forecast at all scales (medium-range, monthly and seasonal).

Therefore given the wide usage of operational products generated by BSC and ECMWF, a sizeable benefit in diverse areas of the public and private sectors across Europe and beyond is highly likely.

b. Commercialisation process and/or any other exploitation process

This project will not develop a product that can be commercialised. Instead it is planned to exploit research results through implementation of a new parameterisation into state-of-the-art operational weather and air quality forecasting systems. This is only possible in close collaboration with operational weather and dust services.

c. Proposed plans

Competitive analysis. The scheme by [6] is a completely new approach not yet realised in operational weather forecasting. The only similar approaches currently existing are basic gust parameterisations for moist convection, which do not take into account the specific behaviour of cold pools (e.g. [25] used in NASA's climate model), and one highly complex parameterisation of propagating, sub-grid cold pools that is fully coupled with the parameterisation of sub-grid convection [26], as currently employed in the French climate model LMDZ but not used for aerosol or weather forecasting. The large complexity of the scheme and the intimate coupling with other schemes makes this approach very hard to port to other models.

Testing, technical reports. As detailed in section 3, there will be ample testing of the new parameterisation at various stages of the work plan. If the parameterisation becomes part of the operational system, the details of the implementation will be documented in technical reports by BSC and ECMWF. This will help propagating the technology to other operational centres, e.g. those involved in SDS-WAS.

IPR position and strategy. The parameterisation by [6] is published and can freely be used. Once implemented into operational models, the concrete realisation of the parameterisation will become part of that model and fall under the pertinent legal regulations. Typically, model code and output are available for non-commercial research purposes and to partner organisations (see e.g. <http://www.ecmwf.int/en/terms-use>).

Industry/sector contacts. In this project academic researchers will interact with operational forecast centres. A wide range of public and private sector users will be affected through the direct or indirect use of operational forecast products (see section 2a). Furthermore, if PACODOM can demonstrate the value of its approach, it will become sufficiently low-risk for private companies (e.g. Fugro-GEOS) or public-private consortia (e.g. DNicast, www.dnicast-project.net) producing dust or solar energy forecasts to consider implementation.

Section 3: The proof of concept plan

a. Plan of the activities

The aim of PACODOM is to lead to a measurable improvement of forecast skill in operational global prediction models. The main target is hazardous convective dust storms, but improvement is expected to reach beyond dust variables (through couplings with radiation), beyond Africa (through teleconnection and long-range transport) and beyond weather timescales (i.e. climate response to aerosol radiative forcing). The main planned activities in chronological order are (timings in Fig. 3):

- **Meeting 1 (M1):** Kick-off meeting at BSC in Barcelona with all team members; introduction of postdocs to senior researchers; discussion of technical and scientific details of the work plan and overall project.
- **Task 1 (T1):** Implementation of the parameterisation code in test versions of the current operational systems at ECMWF and BSC, including the coupling between the cold pool parameterisation and the dust scheme; initial tests of the performance relative to the original system using the most advanced forecast verification methods (i.e. computing skill scores comparing forecasts with available satellite and in-situ observations) established at the two centres and the WMO SDS-WAS Regional Centre.
- **Task 2 (T2):** Separate calibration of the parameterisation for BSC and ECMWF models using the approach and high-resolution COSMOS model data as employed by [7]; comparison between the two systems.
- **Meeting 2 (M2):** Midterm meeting at KIT in Karlsruhe with all team members; discussion of achievements, surprises and problems; potentially decision about application of contingency options (see below).
- **Task 3 (T3):** Sensitivity tests with respect to the treatment of soil moisture generated by convective precipitation in the dust emission process (disregarded in [6,7]); possibly re-tuning using same data as in T2.
- **Task 4 (T4):** Generation of hindcasts for a longer period in a pre-operational mode; evaluation of hindcasts, again using the same forecast verification methods as in T1 to test effects on forecasts worldwide.
- **Meeting 3 (M3):** Concluding meeting at UoL in Leeds; discussions of project results and possible follow-up activities, e.g. as part of SDS-WAS; writing of final report and technical documentations.

Tasks 1–4 will be largely executed in parallel with the BSC and ECMWF modelling systems. Direct exchanges between the postdocs and discussions at the project meetings will ensure model intercomparison and consistency of implementation, although different choices may be made due to the differences between the two models. The use of two models will allow us to evaluate the impact of the parent model on the success of the parametrisation.

Activity / Month	01	02	03	04	05	06	07	08	09	10	11	12	13	14	15	16	17	18
T1: Implementation																		
T2: Calibration																		
T3: Soil Moisture																		
T4: Pre-operational mode																		
Project meetings	M1								M2									M3

FIG. 3: Gantt chart indicating planned timings of the activities in PACODOM.

The risk of failure for the PACODOM project are very small because:

- The project builds on pre-existing knowledge from [6,7] that will be integrated into operational systems.
- Data necessary for tuning the operational implementations already exist (1-year COSMO simulation [7])
- Consortium has strong expertise in all relevant areas (atmospheric dynamics, modelling, data assimilation, forecasting, validation, interactions with users). All members are recognised at the international level.

A number of risks have been identified for which specific responses can be prepared to avoid negative impacts:

- Senior researcher leaving the project. This risk is very small as all involved PIs are well-established scientists with long-term positions. Since all partners are strongly committed to the project, there will be a clear motivation for the respective institute to nominate a suitable colleague to take over the vacated position.
- Postdoc leaving the project. This risk is very small, as we are seeking to find experienced people to be shared with other projects (50% posts), who have a longer-term perspective at UoL and BSC. If such a case occurs, we will distribute the work to other existing postdocs in these institutions with similar experience.
- A critical task is delayed or of unsatisfactory result. Risk is very small, because any problem will be discussed in regular telecons or meetings and the project relies to a large extent on pre-existing knowledge.
- Consortium not agreeing on an issue. There is a clear plan of actions and common goal to improve forecasts.

Generally, the PIs will identify risks at the earliest possible stage and suggest efficient countermeasures.

b. Project-management plan

PI Knippertz will have the overall responsibility of the project coordination (see Fig. 4), ensuring execution of tasks in an efficient and timely manner. Lead beneficiary KIT will be responsible for the financial and scientific reporting to the EU. Technical work and other day-to-day tasks related to the two operational models will be executed by two postdocs supervised by Carlos Pérez García-Pando at BSC and John Marsham at UoL. Marsham will coordinate interaction with others at UoL working on the CAMS system (e.g. Graham Mann, see section 4). Pérez García-Pando and Benedetti will serve as main points of contact at BSC and ECMWF, respectively, and make sure access to all necessary resources is provided. Benedetti will organize the UoL postdoc's visits to ECMWF and introduce her/him to the CAMS system and relevant individuals at ECMWF. Direct exchanges between the postdocs will ensure model intercomparison and consistency of implementation. Effective communication between all team members will be achieved through e-mail and bi-monthly telephone- or videoconferences, where problems or delays in the technical work and scientific interpretation of results will be discussed. Three project meetings (section 3a) will provide a forum for more extensive and detailed discussions on all relevant project matters.

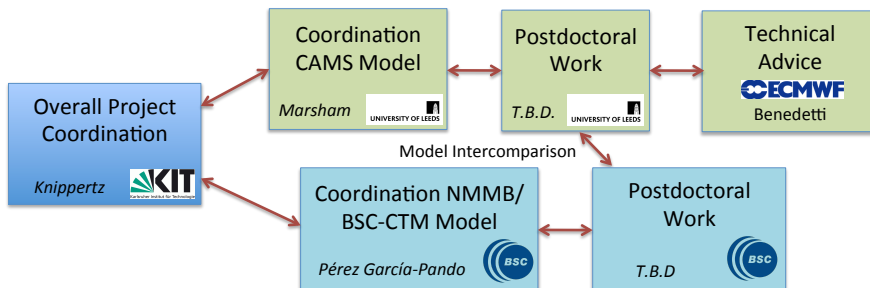


FIG. 4: Schematic depiction of the implementation of PACODOM showing the roles of the six involved scientists together with the main communication pathways. Green / turquoise colours indicate the two modelling systems.

c. Description of the team

Prof Dr Peter Knippertz (PI), Professor of Meteorology at **KIT**, initiated, conceived and successfully led ERC Desert Storms from 2010–2015. He is an internationally renowned expert on the dynamics of dust storms and lead editor of a comprehensive book on Mineral Dust. He (co-)authored 93 journal articles, 45 of which address dust-related topics (h-index 27, Web of Science). He has led several national and international projects and currently coordinates the EU consortium DACCWA (www.dacciwa.eu). Knippertz has (co-)convened a session on dust at the European Geosciences Union Annual Assembly for 9 years. The main developer of the new parameterisation, **Dr Florian Pantillon**, recently moved to a 4-year position at KIT. He is keen to support PACODOM through advice on technical and scientific detail and participation in project meetings.

Dr John H. Marsham, Associate Professor at **UoL**, has been involved in Desert Storms from the proposal stage and took over the UoL component in 2013. He is an expert in atmospheric dust (21 papers, 433 citations), tropical meteorology and convection (h-index 16, Web of Science). He was awarded the *RMetS's L F Richardson prize* and the *EMS's Young Scientist Award* for his outstanding publications. He has been PI or Co-I of several projects on dust, African meteorology and forecasting (Fennec, IFADS, SWAMMA, Future Climate for Africa). **Dr Graham Mann** will support activities at UoL through his expertise with the CAMS model.

Dr Angela Benedetti, Senior Scientist at **ECMWF**, has over a decade of expertise in aerosol assimilation. She has been involved in the GEMS and MACC projects from the outset, and she still closely works with the CAMS team. She collaborates with several international scientists on aerosol prediction issues and has recently coordinated a chapter on dust numerical prediction [2]. Benedetti has co-authored numerous publications in aerosol science and serves in various international panels (WMO SDS-WAS, WMO Global Atmosphere Watch (GAW) Science Advisory Group on Aerosols, Aeolus-ADM Mission Advisory Group).

Dr Carlos Pérez García-Pando, currently Associate Research Scientist at the NASA Goddard Institute for Space Studies and Columbia University, will return to **BSC** in September 2016 as Group Leader of the Atmospheric Composition group. Thanks to the international recognition of his contributions to basic, applied and cross-disciplinary aspects of SDS, he was awarded with an AXA Research Fund Chair in October 2015. He is the main developer of the aerosol component of the NMMB/BSC-CTM model and played a key role in establishing WMO SDS-WAS and the Regional Center in Barcelona. He has 46 peer-reviewed papers (h-Index: 24, 2370 citations, Google Scholar), 20 chapters in books, proceedings and reports and 26 invited presentation. He has participated in 27 international and national projects (in 6 of them as PD, PI or co-PI).

Section 4: *The budget***a. Resources (incl. project costs)**

Cost Category			Total in Euro
Direct Costs	Personnel	PI	7,100
		Senior Staff	8,819
		Postdocs	86,413
		Students	0
		Other	0
	i. Total Direct costs for Personnel (in Euro)		102,332
	Travel		14,900
	Equipment		0
	Other goods and services	Consumables	0
		Publications (including Open Access fees), etc.	0
		Other (please specify)	2000
	ii. Total Other Direct Costs (in Euro)		16,900
A – Total Direct Costs (i + ii) (in Euro)			119,232
B – Indirect Costs (overheads) 25% of Direct Costs (in Euro)			29,808
C1 – Subcontracting Costs (no overheads) (in Euro)			0
C2 – Other Direct Costs with no overheads (in Euro)			0
Total Estimated Eligible Costs (A + B + C) (in Euro)			149,040
Total Requested EU Contribution (in Euro)			149,040

b. Justification (description of the budget)*Personnel*

The main resource needed in this project is postdoc hours to do the implementation, testing and tuning of the parameterisation with the operational forecasting systems. The project is tentatively planned to start on 01 December 2016 and to run for 18 months with both postdocs working 50% of their time on the project.

The first postdoc position is requested for the BSC (35,000€) under the supervision of Carlos Pérez García-Pando. We will seek a person with experience and knowledge of the operational system at BSC, including the dust component, who will be able to execute the work in an efficient and competent way.

The second postdoc position is requested for the University of Leeds (51,413€) under the supervision of John Marsham and will concentrate on the work with the CAMS model through a remote log-on to the ECMWF system. Working at the university guarantees close contact with related research in projects building on Desert Storms and an integration of the researcher in an academic environment. At the same time there is long-standing experience at UoL in working with the ECMWF model remotely (particularly in the group led by Ken Carslaw and involving Graham Mann), such that direct exchange with other more experienced staff is possible, particularly if technical problems arise. Three one-week long stays of the Leeds postdoc at the ECMWF in Reading are planned to directly work with involved ECMWF scientists and operational experts.

2% of the salary of Co-PI Marsham (3,039€), 3% of the salary of Perez García-Pando (4,410€) and 5% of the salary of project leader Knippertz (7,100€) are requested to cover the time they will dedicate to the supervision and management of the project. At UoL, Dr Graham Mann has long-standing expertise with technical

development work using the ECMWF CAMS model. 1% of his salary (1,370€) is requested to facilitate the UoL Postdoc's work with this system.

Other direct costs

As explained in section 3, three one-day project meetings are planned (beginning, middle and end of project period). These will take place in Barcelona, Karlsruhe and Leeds. In total this will require 1 trip within the UK (300€) and 13 international trips for about 800€ each (including a trip of Florian Pantillon to the kick-off meeting in Barcelona), totalling 10,700€. In addition, funds are requested for each postdoc to attend one international conference or workshop, totalling 2,400€. Travel funds are also needed for three one-week long stays of the Leeds postdoc at ECMWF (1,800€ in total). Therefore a total travel budget of 14,900€ is requested.

Towards the end of the project, the results of the implementation of the scheme in the two operational models as well as some evaluation results showing the expected added value will be published in technical reports that should enable other centres to use this approach in their own models. The results will also be advertised through information channels established by the SDS-WAS. 1500€ are requested to cover expenses related to these outreach activities (e.g. costs of publishing technical reports, travel to WMO meetings).

Technical support, computer hardware and computing time, as well as data storage, are in kind contributions from BSC and ECMWF. At UoL 500€ are requested for data storage, particularly the large COSMO model dataset used for the calibration of the parameterisation in the CAMS model.

No equipment or consumables are requested for this project.

References

- [1] <http://www.aljazeera.com/weather/2014/06/dust-storms-modern-plague-iran-20146475257821125.html>
- [2] Benedetti, A. and co-authors, 2014: Operational dust prediction. Chapter 10 in: Knippertz, P. and J.-B. Stuut (eds.), *Mineral Dust – A Key Player in the Earth System*, Springer Netherlands, ISBN 978-94-017-8977-6, doi:10.1007/978-94-017-8978-3_10.
- [3] Huneeus, N. and co-authors, 2011: Global dust model intercomparison in AeroCom phase I. *Atmos. Chem. Phys.*, 11, 7781–7816, doi:10.5194/acp-11-7781-2011.
- [4] Heinold, B., Knippertz, P., Marsham, J. H., Fiedler, S., Dixon, N. S., Schepanski, K., Laurent, B., Tegen, I., 2013: The role of deep convection and low-level jets for dust emissions in West Africa. *J. Geophys. Res.*, 118(10), 4385–4400.
- [5] Marsham, J. H. and co-authors, 2013: Meteorology and dust in the central Sahara: Observations from Fennec supersite-1 during the June 2011 Intensive Observation Period. *J. Geophys. Res. Atmos.*, 118, 4069–4089, doi:10.1002/jgrd.50211.
- [6] Pantillon, F., Knippertz, P., Marsham, J. H., Birch, C., 2015: A parameterization of convective dust storms for models with mass-flux convection schemes. *J. Atmos. Sci.*, 72(6), 2545–2561, doi:10.1175/JAS-D-14-0341.1.
- [7] Pantillon, F., Knippertz, P., Marsham J. H., Panitz, H.-J., Bischoff-Gauss, I., 2016: Modeling haboobs in large-scale weather and climate models. *J. Geophys. Res.*, in press, doi:10.1002/2015JD024349.
- [8] Knippertz, P., 2014: Meteorological aspects of dust storms. Chapter 6 in: Knippertz, P. and J.-B. Stuut (eds.), *Mineral Dust – A Key Player in the Earth System*, Springer Netherlands, ISBN 978-94-017-8977-6, doi:10.1007/978-94-017-8978-3_6.
- [9] Pérez, C., Haustein, K., Janjic, Z., Jorba, O., Huneeus, N., Baldasano, J. M., Black, T., Basart, S., Nickovic, S., Miller, R. L., Perlwitz, J. P., Schulz, M., and Thomson, M., 2011: Atmospheric dust modeling from meso to global scales with the online NMMB/BSC-Dust model – Part 1: Model description, annual simulations and evaluation. *Atmos. Chem. Phys.*, 11, 13001–13027, doi: 10.5194/acp-11-13001-2011.
- [10] Morman, S. A., Plumley, G. S., 2014: Dust and human health. Chapter 15 in: Knippertz, P. and J.-B. Stuut (eds.), *Mineral Dust – A Key Player in the Earth System*, Springer Netherlands, 121–148, ISBN 978-94-017-8977-6. doi:10.1007/978-94-017-8978-3_15
- [11] http://acm.eionet.europa.eu/docs/ETCACM_TP_2011_4_health_effects_sahara_dust.pdf
- [12] Escudero, M., Castillo, S., Querol, X., Avila, A., Alarcon, M., Viana, M.M., Alastuey, A., Cuevas, E., Rodriguez, S., 2005: Wet and dry African dust episodes over Eastern Spain. *J. Geophys. Res.*, 110, D18S08.
- [13] <http://www.theguardian.com/uk-news/2014/apr/02/smog-alert-england-wales-air-pollution-saharan-dust>
- [14] Pérez García-Pando, C., Stanton, M. C., Diggle, P. J., Trzaska, S., Miller, R. L., Perlwitz, J. P., Baldasano, J. M., Cuevas, E., Ceccato, P., Yaka P., Thomson, M. C., 2014: Soil dust aerosols and wind as predictors of seasonal meningitis incidence in Niger. *Environmental Health Perspectives*, doi:10.1289/ehp.1306640
- [15] World Health Organization (WHO), 2012: *World health statistics 2012*. World Health Statistics Annual, ISBN 9789241564441, 170pp.
- [16] Stefanski R., Sivakumar, M. V. K., 2009: Impacts of sand and dust storms on agriculture and potential agricultural applications of a SDSWS IOP. *Conf. Ser.: Earth Environ. Sci.* 7 012016.
- [17] Schroedter-Homscheidt, M., Oumbe, A., Benedetti, A., Morcrette, J.-J., 2012: Aerosols for concentrating solar electricity production forecasts: requirement quantification and ECMWF/MACC aerosol forecast assessment. *Bull. Amer. Meteor. Soc.*, 94, 903–914, doi:10.1175/BAMS-D-11-00259.
- [18] Tompkins, A. M., Cardinali, C., Morcrette, J.-J., Rodwell, M., 2005: Influence of aerosol climatology on forecasts of the African Easterly Jet. *Geophys. Res. Lett.*, 32, L10801, doi:10.1029/2004GL022189.
- [19] Pérez, C., Nickovic, S., Pejanovic, G., Baldasano, J. M., Özsoy, E., 2006: Interactive dust-radiation modeling: A step to improve weather forecasts. *J. Geophys. Res.*, 111, D16206, doi:10.1029/2005JD006717.
- [20] Milton S. F., Greed, G., Brooks, M. E., Haywood, J., Johnson, B., Allan, R. P., Slingo, A., Grey, W. M. F., 2008: Modeled and observed atmospheric radiation balance during the West African dry season: Role of

- mineral dust, biomass burning aerosol, and surface albedo. *J. Geophys. Res.*, 113, doi:10.1029/2007JD009741.
- [21] Mulcahy, J. P., Walters, D. N., Bellouin, N., Milton, S. F., 2014: Impacts of increasing the aerosol complexity in the Met Office global numerical weather prediction model. *Atmos. Chem. Phys.*, 14, 4749–4778, doi:10.5194/acp-14-4749-2014.
- [22] Rémy, S. and co-authors, 2014: Positive feedback of dust aerosol via its impact on atmospheric stability during dust storms in the Eastern Mediterranean. *Atmos. Chem. Phys. Discuss.*, 14, 28147–28201, doi:10.5194/acpd-14-28147-2014.
- [23] Boucher, O. and co-authors, 2013: Clouds and aerosols. In: *Climate Change 2013: The Physical Science Basis. Contribution of Working Group I to the Fifth Assessment Report of the Intergovernmental Panel on Climate Change*, Eds. Stocker, T. F. et al., Cambridge University Press, Cambridge, United Kingdom and New York, NY, USA.
- [24] Palmer T.N., Doblas-Reyes, F. J., Weisheimer, A., Rodwell, M. J., 2008: Toward seamless prediction: Calibration of climate change projections using seasonal forecasts. *Bull. Amer. Meteor. Soc.*, 89, 459–470. doi:10.1175/BAMS-89-4-459.
- [25] Cakmur, R. V., Miller, R. L., Torres, O., 2004: Incorporating the effect of small-scale circulations upon dust emission in an atmospheric general circulation model. *J. Geophys. Res.*, 109, D07201, doi:10.1029/2003JD004067.
- [26] Grandpeix, J.-Y., Lafore, J.-P. 2010: A density current parameterization coupled with Emanuel's convection scheme. Part I: The models. *J. Atmos. Sci.*, 67 (4), 881–897, doi: 10.1175/2009JAS3044.1.

Publications from ERC Desert Storms project 2011–2015 (Desert Storms authors in bold)

- [01] **Pantillon, F.; Knippertz, P.; Marsham J. H.**; Panitz, H.-J.; Bischoff-Gauss, I., 2016: Modeling haboobs in large-scale weather and climate models. *J. Geophys. Res.*, doi:10.1002/2015JD024349.
- [02] Redl, R.; Fink, A. H.; **Knippertz, P.**, 2015: An objective detection method for convective cold pool events and its application to northern Africa. *Mon. Wea. Rev.*, 143, 5055–5072. doi:10.1175/MWR-D-15-0223.1
- [03] **Fiedler, S.**; Kaplan, M. L.; **Knippertz, P.**, 2015: The importance of Harmattan surges for the emission of North African dust aerosol. *Geophys. Res. Lett.*, 42, 9495–9504, doi:10.1002/2015GL065925.
- [04] **Cowie, S.; Marsham, J. H.; Knippertz, P.**, 2015: The importance of rare, high-wind events for dust uplift in northern Africa. *Geophys. Res. Lett.*, 42, 8208–8215, doi:10.1002/2015GL065819.
- [05] Sodemann, H.; Lai, M.; Marengo, F.; Ryder, C.; Flamant, C.; **Knippertz, P.**; Rosenberg, P.; Bart, M.; McQuaid, J. B., 2015: Lagrangian dust model simulations for a case of moist convective dust emission and transport in the western Sahara region during Fennec/LADUNEX. *J. Geophys. Res.*, 120 (12), 6117–6144, doi:10.1002/2015JD023283.
- [06] **Fiedler, S.; Knippertz, P.**; Woodward, S.; Martin, G.; Bellouin, N.; Birch, C.; **Heinold, B.; Schepanski, K.**; Tegen, I., 2015: A process-based evaluation of winds for dust emission in the CMIP5 simulation of HadGEM2-ES. *Clim. Dyn.*, doi:10.1007/s00382-015-2635-9.
- [07] **Pantillon, F.; Knippertz, P.; Marsham J. H.**; Birch, C., 2015: A parameterization of convective dust storms for models with mass-flux convection schemes. *J. Atmos. Sci.*, 72(6), 2545–2561. doi:10.1175/JAS-D-14-0341.1
- [08] **Jemmet-Smith, B. C.; Marsham, J. H.; Knippertz, P.; Gilkeson, C. A.**, 2015: Quantifying global dust devil occurrence from meteorological analyses. *Geophys. Res. Lett.*, 42, 1275–1282 doi:10.1002/2015GL063078.
- [09] Evan, A. T.; **Fiedler, S.**; Zhao, C.; Menut, L.; **Schepanski, K.**; Flamant, C.; Doherty, O., 2015: Derivation of an observation-based map of North African dust emission. *Aeolian Research*, 16, 153–162. doi:10.1016/j.aeolia.2015.01.001

- [10] Newton, B.; **Cowie, S.**; Rijks, D.; Banks, J.; Brindley, H.; **Marshall, J. H.**, 2014: Solar cooking in the Sahel. *Bull. Amer. Meteor. Soc.*, 95, 1325–1328.
- [11] Roberts, A.; **Knippertz, P.**; **Marshall, J. H.**, 2014: Disagreements in low-level moisture between (re)analyses over summertime West Africa. *Mon. Wea. Rev.*, [doi:10.1175/MWR-D-14-00218.1](https://doi.org/10.1175/MWR-D-14-00218.1)
- [12] **Heinold, B.**; **Knippertz, P.**; Beare, R. J., 2014: Idealised large-eddy simulations of nocturnal low-level jets over subtropical desert regions and implications for dust-generating winds. *Quart. J. Roy. Meteorol. Soc.*, [doi:10.1002/qj.2475](https://doi.org/10.1002/qj.2475)
- [13] **Schepanski K.**; **Knippertz, P.**; Fiedler, S.; Timouck, F.; Dermaty, J., 2014: The sensitivity of nocturnal low-level jets and near-surface winds over the Sahel to resolution, initial conditions and boundary-layer setup. *Quart. J. Roy. Meteorol. Soc.*, [doi:10.1002/qj.2453](https://doi.org/10.1002/qj.2453).
- [14] Fiedler, S.; **Schepanski, K.**; **Knippertz, P.**; **Heinold, B.**; Tegen, I., 2014: How important are atmospheric depressions and mobile cyclones for emitting mineral dust aerosol in North Africa? *Atm. Chem. Phys.*, 14, 8983–9000. [doi:10.5194/acp-14-8983-2014](https://doi.org/10.5194/acp-14-8983-2014)
- [15] **Cowie, S.**; **Knippertz, P.**; **Marshall, J. H.**, 2014: A climatology of dust emission events from northern Africa using long-term surface observations. *Atm. Chem. Phys.*, 14, 8579–8597. [doi:10.5194/acp-14-8579-2014](https://doi.org/10.5194/acp-14-8579-2014)
- [16] Roberts, A.; **Knippertz, P.**, 2014: The Formation of a large summertime Saharan dust plume: Convective and synoptic-scale analysis. *J. Geophys. Res.*, 19(4), 1766–1785. [doi:10.1002/2013JD020667](https://doi.org/10.1002/2013JD020667)
- [17] **Knippertz, P.**, 2013: Dust may cool polar regions. *Nature Clim. Change*, 3(5), 443–444. [doi:10.1038/nclimate1880](https://doi.org/10.1038/nclimate1880)
- [18] **Marshall, J.**; Dixon, N.; Garcia-Carreras, L.; Lister, G. M. S.; Parker, D. J.; **Knippertz, P.**, 2013: The role of moist convection in the West African monsoon system - insights from continental-scale convection-permitting simulations. *Geophys. Res. Lett.*, 40(9), 1843–1849. [doi:10.1002/grl.50347](https://doi.org/10.1002/grl.50347)
- [19] Fiedler, S.; **Schepanski, K.**; **Heinold, B.**; **Knippertz, P.**; Tegen, I., 2013: Climatology of nocturnal low-level jets over North Africa and implications for modeling mineral dust emission. *J. Geophys. Res.*, 118(12), 6100–6121. [doi:10.1002/jgrd.50394](https://doi.org/10.1002/jgrd.50394)
- [20] **Heinold, B.**; **Knippertz, P.**; **Marshall, J. H.**; Fiedler, S.; Dixon, N. S.; **Schepanski, K.**; Laurent, B.; Tegen, I., 2013: The role of deep convection and low-level jets for dust emissions in West Africa. *J. Geophys. Res.*, 118(10), 4385–4400. [doi:10.1002/jgrd.50402](https://doi.org/10.1002/jgrd.50402)
- [21] **Cowie, S.**; **Knippertz, P.**; **Marshall, J. H.**, 2013: Are vegetation-related roughness changes the causes of the recent decrease in dust emission from the Sahel? *Geophys. Res. Lett.*, 40(9), 1868–1872. [doi:10.1002/grl.50273](https://doi.org/10.1002/grl.50273)
- [22] **Schepanski, K.**; Flamant, C.; Chaboureaud, J.-P.; Kocha, C.; Banks, J. R.; Brindley, H. E.; Lavaysse, C.; Marnas, F.; Pelon, J.; Tulet, P., 2013: Characterization of dust emission from alluvial sources using aircraft observations and high-resolution modeling. *J. Geophys. Res.*, 118, 7237–7259. [doi:10.1002/jgrd.50538](https://doi.org/10.1002/jgrd.50538)
- [23] **Schepanski, K.**; Wright, T. J.; **Knippertz, P.**, 2012a: Evidence for flash floods over deserts from loss of coherence in InSAR imagery. *J. Geophys. Res.*, 117, D20101, [doi:10.1029/2012JD017580](https://doi.org/10.1029/2012JD017580).
- [24] **Schepanski, K.**; Tegen, I.; Macke, A., 2012b: Comparison of satellite observations of Saharan dust source areas. *Rem. Sens. Env.*, 123, 90–97. [doi:10.1016/j.rse.2012.03.019](https://doi.org/10.1016/j.rse.2012.03.019)
- [25] Gläser, G.; **Knippertz, P.**; **B. Heinold**, 2012: Orographic effects and evaporative cooling along a subtropical cold front: The case of the spectacular Saharan dust outbreak of March 2004. *Mon. Wea. Rev.*, 140(8), 2520–2533. [doi:10.1175/MWR-D-11-00315.1](https://doi.org/10.1175/MWR-D-11-00315.1)
- [26] Roberts, A.; **Knippertz, P.**, 2012: Haboobs: Convectively generated dust storms in West Africa. *Weather*, 67(12), 311–315. [doi:10.1002/wea.1968](https://doi.org/10.1002/wea.1968)

- [27] **Knippertz, P.**; Todd, M. C., 2012: Mineral dust aerosols over the Sahara: Processes of emission and transport, and implications for modeling. *Rev. Geophys.*, 50, RG1007, [doi:10.1029/2011RG000362](https://doi.org/10.1029/2011RG000362).
- [28] Brindley, H.; **Knippertz, P.**; Ryder, C.; Ashpole, I., 2012: A critical evaluation of the ability of SEVIRI thermal IR RGB rendering to identify dust events. Part A: Theoretical analysis. *J. Geophys. Res.*, 117, D07201, [doi:10.1029/2011JD017326](https://doi.org/10.1029/2011JD017326).
- [29] **Marsham, J. H.**; **Knippertz, P.**; Dixon, N.; Parker, D. J.; Lister, G. M. S., 2011: The importance of the representation of deep convection for modeled dust-generating winds over West Africa during summer. *Geophys. Res. Lett.*, 38, L16803, [doi:10.1029/2011GL048368](https://doi.org/10.1029/2011GL048368).
- [30] Okin, G. S.; Bullard, J. E.; Reynolds, R. L.; Ballantine, J.-A. C.; **Schepanski, K.**; Todd, M. C.; Belnap, J.; Baddock, M. C.; Gill, T. E.; Miller, M. E., 2011: Dust emissions: small-scale processes with global-scale consequences. *EOS, Transactions American Geophysical Union*, 92(29), 241–248, [doi:10.1029/2011EO290001](https://doi.org/10.1029/2011EO290001).
- [31] Johnson, B. T.; Brooks, M. E.; Walters, D.; Woodward, S.; Christopher, S.; **Schepanski, K.**, 2011: Assessment of the Met Office dust forecast model using observations from the GERBILS campaign. *Quart. J. Roy. Met. Soc.*, 137, 1131–1148, [doi:10.1002/qj.736](https://doi.org/10.1002/qj.736).



Re: **ERC-2016-PoC**

Commitment of the host institution

The Karlsruhe Institute of Technology, which is the applicant legal entity, confirms its intention to host and engage with the following 'principal investigator' **Prof. Dr. Peter Knippertz** in which the obligations listed below will be addressed should the proposal entitled **"PACODOM: Parameterising Convective Dust Storms in Operational Forecast Models"** be retained.

Performance obligations of the applicant legal entity that will become the beneficiary of the grant agreement, should the proposal be retained and the preparation of the grant agreement be successfully concluded:

The applicant legal entity commits itself to host and engage the principal investigator for the duration of the grant and to:

- a) ensure that the work will be performed under the guidance of the principal investigator.
- b) carry out the work to be performed, as it will be identified in Annex I and in compliance with the provisions of the ERC Grant Agreement, and all legal obligations under applicable EU, international and national law.

For the host institution (applicant legal entity):

05. Feb. 2016



Prof. Dr. Oliver Kraft
Vice President Research
oliver.kraft@kit.edu



Karlsruher Institut für Technologie



Prof. Dr. Christoph Kottmeier
Head of Institute of Meteorology and
Climate Research -
Troposphere Research
christoph.kottmeier@kit.edu

A Parameterization of Convective Dust Storms for Models with Mass-Flux Convection Schemes

FLORIAN PANTILLON AND PETER KNIPPERTZ

Institut für Meteorologie und Klimaforschung, Karlsruher Institut für Technologie, Karlsruhe, Germany

JOHN H. MARSHAM

Water@Leeds, National Centre for Atmospheric Science, University of Leeds, Leeds, United Kingdom

CATHRYN E. BIRCH

Met Office, University of Leeds, Leeds, United Kingdom

(Manuscript received 20 November 2014, in final form 20 February 2015)

ABSTRACT


Cold pool outflows, generated by downdrafts from moist convection, can generate strong winds and therefore uplift of mineral dust. These so-called haboob convective dust storms occur over all major dust source areas worldwide and contribute substantially to emissions in northern Africa, the world's largest source. Most large-scale models lack convective dust storms because they do not resolve moist convection, relying instead on convection schemes. The authors suggest a parameterization of convective dust storms to account for their contribution in such large-scale models. The parameterization is based on a simple conceptual model, in which the downdraft mass flux from the convection scheme spreads out radially in a cylindrical cold pool. The parameterization is tested with a set of Met Office Unified Model runs for June and July 2006 over West Africa. It is calibrated with a convection-permitting run and applied to a convection-parameterized run. The parameterization successfully produces the extensive area of dust-generating winds from cold pool outflows over the southern Sahara. However, this area extends farther to the east and dust-generating winds occur earlier in the day than in the convection-permitting run. These biases are caused by biases in the convection scheme. It is found that the location and timing of dust-generating winds are weakly sensitive to the parameters of the conceptual model. The results demonstrate that a simple parameterization has the potential to correct a major and long-standing limitation in global dust models.

1. Introduction

In a thunderstorm, the melting, evaporation, and sublimation of hydrometeors generate downdrafts that form a spreading cold pool at low levels (Byers 1949). The cold pool is denser than its environment and therefore spreads as a density current (e.g., Simpson 1999). The cold pool plays a dual role in the life cycle of the

thunderstorm: it increases the low-level atmospheric stability and locally inhibits convection but additionally lifts the surrounding, warmer air and triggers new convective cells (Byers 1949).

The cold pool outflow creates a front of wind gusts at its leading edge. Over arid ground, the wind gusts can be strong enough to lift mineral dust. This process was first documented in peer-reviewed literature for Karthoum and described as “haboob” (Sutton 1925). Since then, haboobs have been reported over all major sources of mineral dust worldwide [see Knippertz (2014), and references therein]. Dust uplift is found in cold pool outflows of different space and time scales: mesoscale convective systems (Houze 2004) can produce long-lived haboobs (Roberts and Knippertz 2014); small, strong downdrafts (microbursts; Fujita 1985) can produce

 Denotes Open Access content.

Corresponding author address: Florian Pantillon, Forschungsbereich Troposphäre, Institut für Meteorologie und Klimaforschung, Karlsruher Institut für Technologie, Kaiserstr. 12, 76128 Karlsruhe, Germany.
E-mail: florian.pantillon@kit.edu

DOI: 10.1175/JAS-D-14-0341.1

© 2015 American Meteorological Society

This proposal version was submitted by Peter KNIPPERTZ on 14/02/2016 18:35:06 Brussels Local Time. Issued by the Participant Portal Submission Service.

short-lived haboobs (Miller et al. 2008); even small cold pools from precipitating congestus can produce dust uplift (Marshall et al. 2009). As all processes are related to convection, they are referred to as convective dust storms.

Convective dust storms of different origins have been observed over the Sahara during recent field campaigns: created by orographic convection over the northwestern Sahara [during the Saharan Mineral Dust Experiment (SAMUM; Knippertz et al. 2007)]; embedded within the monsoon flow over the southern Sahara [during the African Monsoon Multidisciplinary Analysis (AMMA; Flamant et al. 2007; Bou Karam et al. 2008)] and over the western Sahara [during the Geostationary Earth Radiation Budget Intercomparison of Longwave and Shortwave Radiation (GERBILS; Marshall et al. 2008b)]; and over the central Sahara, from locally generated moist convection, as well as mesoscale convective systems that propagate from the Sahel [from Fennec supersite observations (Marshall et al. 2013b; Allen et al. 2013)]. Observational (Marshall et al. 2008b, 2013b) and modeling studies (Heinold et al. 2013) suggest that convective dust storms contribute a large fraction of dust emission over the Sahara in summer. The Sahara is the main source of mineral dust worldwide, and convective dust storms may contribute to the local and remote impacts of Saharan dust on health, oceanic biogeochemistry, and atmospheric dynamics [see Knippertz and Todd (2012) for a review of mineral dust over the Sahara].

Investigating the systematic impact of convective dust storms is challenging: the ground observation network is sparse over the Sahara, and convective clouds often hide dust in satellite observations (Heinold et al. 2013; Kochar et al. 2013). Furthermore, most operational models lack convective dust storms (Marshall et al. 2011; Garcia-Carreras et al. 2013), since they do not explicitly resolve convection and rely on parameterization schemes. Parameterization schemes lack microbursts, because they do not account for subgrid-scale winds. Parameterization schemes also lack mesoscale convective systems, because they do not account for grid-scale organization of convection (e.g., Knippertz and Todd 2012). A parameterization of convective dust storms is needed to account for their contribution to dust uplift in large-scale models.

Several authors have parameterized wind gusts according to convective downdrafts: Nakamura et al. (1996) assumed conservation of horizontal momentum in downdrafts to compute peak wind gusts in numerical weather prediction models; Redelsperger et al. (2000) defined subgrid gustiness as a function of the downdraft mass flux to enhance surface fluxes in global circulation models; Cakmur et al. (2004) scaled a probability

distribution of subgrid wind with the downdraft mass flux to compute dust uplift in global circulation models. Building on these previous studies, we suggest a parameterization of subgrid winds for dust uplift based on the downdraft mass flux of a convective parameterization scheme. Our parameterization aims at remaining simple in order to be applied online or offline to any model with a mass-flux convection scheme. It contrasts with the integrated approach of Hourdin et al. (2014), which improves the representation of wind and dust emissions in a global model—although it does not address the issue of convective dust storms—but requires a complete modification of subgrid parameterization schemes. Our parameterization also complements statistical downscaling methods, which improve dust emissions in global models but still lack the contribution from convective dust storms, such as the one by Ridley et al. (2013).

Section 2 describes the configuration of the model runs used to formulate the parameterization, compares their representation of cold pools and dust-generating winds, and details the reference used to calibrate the parameterization. Section 3 explains and illustrates the conceptual model of the parameterization and its tuning. Section 4 gives the results of the parameterization for both the geographical distribution and diurnal cycle. Finally, section 5 concludes the paper and discusses perspectives for future work.

2. Model runs

a. Configuration

The parameterization of convective dust storms is based on a set of model runs with the Met Office Unified Model. The Unified Model uses a seamless approach, from weather forecast to climate projection and from limited area to global domain (Walters et al. 2011). In the framework of the Cascade project, the model was run in a limited area configuration over West Africa at different spatial resolutions, with and without parameterizations of moist convection and for different time periods during the summer 2006. The Cascade project allowed an investigation of the representation of tropical convection (Pearson et al. 2010, 2014; Birch et al. 2014a), its impact on the monsoon (Marshall et al. 2013a; Birch et al. 2014b), and its impact on dust emission (Marshall et al. 2011; Heinold et al. 2013).

The present study is mainly based on two runs with 4- and 12-km grid spacings for the 60-day period from 1 June to 30 July 2006. Diagnostics for convective mass fluxes, which are essential for the formulation of the parameterization of convective dust storms, were saved during this time period only. Additional runs for the

TABLE 1. Relevant characteristics of the model runs discussed in the text.

Period (days)	Dates	Grid spacing (km)	Vertical levels	Lateral boundaries	Convection	Mass-flux diagnostics
10	25 Jul–3 Aug	1.5	70	4-km run	Explicit	
10	25 Jul–3 Aug	4	70	12-km run	Explicit	
10	25 Jul–3 Aug	12	38	ECMWF analyses	Parameterized	Not available
60	1 Jun–30 Jul	4	70	12-km run	Explicit	
60	1 Jun–30 Jul	12	38	ECMWF analyses	Parameterized	Available

10-day period from 25 July to 3 August 2006 are also discussed, because the model was run at higher resolution with 1.5-km grid spacing for this time period, in addition to the 4- and 12-km grid spacings. As convective mass fluxes were not saved for this 10-day period, the additional runs cannot be used for the parameterization of convective dust storms. The relevant characteristics of the different runs are summarized in Table 1.

The model was run over limited area domains on a rotated cylindrical grid. Figure 1 illustrates the orography, soil fraction, and surface roughness over the 12-km domain. Figure 1a further displays the 4- and 1.5-km domains. Operational analyses from the European Centre for Medium-Range Weather Forecasts (ECMWF) provided the initial conditions and lateral boundaries for the 12-km runs (Table 1). The 12-km runs provided the lateral boundaries conditions for the nested 4-km runs. The 4-km run for the 10-day period, in turn, provided the lateral boundaries for the nested 1.5-km run. Terrain-following hybrid coordinates were used in the vertical, with 70 levels starting at 2.5 m in the 4- and 1.5-km runs and with 38 levels starting at 10 m in the 12-km run (Table 1). The model configuration is detailed in Pearson et al. (2010).

The 1.5- and 4-km runs fundamentally differ in their representation of convection, as compared to the 12-km run: the convection is permitted to develop explicitly with 1.5- and 4-km grid spacings, while it is parameterized with 12-km grid spacing (Table 1). In the Unified Model, the parameterization of moist convection is based on a convective available potential energy (CAPE) closure (Gregory and Rowntree 1990). Following a parcel theory modified by entrainment and detrainment, an ensemble of subgrid convective clouds is described by updraft and downdraft mass fluxes. Updrafts are initiated if a layer is positively buoyant; ascent occurs until the parcel becomes negatively buoyant. In turn, downdrafts are initiated as a fraction of updrafts if a layer is negatively buoyant; descent occurs until the parcel becomes positively buoyant or too close to the surface.

b. Representation of cold pools

Figure 2 compares the representation of cold pools in the 1.5-, 4-, and 12-km runs on 31 July 2006 (10-day period; Table 1). The respective peak of the diurnal cycle of

precipitation is illustrated; it occurs at 1200 UTC in the 12-km run (Fig. 2g), instead of at 1700 UTC in the 1.5- and 4-km runs (Figs. 2a,d). The parameterization scheme triggers convection too early in the 12-km run (Marshall et al. 2013a; Birch et al. 2014b; Pearson et al. 2014), which is a common and well-documented issue in tropical regions (Yang and Slingo 2001; Dai 2006; Nikulin et al. 2012; Bechtold et al. 2014). Note that the three runs are not expected to look the same at any particular time because they are only constrained at the lateral boundaries. The panels in Fig. 2 are used for illustration purposes only.

In both the 1.5- and 4-km runs, convective cells produce strong precipitation above 10 mm h^{-1} (Figs. 2a,d). The evaporation, melting, and sublimation of hydrometeors create cold pools at low levels with temperature contrast above 5 K (Figs. 2b,e). The outflow of cold pools produces strong surface winds above 10 m s^{-1} (Figs. 2c,f). Convective cells produce small, circular cold pools, which grow and merge into larger, more complex structures. In contrast, the convection scheme produces weak precipitation below 10 mm h^{-1} in the 12-km run (Fig. 2g). The evaporation of precipitation is too weak and too widespread to produce distinct cold pools (Fig. 2h). The 12-km run therefore lacks high winds resulting from convective cold pool outflows (Fig. 2i).

This qualitative comparison suggests that the 4- and 1.5-km runs offer a similar representation of convection and strongly contrast with the 12-km run. Earlier studies showed that convection in the 1.5- and 4-km runs occurs with a good timing compared to satellite observations, while convection occurs too early in the 12-km run (Marshall et al. 2013a; Birch et al. 2014b; Pearson et al. 2014). Furthermore, the development and growth of convective organization is weakly sensitive to the resolution between the 1.5- and 4-km runs (Pearson et al. 2014). Weisman et al. (1997) also found that the structure and evolution of mesoscale convective systems varied little between runs with 4- and 1-km grid spacing, although convection was slightly delayed with the coarser grid spacing. In contrast with the 1.5- and 4-km runs, the 12-km run lacks organized convection (Birch et al. 2014a; Pearson et al. 2014) and cold pools (Marshall et al. 2011, 2013a; Heinold et al. 2013).

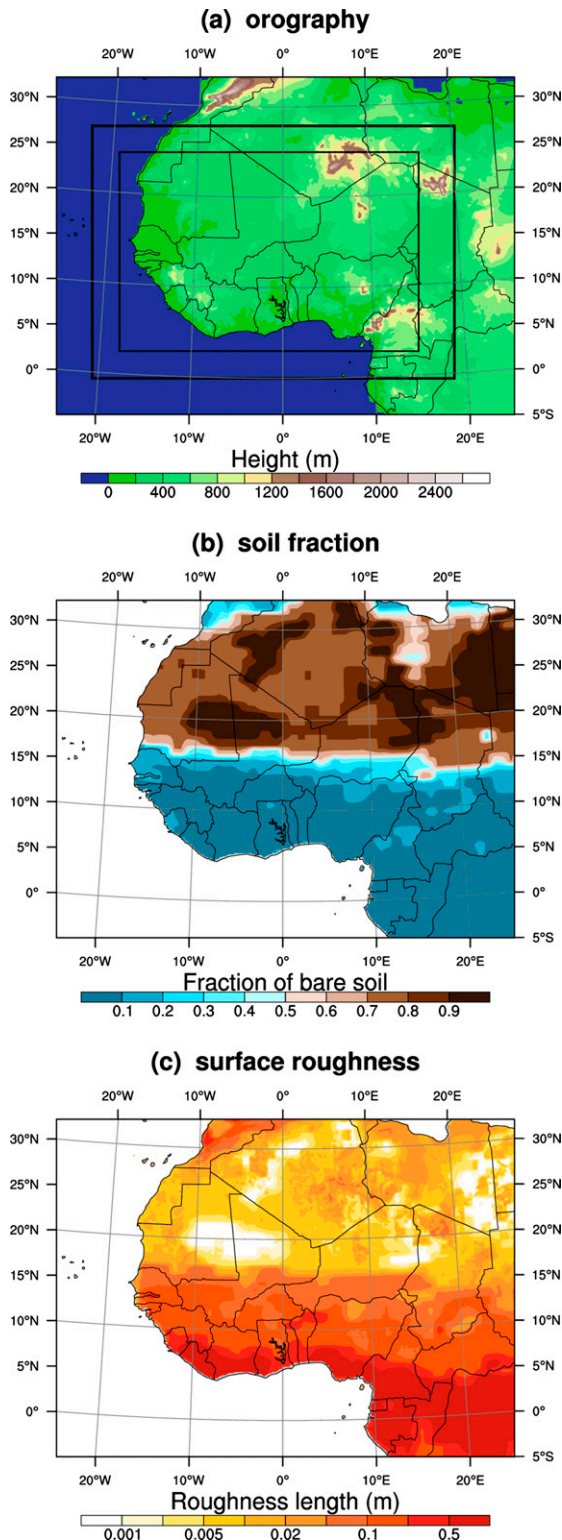


FIG. 1. (a) Orography, (b) soil fraction, and (c) surface roughness in the 12-km run. The thick and thin boxes in (a) show the nested 4- and 1.5-km domains, respectively.

A quantitative comparison is given by the frequency of surface wind speed over the Sahara in the runs during the 10-day period (Fig. 3). While the 12-km-run distribution drops near 12 m s^{-1} , the 4-km run matches the 1.5-km run and captures the tail of distribution up to 20 m s^{-1} . Convective dust storms contribute most of the tail of distribution (not shown). This further supports that the representation of cold pool outflows is similar in the 4- and 1.5-km runs. Johnson et al. (2014) also show that the timing and structure of a convective outflow are successfully represented with a 4-km grid spacing. The 4-km run is then the only available run that explicitly represents convection and captures the cold pool outflows during the 60-day period, for which the convective mass-flux diagnostics were saved (Table 1). As observations are sparse over the Sahara, the 4-km run is used as a reference for the parameterization of convective dust storms. It provides robust statistics with a large number (many hundreds) of convective dust storms that develop during the 60-day period.

c. Dust uplift potential

Dust uplift occurs when the friction velocity reaches a threshold that depends on soil properties, such as mineralogy, roughness elements, and moisture (Marticorena and Bergametti 1995; Shao and Lu 2000). The friction velocity was not saved in the runs. We therefore estimate dust uplift from the 10-m wind speed, which largely controls the friction velocity. Several authors have directly computed the friction velocity from the 10-m wind speed (e.g., Cakmur et al. 2004; Miller et al. 2008; Ridley et al. 2013; Fiedler et al. 2013). Here we follow Marsham et al. (2011) and compute the dust uplift potential (DUP):

$$\text{DUP} = \nu U_{10}^3 \left(1 + \frac{U_t}{U_{10}} \right) \left(1 - \frac{U_t^2}{U_{10}^2} \right), \quad (1)$$

with ν the fraction of bare soil, U_{10} the 10-m wind speed, and $U_t = 7 \text{ m s}^{-1}$ a fixed threshold for dust uplift. DUP isolates the atmospheric control from the soil control on dust uplift and thus can easily be computed offline without a full model for dust emission. Heinold et al. (2013) showed that DUP is largely consistent with both the diurnal cycle and the geographical distribution of dust emission fluxes from such a full model. Marsham et al. (2013b) further showed that DUP correlates with observed dust over the central Sahara.

The geographical distribution of DUP exhibits similar patterns in the 4- and 12-km runs (Fig. 4). Highest DUP is found over the Saharan heat-low region from eastern Mauritania to northern Mali ($18^\circ\text{--}22^\circ\text{N}$, $12^\circ\text{--}2^\circ\text{W}$) and over the Bodélé Depression in northern Chad ($16^\circ\text{--}20^\circ\text{N}$, $15^\circ\text{--}20^\circ\text{E}$). High DUP is found over southwestern Algeria

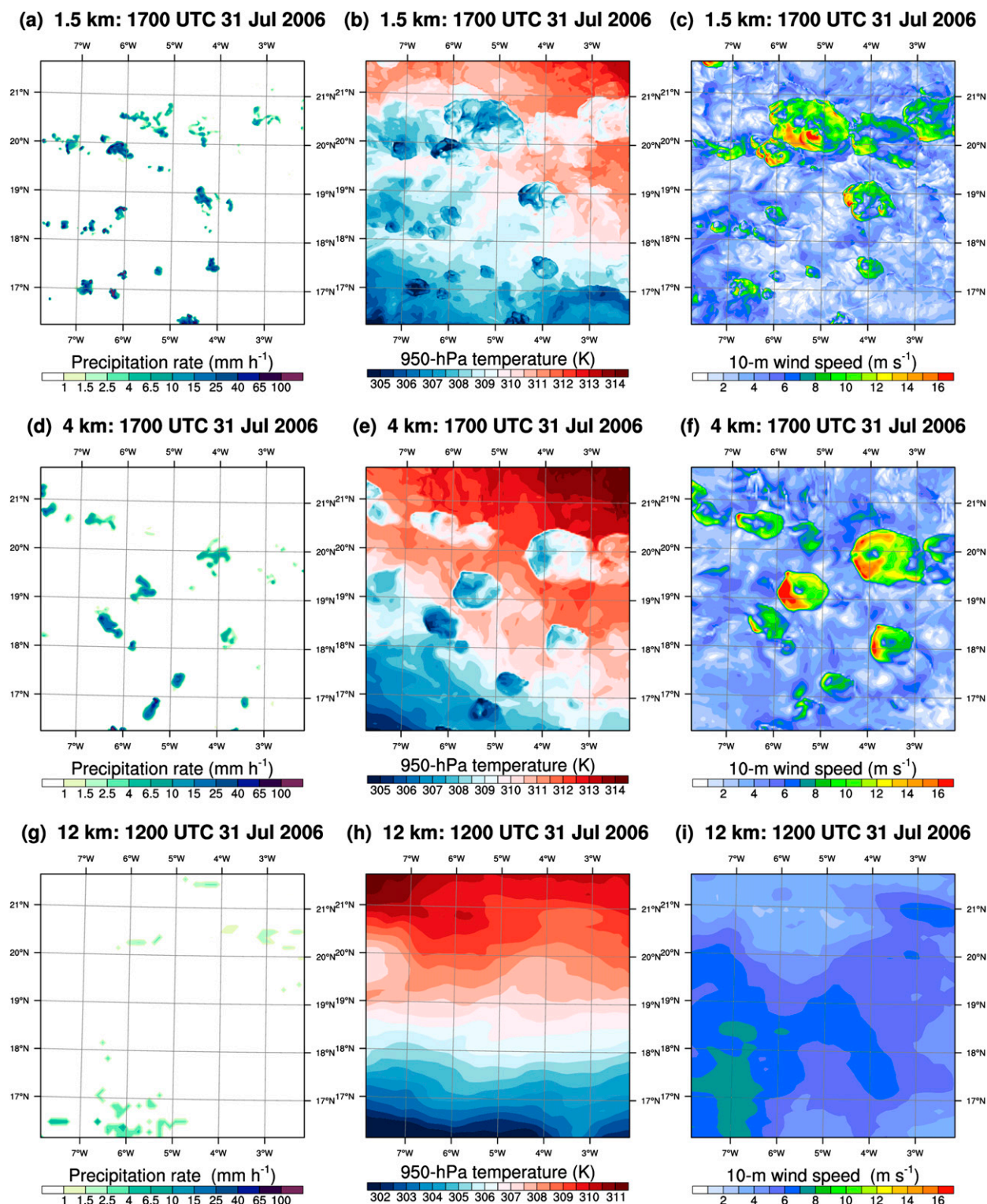


FIG. 2. Example of convection on 31 Jul 2006 in the (a)–(c) 1.5-, (d)–(f) 4-, and (g)–(i) 12-km runs: (a),(d),(g) instantaneous precipitation rate (mm h^{-1}); (b),(e),(h) 950-hPa temperature (K); and (c),(f),(i) 10-m wind speed (m s^{-1}).

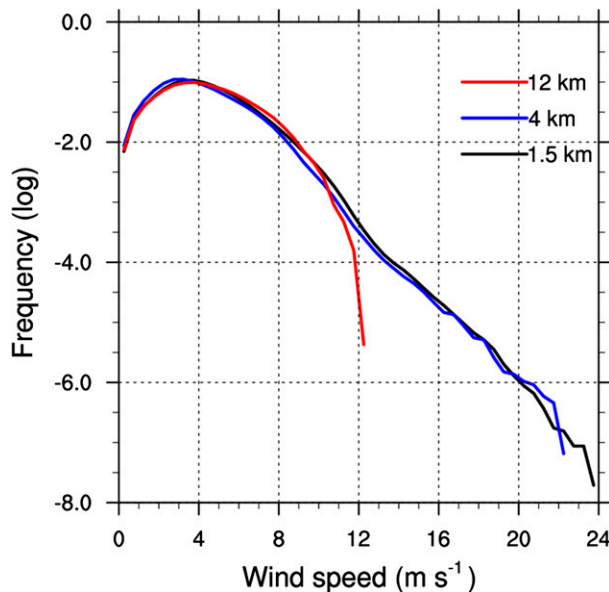


FIG. 3. Probability density function of the 10-m wind speed in the 1.5- (black curve), 4- (blue curve), and 12-km runs (red curve). The wind speed is taken from 25 Jul to 3 Aug 2006 over the area indicated by the boxes in Fig. 4.

(24°–27°N, 5°W–0°), where it is related to the flow around the Hoggar Mountains (Birch et al. 2012) and over northeastern Niger (20°–24°N, 10°–18°E). High DUP is also found along the coast of Mauritania and Western Sahara, where the Atlantic inflow produces strong winds during the afternoon and evening (Grams et al. 2010).

Apart from the Atlantic coast, the areas of high DUP coincide with the areas of highest fraction of bare soil (Fig. 1b). However, the pattern of bare soil does not directly impact the pattern of DUP: omitting ν in Eq. (1) produces a similar pattern of DUP (not shown). Instead, the low roughness length over bare soil (Fig. 1c) allows for strong winds that result in high DUP (Fig. 4). The sharp border in DUP along the Sahel (near 16°N in Fig. 4) matches the strong gradient in roughness length (Fig. 1c). The roughness length increases over mountain ranges, because it accounts for subgrid orography (Fig. 1a). High roughness length prevents strong winds and DUP over the Tibesti (19°–24°N, 16°–20°E) and Hoggar (22°–27°N, 3°–13°E) mountain ranges (Fig. 4).

Figure 5 displays the diurnal cycle of DUP over the Sahara. A strong peak occurs in the morning and is attributed to the breakdown of the nocturnal low-level jet (Knippertz 2008; Fiedler et al. 2013). The 12-km run underestimates the amplitude of the peak compared to the 4-km run (Fig. 5). In contrast, the 12-km run overestimated the amplitude of the peak during the 10-day period, because of a deeper Saharan heat low and, thus, a stronger pressure gradient compared to the 4-km

run (Marsham et al. 2013a; Heinold et al. 2013). Here, the 12-km run exhibits a shallower Saharan heat low than the 4-km run (contours in Fig. 4). This demonstrates how sensitive the monsoon circulation is to the time period and representation of convection in a given model (Marsham et al. 2013a). The weaker pressure gradient in the 12-km run results in weaker nocturnal low-level jets and therefore weaker DUP in the morning compared to the 4-km run (Fig. 5). Heinold et al. (2013) showed that low-level jets can form in aged cold pools such that some of the differences between the two runs may indirectly be related to the lack of organized convection in the 12-km run.

A second, weaker peak in DUP occurs in the afternoon, in both 4- and 12-km runs (Fig. 5). This peak is attributed to dry convection in the boundary layer, which reaches its peak in the afternoon and which was observed to enhance dust uplift (Chaboureaud et al. 2007; Marsham et al. 2008a). DUP then remains high in the evening in the 4-km run, while it drops in the 12-km run. The weaker DUP in the 12-km run was attributed to the lack of convective dust storms in the evening during the 10-day period (Marsham et al. 2011; Heinold et al. 2013). The contribution of convective dust storms to DUP in the 4-km run is discussed below.

d. Identification of convective dust storms

Convective dust storms need to be identified in the 4-km run, which is used as a reference to calibrate the parameterization. Following Heinold et al. (2013), surface winds are attributed to convective dust storms if they occur within 40 km of a grid point of rapid cooling and strong vertical velocities. These conditions are met at the leading edge of cold pool outflows (see example of cold pool outflow in section 3a). Additional conditions in potential temperature and wind divergence suggested by Heinold et al. (2013) were found redundant here with the conditions in cooling and vertical velocity, respectively.

A visual inspection of several cold pool outflows in the 4-km run delivered thresholds $\dot{T}_t = -1 \text{ K h}^{-1}$ for temperature tendency and $|w|_t = 0.5 \text{ m s}^{-1}$ for vertical velocity of updrafts and downdrafts. The 1-h temperature tendency is computed on the 133-m model level and defined as the anomaly with respect to the 5-day average of the diurnal cycle, while the vertical velocity is taken on the 1605-m model level. The choice of 1-h tendency and 5-day average was constrained by the organization of model data, while the choice of model levels was driven by the strongest signature of cold pools in temperature tendency and vertical velocity.

The thresholds are close to those defined by Heinold et al. (2013). Figure 6 shows the diurnal cycle of identified convective dust storms using a range of \dot{T}_t and $|w|_t$. Regardless

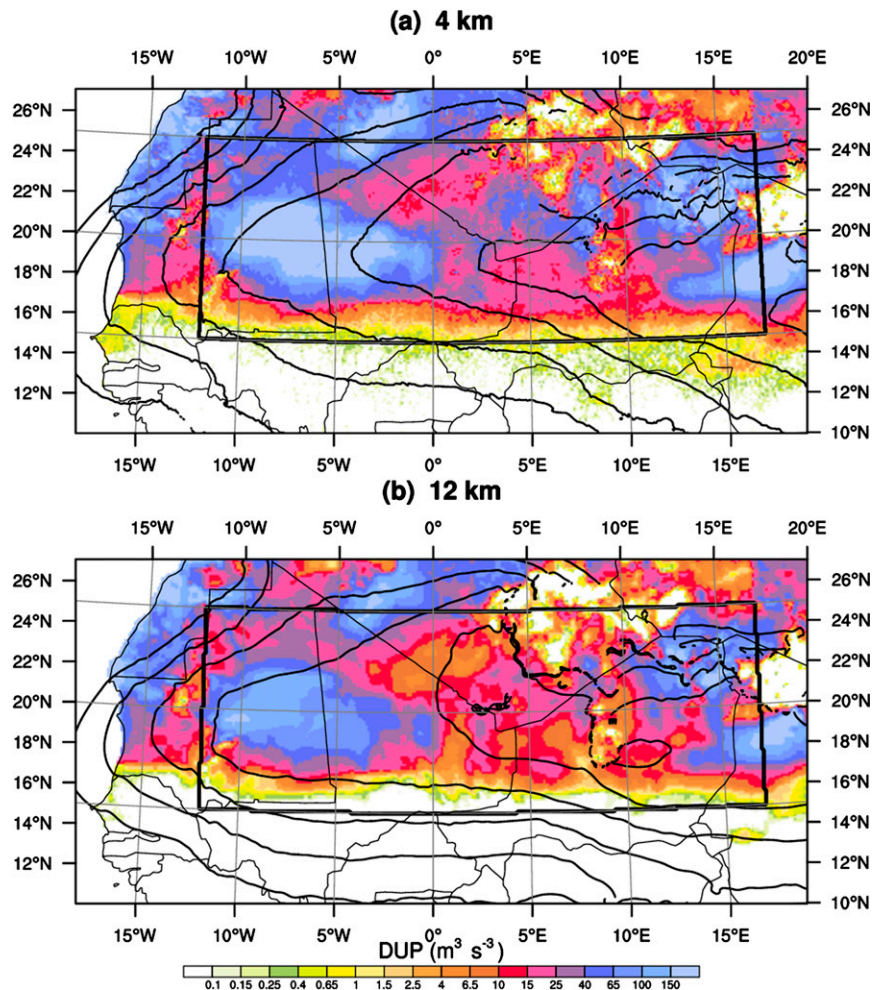


FIG. 4. Dust uplift potential from the model wind (shading; $\text{m}^3 \text{s}^{-3}$) and 925-hPa geopotential height (contours below 790 m; interval of 5 gpm) averaged from 1 Jun to 30 Jul 2006 in the (a) 4- and (b) 12-km runs. The geopotential height is omitted where it lies below the model orography. The displayed area is the northern part of the 4-km domain (Fig. 1). The dust uplift potential is defined in section 2c. The boxes show the area used to compute the probability density function in Fig. 3 and the diurnal cycles in Figs. 5 and 6.

of thresholds, DUP from convective dust storms quickly increases from 1300 UTC to reach its peak at 1800 UTC, consistent with the peak rain at this time (Marshall et al. 2013a; Birch et al. 2014b; Pearson et al. 2014). This contributes to the overall DUP peak in the afternoon (blue curve in Fig. 5). DUP from convective dust storms then declines until 0600 UTC (Fig. 6), when rainfall is low and the strong surface stable layer inhibits cold pool momentum from reaching the surface. A weak peak occurs at 0900 UTC during the breakdown of the nocturnal low-level jet (Fig. 5). This is consistent with cold pool momentum being mixed down to the surface as dry convection erodes the stable layer (Heinold et al. 2013).

Heinold et al. (2013) found low sensitivity to the exact thresholds used. Here, multiplying \dot{T}_t or $|w|_t$ by a factor of

2 increases DUP by 33% and 24%, respectively (red curves in Fig. 6). Dividing \dot{T}_t or $|w|_t$ by a factor of 2 decreases DUP by 42% and 20%, respectively (blue curves in Fig. 6). These results suggest that the uncertainty in the contribution of convective dust storms is on the order of 30%. The uncertainty accounts both for spurious rejection of cold pool outflows and for spurious identification of other processes. While isolated cold pools are distinct, however, their identification is ambiguous when they are embedded in the monsoon flow or evolve into nocturnal low-level jets (Heinold et al. 2013).

3. Conceptual model

To address the problem of lacking cold pool dust emission in models with parameterized convection, we

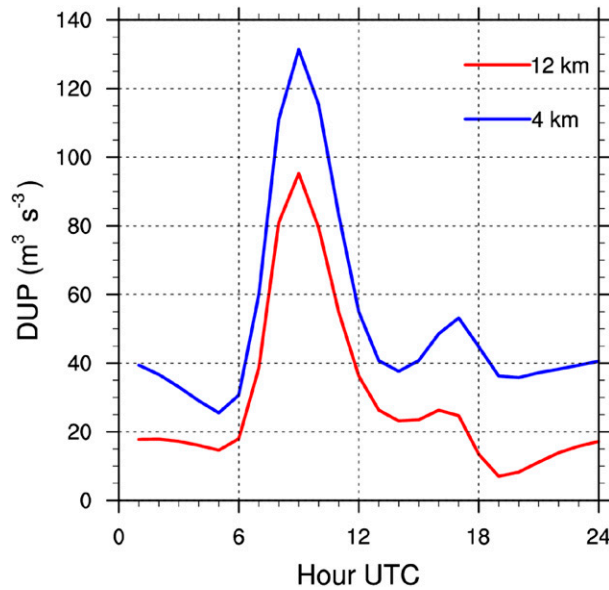


FIG. 5. Diurnal cycle of dust uplift potential from the model wind in the 4- (blue curve) and 12-km runs (red curve). The dust uplift potential is averaged from 1 Jun to 30 Jul 2006 over the area displayed in Fig. 4.

now present the conceptual model on the basis of which our parameterization of convective dust storms is built. Section 3a presents the general formulation, while section 3b shows an illustrative example, which is used to tune the parameterization in section 3c.

a. Formulation

The parameterization is based on the conceptual model of convective dust storms that is illustrated in Fig. 7: the downdraft mass flux M_{dd} (kg s^{-1}) spreads out radially in a cylindrical cold pool of radius R and height h . To ensure conservation of mass, the propagation speed of the cold pool must be

$$C = \frac{M_{dd}}{2\pi R h \rho}, \quad (2)$$

with ρ the average density of the cold pool. The conceptual model matches a developing cold pool in the 4-km run: a strong convective downdraft (Figs. 8b,d) spreads out radially in a cylindrical cold pool and creates strong winds at its leading edge (Figs. 8a,c).

When a cold pool propagates as a density current, its radius increases and its propagation speed decreases.¹ In

¹ The theoretical propagation speed of a cold pool follows $C \propto R^{-1/3} \propto t^{-1/4}$ if the downdraft mass flux is sustained (Parker 1996) and $C \propto R^{-1} \propto t^{-1/2}$ if the downdraft mass flux is stopped at some point (Simpson 1999).

contrast, convective parameterizations assume the quasi equilibrium of subgrid boundary layer processes (Bechtold et al. 2014). A parameterization of propagating subgrid cold pools therefore requires the complete coupling with the parameterization of subgrid convection (Grandpeix and Lafore 2010). Such a coupling is beyond the scope of our work. We rather base our parameterization on a single, static cold pool of representative size (with sensitivity to assumptions of size tested in section 3c). The conceptual model is therefore independent of the model time step if applied online or of the temporal sampling of model output if applied offline.

Surface friction lifts the leading edge of a density current, which forms a “nose” (Simpson 1999). The developing cold pool in the 4-km run exhibits such a nose, with its strongest wind at height $z_{\max} \approx 100$ m (Fig. 8c). Below z_{\max} , turbulence mixes the surface layer. We assume the surface layer has constant potential temperature (i.e., neutral stability) and that below z_{\max} the radial wind speed follows a logarithmic profile:

$$U_r(z) = \frac{u^*}{\kappa} \ln(z_{\max}/z_0), \quad (3)$$

with z the height above ground, u^* the friction velocity, $\kappa = 0.41$ the von Kármán constant, and z_0 the roughness length. Above z_{\max} , the radial wind speed decreases with height (Fig. 8c). While the internal flow of the cold pool is directed forward at low levels, it is directed backward closer to the top levels (Simpson 1999). For simplicity, we assume the radial wind speed decreases linearly with height above z_{\max} and vanishes at height h . The thin black arrows illustrate the vertical profile of the radial wind in Fig. 7.

Combining the logarithmic profile below z_{\max} and the linear profile above, the maximum radial wind speed at the leading edge must satisfy

$$U_r(z_{\max}) = \alpha C \quad (4)$$

at z_{\max} , with

$$\alpha = h \left[z_{\max} \frac{\ln(z_{\max}/z_0) - 1}{\ln(z_{\max}/z_0)} + \frac{1}{2}(h - z_{\max}) \right]^{-1} \quad (5)$$

to ensure conservation of mass. With typical values $z_{\max} = 100$ m and $z_0 = 10^{-3}$ m, α increases from $\alpha \approx 1.1$ for $h = z_{\max}$ to $\alpha = 2$ for $h \gg z_{\max}$; a height $h = 240$ m delivers the value $\alpha = 1.5$ that was observed in thunderstorm outflows (Goff 1976).

Within the cold pool, we assume M_{dd} to be homogeneous. To ensure conservation of mass, the radial wind speed must read

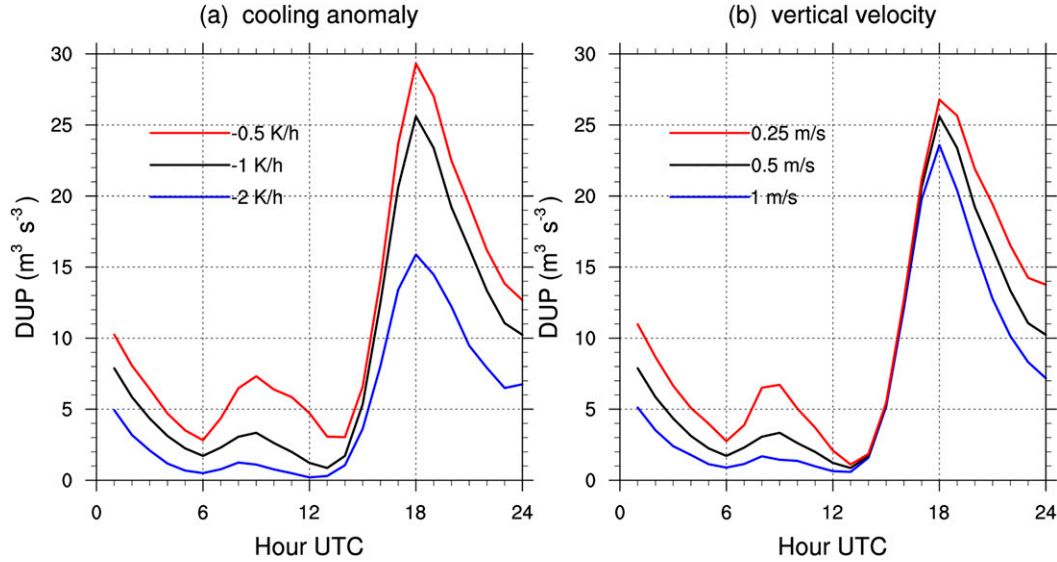


FIG. 6. Diurnal cycle of dust uplift potential attributed to convective dust storms in the 4-km run: sensitivity to thresholds in (a) \bar{T}_t and (b) $|w|_t$. The dust uplift potential is averaged from 1 Jun to 30 Jul 2006 over the area indicated by the boxes in Fig. 4.

$$U_r(r) = \frac{r}{R} U_r(R), \quad (6)$$

with r the distance from the center of the cold pool (thin black arrows in Fig. 7). Based on observations of strong downdrafts, Holmes and Oliver (2000) also used Eq. (6) to describe the wind speed for $r < R$. In addition, they suggested an empirical model of the form

$$U_r(r) = e^{-[(r-R)/R_0]^2} U_r(R) \quad (7)$$

for $r > R$, with $R_0 \approx 0.5R$ a radial length scale. We apply this empirical model to account for the smooth decrease in wind speed beyond the leading edge of the cold pool (Figs. 8a,c).

The developing cold pool in the 4-km run exhibits asymmetric wind speeds (Figs. 8a,c), because the downdraft transports horizontal momentum from higher levels (Figs. 8b,d). Following Parker (1996), we write the steering speed of the cold pool:

$$C_{st} = 0.65 U_{env}, \quad (8)$$

where U_{env} is the environmental steering wind. The relevant layer for U_{env} is where the downdraft originates from and not where it spreads out (Fig. 7). We assume that the steering wind within the cold pool (gray arrows) follows the vertical profile of the radial wind (black arrows). The maximum steering wind therefore reads

$$U_{st}(z_{max}) = \alpha C_{st} \quad (9)$$

at z_{max} , with α given by Eq. (5).

Following Holmes and Oliver (2000), the total wind is obtained from the vector addition of radial and steering wind:

$$\mathbf{U}_{tot}(\mathbf{r}) = \frac{\mathbf{r}}{R} U_r(r) + \mathbf{U}_{st}. \quad (10)$$

The conceptual model does not explicitly account for the vertical wind shear. The wind shear sustains cold pools in organized convective systems (Rotunno et al. 1988) but does not impact the propagation of a cold pool as a density current (Parker 1996).

b. Illustration

Equations (2)–(10) describe the conceptual model. In the following, we apply them to the developing cold pool in the 4-km run (Fig. 8). The downdraft mass flux is computed from the vertical velocity w_{dd} of downdrafts as

$$M_{dd} = \int_A \rho w_{dd} dA, \quad (11)$$

with A the area of the cold pool. The downdraft mass flux reaches its peak $M_{dd} = 1.5 \times 10^9 \text{ kg s}^{-1}$ on the 1605-m model level (Fig. 8b). The average environmental wind within the cold pool reaches $U_{env} = 4.5 \text{ m s}^{-1}$ and blows west-southwestward on the same model level. A visual estimate gives parameters $R = 20 \text{ km}$, $R_0 = 0.33R$ (Fig. 8a), $h = 2 \text{ km}$, and $z_{max} = 100 \text{ m}$ (Fig. 8c); additional parameters are $\rho = 1 \text{ kg m}^{-3}$ and $z_0 = 5 \times 10^{-3} \text{ m}$ in the model run.

Given the estimated parameters, the conceptual model yields $C = 6.0 \text{ m s}^{-1}$ [Eq. (2)], $\alpha = 1.9$ [Eq. (5)],

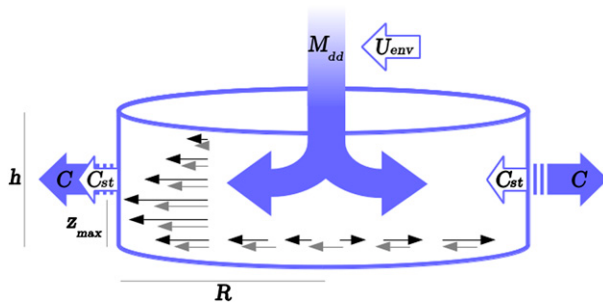


FIG. 7. Schematic of the conceptual model, with M_{dd} as the downdraft mass flux; U_{env} as the environmental steering wind; C and C_{st} as the propagation and steering speeds of the cold pool, respectively; h and R as the height and radius of the cold pool, respectively; and z_{max} as the height of maximum wind. Thin black and gray arrows illustrate the radial and the steering wind within the cold pool, respectively. See section 3a for a detailed discussion.

$U_r(z_{max}) = 11.5 \text{ m s}^{-1}$ [Eq. (4)], and $U_{st}(z_{max}) = 5.7 \text{ m s}^{-1}$ [Eqs. (8) and (9)]. The radial wind at z_{max} is computed from Eqs. (6) and (7); then the total wind at z_{max} is computed from Eq. (10). Finally, the total wind is extrapolated to $z = 10 \text{ m}$ from Eq. (3). Alternatively, the friction velocity can be computed from the total wind in Eq. (3). The total wind is set to vanish at distance $r = R + R_0$ from the center, to avoid the environmental wind extending outside of the cold pool.

Figure 9 illustrates the resulting wind field. The conceptual model captures the asymmetric structure of the cold pool outflow and its magnitude in the 4-km run (Figs. 8a,c). The exact intensity of surface winds can be obtained by tuning the parameters carefully. The strong wind speed along the downdraft at the center of the cold pool (Figs. 8c,d) is lacking in the conceptual model (Fig. 9b), but it does not affect the surface wind. New updrafts and downdrafts at the leading edge of the cold pool (Figs. 8b,d) are also lacking, as expected, in the conceptual model, but they play a minor role during the early development of the cold pool.

The 4-km run exhibits variability in the structure of cold pool outflows (Fig. 2f). The conceptual model does not account for finescale processes that impact the development of cold pools [e.g., surface inhomogeneities; Lothon et al. (2011)]. However, the crescent shape of surface winds (Fig. 9) matches the typical structure of cold pool outflows in the 4-km run (Fig. 2f). This suggests that the simple assumptions of the conceptual model (Fig. 7) deliver a realistic, albeit idealized, representation of cold pool outflows.

c. Tuning

The downdraft mass flux computed from the vertical velocity of downdrafts [Eq. (11)] reaches $M_{dd} = 1.5 \times 10^9 \text{ kg s}^{-1}$ in the developing cold pool of the 4-km run

(Fig. 8). In contrast, the downdraft mass-flux diagnostic computed in the convective parameterization scheme barely reaches $1.5 \times 10^7 \text{ kg s}^{-1}$ over the Sahara in the 12-km run (Fig. 10a). Two reasons explain this difference in magnitude. First, the radius of parameterized convective cells in the 12-km run must be on the order of 1 km to remain of subgrid size, while the radius of the developing cold pool in the 4-km run reaches $R = 20 \text{ km}$. Second, the downdraft mass flux of the convection scheme is typically too weak, because of the lack of explicit representation of subgrid variability. In particular, a more intense downdraft mass flux would overstabilize the lower layers (B. Shipway 2014, personal communication). Cakmur et al. (2004) scaled the downdraft mass flux of the convection scheme with an empirical constant $\beta = 10$ to compute subgrid wind for dust uplift. Following Cakmur et al. (2004), we scale M_{dd} with an arbitrary factor $f = 10$ in the conceptual model, unless stated otherwise.

Several parameters control the wind speed in the conceptual model: R [Eq. (2)], h [Eqs. (2) and (5)], z_{max} [Eqs. (3) and (5)], and R_0 [Eq. (7)]. We constrain the geometry of cold pool outflows to reduce the number of free parameters to one: based on the developing cold pool in the 4-km run (Fig. 8), we set $h/R = 0.1$, $z_{max} = 100 \text{ m}$, and $R_0/R = 0.33$. The parameterization now depends on R only. Using a different constraint on the geometry of the cold pool requires a different tuning of R but weakly impacts the resulting DUP.

The free parameter R is tuned for the average parameterized DUP to match the average reference DUP (the calibration area is discussed in section 4). The parameterized DUP is computed from the parameterized subgrid wind and averaged over the grid cells in the 12-km run, while the reference DUP is computed from the model wind attributed to convective dust storms in the 4-km run. Using a trial-and-error method, the best match of the parameterized DUP with the reference DUP is found for $R = 2.0 \text{ km}$. The constraint on the geometry of cold pools gives $h = 0.2 \text{ km}$. Parameterized downdrafts of subgrid scale spread out in cold pools of subgrid scale as expected. Their radius corresponds to the typical radius of microbursts (Fujita 1985).

An additional, hidden parameter of the conceptual model is the height at which U_{env} is taken. Figure 10b illustrates the distribution of U_{env} over the Sahara at different model levels in the 12-km run. The distribution of U_{env} is computed where M_{dd} is positive only (i.e., where the parameterization will be applied). Increasing the height between 2210 and 4210 m quickly shifts the distribution to stronger U_{env} . The distribution is more stable below and above this range of heights (not shown). This shows that the chosen level strongly impacts the value of U_{env} in the

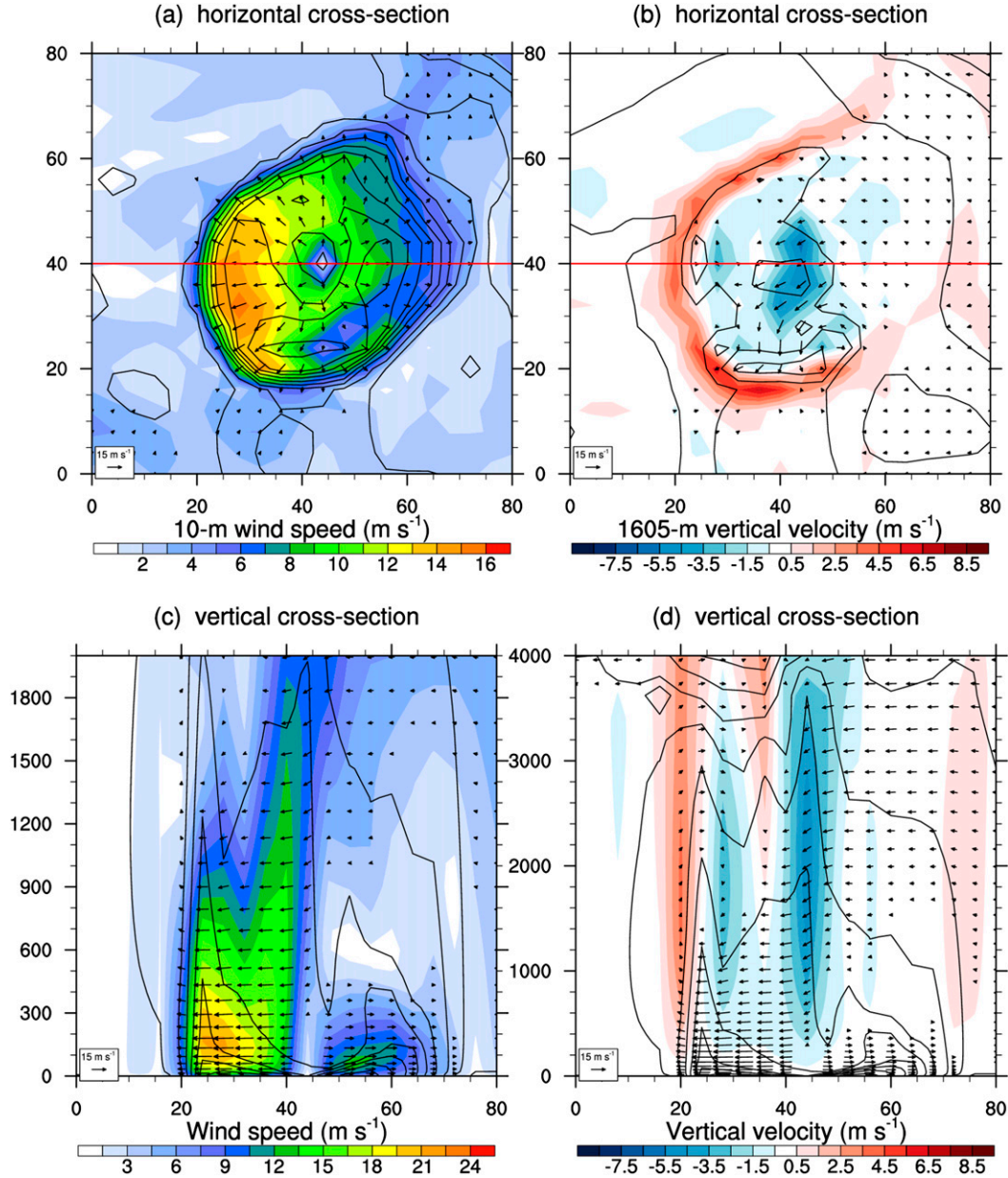


FIG. 8. Example of a cold pool outflow at 1500 UTC 1 Jul 2006 in the 4-km run: (a),(c) wind speed (shading; m s^{-1}) and (b),(d) vertical velocity (shading; m s^{-1}), in (a),(b) horizontal and (c),(d) vertical cross sections, showing the section-parallel wind (vectors above 3 m s^{-1} according to the scale) and potential temperature (contours every 1 K) in the cross sections. Horizontal scales are in kilometers, and vertical scales are in meters. The red lines in (a) and (b) show the trace of (c) and (d), respectively.

parameterization. However, the chosen level weakly impacts the surface wind: a typical $U_{\text{env}} = 5 \text{ m s}^{-1}$ (Fig. 10b) yields $C_{\text{st}} = 3 \text{ m s}^{-1}$ [Eq. (8)]. In comparison, a typical $M_{\text{dd}} = 5 \times 10^6 \text{ kg s}^{-1}$ (Fig. 10a) scaled by $f = 10$ yields $C = 20 \text{ m s}^{-1}$ [Eq. (2)]. The height at which U_{env} is taken is therefore not expected to strongly affect the DUP overall but may impact DUP locally if high U_{env} combines with low M_{dd} . Here, the 3130-m level was chosen

as a compromise between weaker and stronger environmental winds (Fig. 10b).

4. Space and time distribution of convective dust storms

DUP from convective dust storms is first discussed in the 4-km run. Identified convective dust storms produce

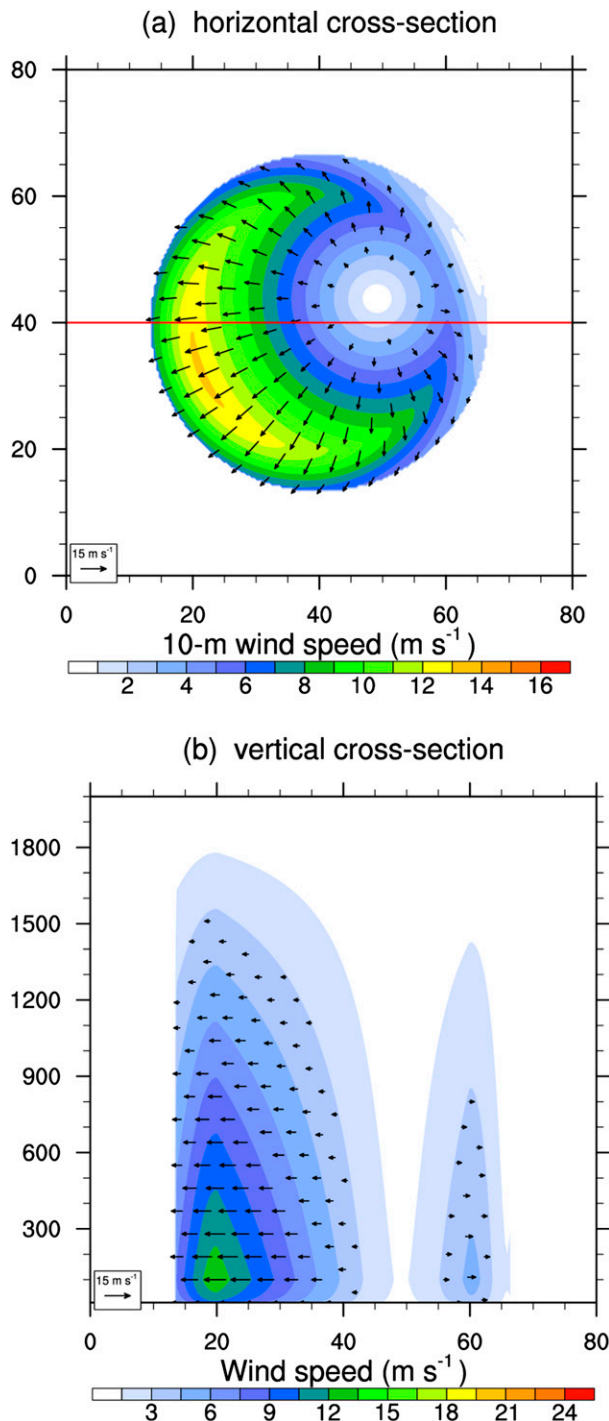


FIG. 9. Parameterization applied to the example of Fig. 8: wind speed (shading; m s^{-1}) and parallel wind (vectors above 3 m s^{-1} according to the scale) in (a) horizontal and (b) vertical cross sections. Horizontal scales are in kilometers, and the vertical scales are in meters. The red line in (a) shows the trace of (b).

DUP over the southern Sahara mainly (around 18°N , Fig. 11a), where the monsoon flow brings the necessary moisture to trigger convection. Highest DUP is found over the Saharan heat low from eastern Mauritania to northern Mali, as for the total DUP (Fig. 4a). In contrast, low DUP is found over the Bodélé Depression in northern Chad and over southwestern Algeria (Fig. 11a), consistent with known wind sources that are not related to cold pools in these regions (Washington and Todd 2005; Birch et al. 2012). Local concentrations of DUP are found over southern Algeria and north-eastern Niger, in the vicinity of mountain ranges (Fig. 4a), consistent with orographic triggering of moist convection.

The parameterization of convective dust storms in the 12-km run succeeds at producing high DUP over the southern Sahara (around 18°N , Fig. 11b). The parameterized DUP is shifted eastward compared to DUP from identified convective dust storms in the 4-km run (Fig. 11a). The eastward shift in the location of DUP is due to the eastward shift in the location of precipitation between the 12- and the 4-km runs (contours in Fig. 11). The location of precipitation is coupled with the pressure gradient of the Saharan heat low (contours in Fig. 4) through the dynamics of the monsoon (Marshall et al. 2013a; Birch et al. 2014b). The parameterized DUP further lacks local concentrations in the vicinity of mountain ranges compared to the 4-km run (Fig. 11) because of the relative lack of moist convection in the vicinity of mountain ranges in the 12-km run.

Although most DUP over the Sahel south of 16°N is attributed to convective dust storms in the 4-km run, it remains small compared to DUP over the Sahara (Figs. 4a and 11a). The parameterized DUP extends farther south across the Sahel (Fig. 11b). This appears more realistic than the sharp border in the 4-km run, as convective dust storms have been observed along a transect around 14°N at the beginning of the monsoon (Marticorena et al. 2010). The high roughness length over the Sahel (Fig. 1c) prevents strong winds in the model runs; it is possibly too high for the beginning of the monsoon, when the vegetation has not yet developed.

High DUP is also attributed to convective dust storms along the coast in the 4-km run (Fig. 11a). The Atlantic inflow is identified as a cold pool outflow, because its front propagates as a density current (Grams et al. 2010). However, the Atlantic inflow does not result from convection; it is therefore excluded from the calibration area (boxes in Fig. 11). The northern and eastern margins of the nested 4-km domain are also excluded from the calibration area to avoid contamination from the lateral boundaries. The calibration area also excludes

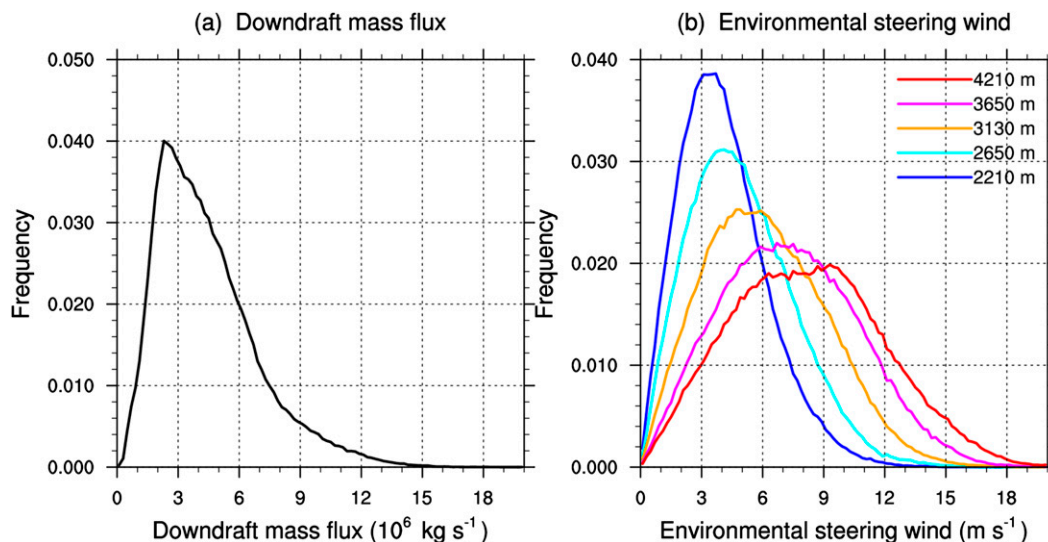


FIG. 10. Schematic of the conceptual model, with M_{dd} as the downdraft mass flux; U_{env} as the environmental steering wind; C and C_{st} as the propagation and steering speeds of the cold pool, respectively; h and R as the height and radius of the cold pool, respectively; and z_{max} as the height of maximum wind.

the area south of 15°N , because the reference 4-km run may underestimate DUP over the Sahel.

As seen in Fig. 6, DUP from convective dust storms exhibits a strong diurnal cycle in the 4-km run (Fig. 12, blue curve). Convective dust storms contribute 27% of the total DUP from 1300 to 0600 UTC and 16% of the total daily DUP over the calibration area displayed in Fig. 11a. The parameterized DUP succeeds at exhibiting a strong diurnal cycle (Fig. 12, red curve). As expected, however, the peak of parameterized DUP occurs at 1200 UTC instead of 1800 UTC in the 4-km run because convection is triggered too early in the 12-km run (Marshall et al. 2013a; Birch et al. 2014b; Pearson et al. 2014). The parameterized DUP then decreases too quickly after the peak since the moist convection is too short lived in the 12-km run. As the parameterization is calibrated with the daily DUP, the amplitude of the peak is overestimated compared to the 4-km run (Fig. 12). Therefore, the main biases in timing and amplitude of DUP are due to biases in the convective parameterization scheme and not to the parameterization of convective dust storms.

5. Conclusions

We suggest a parameterization of convective dust storms for models with mass-flux convection schemes. The parameterization is based on a set of Unified Model runs over West Africa for June and July 2006. It is applied to a convection-parameterized run with 12-km grid spacing, which lacks convective dust storms. A convection-permitting run with 4-km grid spacing

captures the dynamics of convective dust storms and is used as a reference for validation and tuning.

Our conceptual model of convective dust storms follows simple assumptions (Fig. 7). The downdraft mass flux—a known value from the convective parameterization scheme—spreads out radially in a static, cylindrical cold pool. The resulting radial wind adds to the steering wind of the downdraft. Together, they follow a logarithmic profile below the “nose” of the cold pool and decrease linearly with height above. The conceptual model reproduces the structure and magnitude of wind speed for a developing cold pool in the reference run.

The parameterization produces a distribution of subgrid wind in each grid cell of the 12-km run. It is calibrated to match the integrated dust-generating winds [dust uplift potential (DUP)] from identified convective dust storms over the Sahara in the reference run. The geometry of the cold pools is constrained in the parameterization based on a developing cold pool in the reference run. The only free parameter is the radius of the cold pools, which is taken as constant for the whole domain and the whole period. The calibration delivers a radius of 2.0 km, consistent with the subgrid downdraft mass fluxes producing subgrid cold pools.

The parameterization of convective dust storms successfully produces high DUP over the southern Sahara. The parameterized DUP is more spread out than in the reference run: it lacks local concentrations over the central Sahara and extends farther east over the southern Sahara. Over the Sahel, the parameterized DUP extends farther south and appears more realistic than

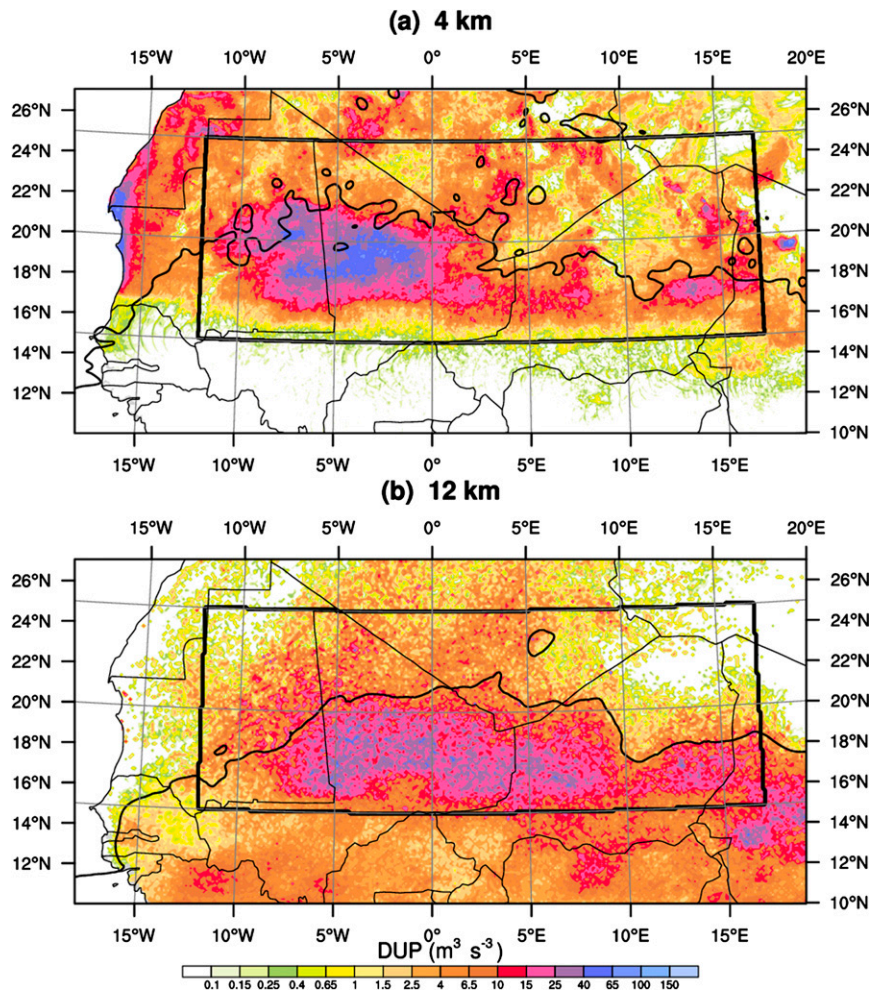


FIG. 11. Dust uplift potential from convective dust storms (shading: $\text{m}^3 \text{s}^{-3}$) and precipitation (smoothed contour at 20 mm) averaged from 1 Jun to 30 Jul 2006 in the (a) 4- and (b) 12-km runs. Convective dust storms are (a) identified in the 4-km run and (b) parameterized in the 12-km run. The boxes show the area used to compute the diurnal cycle in Fig. 12.

the reference run, which shows a sharp border at 16°N. The parameterization of convective dust storms also successfully produces a strong diurnal cycle of DUP. The parameterized DUP peaks 6 h earlier and reaches higher amplitude than in the reference run.

Compared to the reference run, differences in the geographical distribution of parameterized convective dust storms originate from differences in the monsoon flow between the model runs. Differences in the timing of convective dust storms also originate from differences in the timing of convection between the model runs. The dynamics of the West African monsoon (e.g., Marsham et al. 2013a) and the diurnal cycle of tropical convection (e.g., Bechtold et al. 2014) are known issues for modeling and are topics of active research. These issues are separate from the lack of convective dust

storms addressed here, and solving them is beyond the scope of this paper.

The results suggest that the new parameterization allows a useful estimate of dust uplift due to convective dust storms. The distribution and timing of DUP are weakly sensitive to the parameters of the conceptual model if the radius of cold pools is carefully calibrated. The main uncertainty originates from the calibration, which is sensitive to the model resolution, the chosen domain and period, the identification of convective dust storms, and the estimate of dust uplift in the reference run. The uncertainty, however, remains small compared to large uncertainties in the estimation of dust uplift from models and observations (Huneus et al. 2011).

As the parameterization produces a distribution of subgrid wind, it can be implemented in a full model for

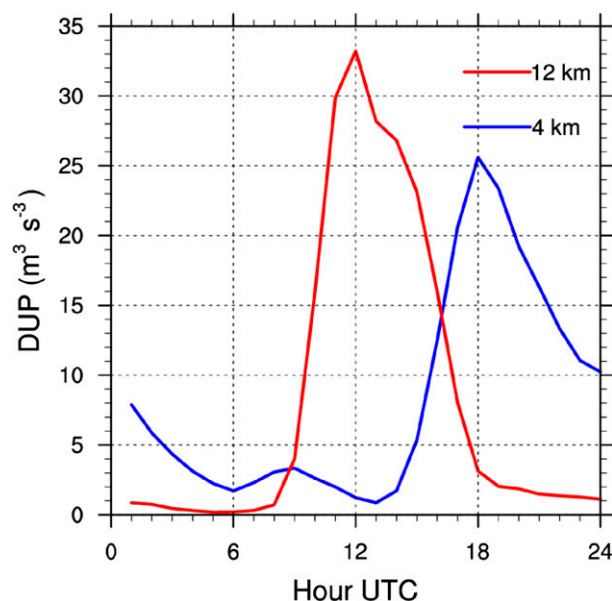


FIG. 12. Diurnal cycle of dust uplift potential from convective dust storms identified in the 4-km run (blue curve) and parameterized in the 12-km run (red curve). The dust uplift potential is averaged from 1 Jun to 30 Jul 2006 over the area indicated by the boxes in Fig. 11.

dust emission. If required, the parameterization can alternatively produce a distribution of subgrid friction velocity. A more accurate estimate of dust uplift can then be used instead of the simple DUP to tune the parameterization for the full model. The uplifted dust will then be transported beyond the grid cell, mixed, or deposited by the meteorology of the model. Through both wetting of the soil and scavenging, convective precipitation within a column may reduce the efficiency of convective dust storms in that column in a full dust model. To account for the spatial separation between the gust front and the precipitation in a realistic convective dust storm, the best approach may be to switch off the soil moisture effect and the scavenging during time steps when the parameterization is activated. A more detailed investigation of this effect is left for future applications in a fully online coupled system.

Further work is needed to test the sensitivity of the parameterization to different periods, grid spacings, and models. Current parameters of the conceptual model may vary: for example, the radius of cold pools, which is expected to increase with increasing grid spacing. Parameterized convective dust storms would have more realistic dimensions with grid spacings on the order of 100 km. Additional parameters may be included in the conceptual model: for example, the vertical wind shear, which is crucial for the organization of convection (Rotunno et al. 1988). If proven

robust, the parameterization will substantially improve the representation of a key ingredient to dust emission and allow studies of the impact of convective dust storms in large-scale weather and climate models that use mass-flux convection schemes.

Acknowledgments. We thank Françoise Guichard and her colleagues at the CNRM in Toulouse for valuable discussions about the parameterization of convective dust storms and Adrian Lock at the Met Office in Exeter for helpful explanations about the boundary layer in the Unified Model. We also thank three anonymous reviewers for their useful comments on an earlier version of this manuscript. This work was funded by ERC Grant 257543 “Desert Storms.” The Cascade project was funded by NERC Grant NE/E003826.

REFERENCES

- Allen, C. J., R. Washington, and S. Engelstaedter, 2013: Dust emission and transport mechanisms in the central Sahara: Fennec ground-based observations from Bordj Badji Mokhtar, June 2011. *J. Geophys. Res. Atmos.*, **118**, 6212–6232, doi:[10.1002/jgrd.50534](https://doi.org/10.1002/jgrd.50534).
- Bechtold, P., N. Semane, P. Lopez, J.-P. Chaboureaud, A. Beljaars, and N. Bormann, 2014: Representing equilibrium and non-equilibrium convection in large-scale models. *J. Atmos. Sci.*, **71**, 734–753, doi:[10.1175/JAS-D-13-0163.1](https://doi.org/10.1175/JAS-D-13-0163.1).
- Birch, C. E., D. J. Parker, J. H. Marsham, and G. M. Devine, 2012: The effect of orography and surface albedo on stratification in the summertime Saharan boundary layer: Dynamics and implications for dust transport. *J. Geophys. Res.*, **117**, D05105, doi:[10.1029/2011JD015965](https://doi.org/10.1029/2011JD015965).
- , J. H. Marsham, D. J. Parker, and C. M. Taylor, 2014a: The scale dependence and structure of convergence fields preceding the initiation of deep convection. *Geophys. Res. Lett.*, **41**, 4769–4776, doi:[10.1002/2014GL060493](https://doi.org/10.1002/2014GL060493).
- , D. J. Parker, J. H. Marsham, D. Copsey, and L. Garcia-Carreras, 2014b: A seamless assessment of the role of convection in the water cycle of the West African Monsoon. *J. Geophys. Res. Atmos.*, **119**, 2890–2912, doi:[10.1002/2013JD020887](https://doi.org/10.1002/2013JD020887).
- Bou Karam, D., C. Flamant, P. Knippertz, O. Reitebuch, J. Pelon, M. Chong, and A. Dabas, 2008: Dust emissions over the Sahel associated with the West African monsoon intertropical discontinuity region: A representative case-study. *Quart. J. Roy. Meteor. Soc.*, **134**, 621–634, doi:[10.1002/qj.244](https://doi.org/10.1002/qj.244).
- Byers, H. R., 1949: Structure and dynamics of the thunderstorm. *Science*, **110**, 291–294, doi:[10.1126/science.110.2856.291](https://doi.org/10.1126/science.110.2856.291).
- Cakmur, R., R. Miller, and O. Torres, 2004: Incorporating the effect of small-scale circulations upon dust emission in an atmospheric general circulation model. *J. Geophys. Res.*, **109**, D07201, doi:[10.1029/2003JD004067](https://doi.org/10.1029/2003JD004067).
- Chaboureaud, J.-P., P. Tulet, and C. Mari, 2007: Diurnal cycle of dust and cirrus over West Africa as seen from Meteosat Second Generation satellite and a regional forecast model. *Geophys. Res. Lett.*, **34**, L02822, doi:[10.1029/2006GL027771](https://doi.org/10.1029/2006GL027771).
- Dai, A., 2006: Precipitation characteristics in eighteen coupled climate models. *J. Climate*, **19**, 4605–4630, doi:[10.1175/JCLI3884.1](https://doi.org/10.1175/JCLI3884.1).

- Fiedler, S., K. Schepanski, B. Heinold, P. Knippertz, and I. Tegen, 2013: Climatology of nocturnal low-level jets over North Africa and implications for modeling mineral dust emission. *J. Geophys. Res. Atmos.*, **118**, 6100–6121, doi:[10.1002/jgrd.50394](https://doi.org/10.1002/jgrd.50394).
- Flamant, C., J.-P. Chaboureaud, D. J. Parker, C. M. Taylor, J.-P. Cammas, O. Bock, F. Timouk, and J. Pelon, 2007: Airborne observations of the impact of a convective system on the planetary boundary layer thermodynamics and aerosol distribution in the inter-tropical discontinuity region of the West African Monsoon. *Quart. J. Roy. Meteor. Soc.*, **133**, 1175–1189, doi:[10.1002/qj.97](https://doi.org/10.1002/qj.97).
- Fujita, T., 1985: The downburst: Microburst and macroburst. Satellite and Mesometeorology Research Project Research Paper 210, Dept. of Geophysical Sciences, University of Chicago, 122 pp.
- Garcia-Carreras, L., and Coauthors, 2013: The impact of convective cold pool outflows on model biases in the Sahara. *Geophys. Res. Lett.*, **40**, 1647–1652, doi:[10.1002/grl.50239](https://doi.org/10.1002/grl.50239).
- Goff, R. C., 1976: Vertical structure of thunderstorm outflows. *Mon. Wea. Rev.*, **104**, 1429–1440, doi:[10.1175/1520-0493\(1976\)104<1429:VSOTO>2.0.CO;2](https://doi.org/10.1175/1520-0493(1976)104<1429:VSOTO>2.0.CO;2).
- Grams, C. M., S. C. Jones, J. H. Marsham, D. J. Parker, J. M. Haywood, and V. Heuveline, 2010: The Atlantic inflow to the Saharan heat low: Observations and modelling. *Quart. J. Roy. Meteor. Soc.*, **136**, 125–140, doi:[10.1002/qj.429](https://doi.org/10.1002/qj.429).
- Grandpeix, J.-Y., and J.-P. Lafore, 2010: A density current parameterization coupled with Emanuel's convection scheme. Part I: The models. *J. Atmos. Sci.*, **67**, 881–897, doi:[10.1175/2009JAS3044.1](https://doi.org/10.1175/2009JAS3044.1).
- Gregory, D., and P. Rowntree, 1990: A mass flux convection scheme with representation of cloud ensemble characteristics and stability-dependent closure. *Mon. Wea. Rev.*, **118**, 1483–1506, doi:[10.1175/1520-0493\(1990\)118<1483:AMFCSW>2.0.CO;2](https://doi.org/10.1175/1520-0493(1990)118<1483:AMFCSW>2.0.CO;2).
- Heinold, B., P. Knippertz, J. Marsham, S. Fiedler, N. Dixon, K. Schepanski, B. Laurent, and I. Tegen, 2013: The role of deep convection and nocturnal low-level jets for dust emission in summertime West Africa: Estimates from convection-permitting simulations. *J. Geophys. Res. Atmos.*, **118**, 4385–4400, doi:[10.1002/jgrd.50402](https://doi.org/10.1002/jgrd.50402).
- Holmes, J., and S. Oliver, 2000: An empirical model of a downburst. *Eng. Struct.*, **22**, 1167–1172, doi:[10.1016/S0141-0296\(99\)00058-9](https://doi.org/10.1016/S0141-0296(99)00058-9).
- Hourdin, F., M. Gueye, B. Diallo, J.-L. Dufresne, L. Menut, B. Marticoréna, G. Siour, and F. Guichard, 2014: Parameterization of convective transport in the boundary layer and its impact on the representation of diurnal cycle of wind and dust emissions. *Atmos. Chem. Phys. Discuss.*, **14**, 27 425–27 458, doi:[10.5194/acpd-14-27425-2014](https://doi.org/10.5194/acpd-14-27425-2014).
- Houze, R. A., Jr., 2004: Mesoscale convective systems. *Rev. Geophys.*, **42**, RG4003, doi:[10.1029/2004RG000150](https://doi.org/10.1029/2004RG000150).
- Huneus, N., and Coauthors, 2011: Global dust model intercomparison in AeroCom phase I. *Atmos. Chem. Phys.*, **11**, 7781–7816, doi:[10.5194/acp-11-7781-2011](https://doi.org/10.5194/acp-11-7781-2011).
- Johnson, R. H., R. S. Schumacher, J. H. Ruppert Jr., D. T. Lindsey, J. E. Rutherford, and L. Kriederman, 2014: The role of convective outflow in the Waldo Canyon fire. *Mon. Wea. Rev.*, **142**, 3061–3080, doi:[10.1175/MWR-D-13-00361.1](https://doi.org/10.1175/MWR-D-13-00361.1).
- Knippertz, P., 2008: Dust emissions in the West African heat trough—The role of the diurnal cycle and of extratropical disturbances. *Meteor. Z.*, **17**, 553–563, doi:[10.1127/0941-2948/2008/0315](https://doi.org/10.1127/0941-2948/2008/0315).
- , 2014: Meteorological aspects of dust storms. *Mineral Dust*, P. Knippertz and J.-B. W. Stuut, Eds., Springer Netherlands, 121–147, doi:[10.1007/978-94-017-8978-3_6](https://doi.org/10.1007/978-94-017-8978-3_6).
- , and M. C. Todd, 2012: Mineral dust aerosols over the Sahara: Meteorological controls on emission and transport and implications for modeling. *Rev. Geophys.*, **50**, RG1007, doi:[10.1029/2011RG000362](https://doi.org/10.1029/2011RG000362).
- , C. Deutscher, K. Kandler, T. Müller, O. Schulz, and L. Schütz, 2007: Dust mobilization due to density currents in the Atlas region: Observations from the Saharan Mineral Dust Experiment 2006 field campaign. *J. Geophys. Res.*, **112**, D21109, doi:[10.1029/2007JD008774](https://doi.org/10.1029/2007JD008774).
- Kocha, C., P. Tulet, J.-P. Lafore, and C. Flamant, 2013: The importance of the diurnal cycle of Aerosol Optical Depth in West Africa. *Geophys. Res. Lett.*, **40**, 785–790, doi:[10.1002/grl.50143](https://doi.org/10.1002/grl.50143).
- Lothon, M., B. Campistron, M. Chong, F. Couvreux, F. Guichard, C. Rio, and E. Williams, 2011: Life cycle of a mesoscale circular gust front observed by a C-band Doppler radar in West Africa. *Mon. Wea. Rev.*, **139**, 1370–1388, doi:[10.1175/2010MWR3480.1](https://doi.org/10.1175/2010MWR3480.1).
- Marsham, J. H., D. J. Parker, C. M. Grams, B. T. Johnson, W. M. F. Grey, and A. N. Ross, 2008a: Observations of mesoscale and boundary-layer scale circulations affecting dust transport and uplift over the Sahara. *Atmos. Chem. Phys.*, **8**, 6979–6993, doi:[10.5194/acp-8-6979-2008](https://doi.org/10.5194/acp-8-6979-2008).
- , —, —, C. M. Taylor, and J. M. Haywood, 2008b: Uplift of Saharan dust south of the intertropical discontinuity. *J. Geophys. Res.*, **113**, D21102, doi:[10.1029/2008JD009844](https://doi.org/10.1029/2008JD009844).
- , C. M. Grams, and B. Möhr, 2009: Photographs of dust uplift from small-scale atmospheric features. *Weather*, **64**, 180–181, doi:[10.1002/wea.390](https://doi.org/10.1002/wea.390).
- , P. Knippertz, N. S. Dixon, D. J. Parker, and G. M. S. Lister, 2011: The importance of the representation of deep convection for modeled dust-generating winds over West Africa during summer. *Geophys. Res. Lett.*, **38**, L16803, doi:[10.1029/2011GL048368](https://doi.org/10.1029/2011GL048368).
- , N. S. Dixon, L. Garcia-Carreras, G. Lister, D. J. Parker, P. Knippertz, and C. E. Birch, 2013a: The role of moist convection in the West African monsoon system: Insights from continental-scale convection-permitting simulations. *Geophys. Res. Lett.*, **40**, 1843–1849, doi:[10.1002/grl.50347](https://doi.org/10.1002/grl.50347).
- , and Coauthors, 2013b: Meteorology and dust in the central Sahara: Observations from Fennec supersite-1 during the June 2011 Intensive Observation Period. *J. Geophys. Res. Atmos.*, **118**, 4069–4089, doi:[10.1002/jgrd.50211](https://doi.org/10.1002/jgrd.50211).
- Marticorena, B., and G. Bergametti, 1995: Modeling the atmospheric dust cycle: 1. Design of a soil-derived dust emission scheme. *J. Geophys. Res.*, **100**, 16 415–16 430, doi:[10.1029/95JD00690](https://doi.org/10.1029/95JD00690).
- , and Coauthors, 2010: Temporal variability of mineral dust concentrations over West Africa: Analyses of a pluriannual monitoring from the AMMA Sahelian Dust Transect. *Atmos. Chem. Phys.*, **10**, 8899–8915, doi:[10.5194/acp-10-8899-2010](https://doi.org/10.5194/acp-10-8899-2010).
- Miller, S. D., A. P. Kuciauskas, M. Liu, Q. Ji, J. S. Reid, D. W. Breed, A. L. Walker, and A. A. Mandoos, 2008: Haboob dust storms of the southern Arabian Peninsula. *J. Geophys. Res.*, **113**, D01202, doi:[10.1029/2007JD008550](https://doi.org/10.1029/2007JD008550).
- Nakamura, K., R. Kershaw, and N. Gait, 1996: Prediction of near-surface gusts generated by deep convection. *Meteor. Appl.*, **3**, 157–167, doi:[10.1002/met.5060030206](https://doi.org/10.1002/met.5060030206).
- Nikulin, G., and Coauthors, 2012: Precipitation climatology in an ensemble of CORDEX-Africa regional climate simulations. *J. Climate*, **25**, 6057–6078, doi:[10.1175/JCLI-D-11-00375.1](https://doi.org/10.1175/JCLI-D-11-00375.1).
- Parker, D. J., 1996: Cold pools in shear. *Quart. J. Roy. Meteor. Soc.*, **122**, 1655–1674, doi:[10.1002/qj.49712253509](https://doi.org/10.1002/qj.49712253509).
- Pearson, K. J., R. J. Hogan, R. P. Allan, G. M. S. Lister, and C. E. Holloway, 2010: Evaluation of the model representation of the

- evolution of convective systems using satellite observations of outgoing longwave radiation. *J. Geophys. Res.*, **115**, D20206, doi:[10.1029/2010JD014265](https://doi.org/10.1029/2010JD014265).
- , G. M. S. Lister, C. E. Birch, R. P. Allan, R. J. Hogan, and S. J. Woolnough, 2014: Modelling the diurnal cycle of tropical convection across the ‘grey zone.’ *Quart. J. Roy. Meteor. Soc.*, **140**, 491–499, doi:[10.1002/qj.2145](https://doi.org/10.1002/qj.2145).
- Redelsperger, J.-L., F. Guichard, and S. Mondon, 2000: A parameterization of mesoscale enhancement of surface fluxes for large-scale models. *J. Climate*, **13**, 402–421, doi:[10.1175/1520-0442\(2000\)013<0402:APOMEO>2.0.CO;2](https://doi.org/10.1175/1520-0442(2000)013<0402:APOMEO>2.0.CO;2).
- Ridley, D. A., C. L. Heald, J. Pierce, and M. Evans, 2013: Toward resolution-independent dust emissions in global models: Impacts on the seasonal and spatial distribution of dust. *Geophys. Res. Lett.*, **40**, 2873–2877, doi:[10.1002/grl.50409](https://doi.org/10.1002/grl.50409).
- Roberts, A. J., and P. Knippertz, 2014: The formation of a large summertime Saharan dust plume: Convective and synoptic-scale analysis. *J. Geophys. Res. Atmos.*, **119**, 1766–1785, doi:[10.1002/2013JD020667](https://doi.org/10.1002/2013JD020667).
- Rotunno, R., J. B. Klemp, and M. L. Weisman, 1988: A theory for strong, long-lived squall lines. *J. Atmos. Sci.*, **45**, 463–485, doi:[10.1175/1520-0469\(1988\)045<0463:ATFSLL>2.0.CO;2](https://doi.org/10.1175/1520-0469(1988)045<0463:ATFSLL>2.0.CO;2).
- Shao, Y., and H. Lu, 2000: A simple expression for wind erosion threshold friction velocity. *J. Geophys. Res.*, **105**, 22 437–22 443, doi:[10.1029/2000JD900304](https://doi.org/10.1029/2000JD900304).
- Simpson, J. E., 1999: *Gravity Currents: In the Environment and the Laboratory*. Cambridge University Press, 262 pp.
- Sutton, L. J., 1925: Haboobs. *Quart. J. Roy. Meteor. Soc.*, **51**, 25–30, doi:[10.1002/qj.49705121305](https://doi.org/10.1002/qj.49705121305).
- Walters, D. N., and Coauthors, 2011: The Met Office Unified Model Global Atmosphere 3.0/3.1 and JULES Global Land 3.0/3.1 configurations. *Geosci. Model Dev.*, **4**, 919–941, doi:[10.5194/gmd-4-919-2011](https://doi.org/10.5194/gmd-4-919-2011).
- Washington, R., and M. C. Todd, 2005: Atmospheric controls on mineral dust emission from the Bodélé Depression, Chad: The role of the low level jet. *Geophys. Res. Lett.*, **32**, L17701, doi:[10.1029/2005GL023597](https://doi.org/10.1029/2005GL023597).
- Weisman, M. L., W. C. Skamarock, and J. B. Klemp, 1997: The resolution dependence of explicitly modeled convective systems. *Mon. Wea. Rev.*, **125**, 527–548, doi:[10.1175/1520-0493\(1997\)125<0527:TRDOEM>2.0.CO;2](https://doi.org/10.1175/1520-0493(1997)125<0527:TRDOEM>2.0.CO;2).
- Yang, G.-Y., and J. Slingo, 2001: The diurnal cycle in the tropics. *Mon. Wea. Rev.*, **129**, 784–801, doi:[10.1175/1520-0493\(2001\)129<0784:TDCITT>2.0.CO;2](https://doi.org/10.1175/1520-0493(2001)129<0784:TDCITT>2.0.CO;2).

Modeling Haboob Dust Storms in Large-Scale Weather and Climate Models

Florian Pantillon¹, Peter Knippertz¹, John H. Marsham², Hans-Jürgen

Panitz¹, and Ingeborg Bischoff-Gauss³

Corresponding author: Florian Pantillon, Institut für Meteorologie und Klimaforschung, Karlsruher Institut für Technologie, Kaiserstr. 12, 76128 Karlsruhe, Germany. (florian.pantillon@kit.edu)

¹Institute of Meteorology and Climate
Research, Karlsruhe Institute of Technology,
Karlsruhe, Germany

²Water@Leeds, National Centre for
Atmospheric Science, University of Leeds,
Leeds, United Kingdom

³Steinbuch Centre for Computing,
Karlsruhe Institute of Technology,
Karlsruhe, Germany

D R A F T

January 14, 2016, 2:57pm

D R A F T

Abstract. Recent field campaigns have shown that haboob dust storms, formed by convective cold pool outflows, contribute a significant fraction of dust uplift over the Sahara and Sahel in summer. However, in-situ observations are sparse and haboobs are frequently concealed by clouds in satellite imagery. Furthermore, most large-scale weather and climate models lack haboobs, because they do not explicitly represent convection. Here a one-year-long model run with explicit representation of convection delivers the first full seasonal cycle of haboobs over northern Africa. Using conservative estimates, the model suggests that haboobs contribute one fifth of the annual dust-generating winds over northern Africa, one fourth between May and October, and one third over the western Sahel during this season. A simple parameterization of haboobs has recently been developed for models with parameterized convection, based on the downdraft mass flux of convection schemes. It is applied here to ~~a set of two~~ model runs with different horizontal resolutions ~~and convection schemes~~, and assessed against the explicit run. The parameterization succeeds in capturing the geographical distribution of haboobs and their seasonal cycle over the Sahara and Sahel. It can be tuned to the different horizontal resolutions ~~and convection schemes but depends on the representation of the monsoon in the parent model. Different formulations are further~~, and different formulations are discussed with respect to the frequency of extreme events. The results show that the parameterization is reliable and may solve a major and long-standing issue in simulating dust storms in large-scale weather and climate models.

D R A F T

January 14, 2016, 2:57pm

D R A F T

1. Introduction

“Haboobs” [Sutton, 1925] are dust storms formed by the cold pool outflows from moist convective storms. Such storms vary in scale from hundreds of metres [Marsham *et al.*, 2009] to hundreds of kilometres [Roberts and Knippertz, 2014]. They are observed over most arid areas around the world, and over the Sahel and Sahara in particular, which are the main sources of mineral dust worldwide [see Knippertz, 2014, for a review]. Recently, the first ever detailed in-situ observations of meteorology and dust over the central Sahara showed that haboobs contribute ~~about~~ at least half of dust emissions in summer [Marsham *et al.*, 2013a; Allen *et al.*, 2013, 2015]. Apart from this and earlier field campaigns over the fringes of the Sahara [Knippertz *et al.*, 2007; Flamant *et al.*, 2007; Bou Karam *et al.*, 2008; Marsham *et al.*, 2008; Marticorena *et al.*, 2010], detailed observations are rare in the region. Haboobs can hardly be distinguished in the sparse surface observations of meteorology and dust, and they are frequently concealed by clouds in satellite imagery [Heinold *et al.*, 2013; Kocha *et al.*, 2013]. Numerical modeling is therefore crucial to better understand the role of haboobs over the Sahara and in the global dust cycle. However, large-scale weather and climate models often lack haboobs, because they rely on parameterization schemes for subgrid convection that do not represent the cold pools and their propagation [Marsham *et al.*, 2011; Garcia-Carreras *et al.*, 2013; Heinold *et al.*, 2013; Largeron *et al.*, 2015; Sodemann *et al.*, 2015]. Statistical parameterizations of subgrid winds can improve the modeling of dust emissions at coarse resolution, but they are not able to represent haboobs [Ridley *et al.*, 2013].

D R A F T

January 14, 2016, 2:57pm

D R A F T

To correct this major and long-standing limitation of large-scale dust models, *Pantillon et al.* [2015, hereafter PKMB15] suggested a simple parameterization of haboobs based on the downdraft mass flux of convection schemes. The parameterization of haboobs requires a model run with explicit convection for calibration. The available model data limited the results of PKMB15 to the western Sahel and Sahara and to the June-July 2006 period. Here, an unprecedented model run with explicit convection over the whole of northern Africa and for the whole year 2006 extends the original work of PKMB15 and offers new perspectives. The new model run allows estimating the seasonal cycle of haboobs and thus testing the parameterization over the different parts of the Sahara, now including the eastern Sahel and Sahara as well as the Atlas Mountains. The parameterization is applied to ~~a set of two~~ model runs with different ~~configurations~~horizontal resolutions, which further allows assessing its sensitivity ~~with respect to the resolution and to the convection scheme of the atmospheric model~~. Different formulations of the parameterization are also discussed to better represent the intensity of haboobs.

Section 2 describes the configuration of the model runs, the estimate of dust-generating winds, the identification of haboobs, and the different formulations of the parameterization. Section 3 evaluates the representation of precipitation and dust-generating winds in the different runs, as compared to satellite and surface observations. Section 4 compares the distribution of explicit and parameterized haboobs in the different model runs and discusses the sensitivity to the model configuration as well as to the formulation of the parameterization. Finally, Section 5 gives the conclusions of the paper and guides the use of the parameterization in large-scale weather and climate models.

D R A F T

January 14, 2016, 2:57pm

D R A F T

2. Data and Methods

2.1. Model Runs

2.1.1. Configuration

This paper is based on one-year-long runs using the model of the Consortium for Small-scale Modeling [COSMO, *Baldauf et al.*, 2011] in Climate Mode (COSMO-CLM). COSMO-CLM is the community model of the German regional climate research. It was run over Africa for the year 2006 using ERA-Interim reanalyses [*Dee et al.*, 2011] as initial and lateral boundary conditions with the different configurations summarized in Table 1.

Based on the configuration of the Coordinated Regional climate Downscaling Experiment [CORDEX; *Panitz et al.*, 2014], COSMO-CLM was run over the whole of Africa in a control run with parameterized convection (hereafter CTRL-P) with 0.44° (about 50 km) grid spacing and in a higher-resolution sensitivity run, also with parameterized convection (hereafter HIRES-P), with 0.22° (about 25 km) grid spacing, both with 35 terrain-following vertical levels. Both runs used the *Tiedtke* [1989] parameterization scheme for moist convection, which is based on a grid-scale moisture convergence closure. The model configuration was identical to that detailed in *Panitz et al.* [2014], except for a shorter time period and for additional model outputs of convective diagnostics.

~~An additional sensitivity run used the ? parameterization scheme for moist convection (hereafter BECH-P), which uses a convective available potential energy (CAPE) closure.~~

In an unprecedented computational effort, COSMO-CLM was also run with 0.025° (about 2.8 km) grid spacing, which allows explicit representation of moist convection and thus of haboobs (hereafter EXPL). Following *Gantner and Kalthoff* [2010], the number

D R A F T

January 14, 2016, 2:57pm

D R A F T

of vertical levels was increased to 50 to better represent tropical deep convection. EXPL was run over a domain spanning almost all of Africa north of the equator (Figure 1). This domain was reduced compared to the other model runs due to high computational costs. Sensitivity runs with 0.44° grid spacing showed that increasing the domain size from northern Africa to the whole of Africa improved the timing of monsoon but did not significantly impact the results overall.

2.1.2. Verification

The Tropical Rainfall Measuring Mission (TRMM) product 3B42 [Huffman *et al.*, 2007] version 7, combining observations from several satellites and from rain gauges, is used to assess the modeled precipitation. It provides 3-hourly, spatially homogeneous observations on a 0.25° horizontal grid.

Surface observations from SYNOP stations are used to assess the modeled wind. They provide 3-hourly observations of 10-m wind averaged over 10 min. Following Cowie *et al.* [2014], reported observations of wind speed above 55 kt (about 28 m s^{-1}) are considered spurious and thus excluded. SYNOP stations are sparse over northern Africa, and over arid zones in particular (see their geographical distribution in Figure 7a). Moreover, the actual frequency of observations varies from region to region, e.g., with night-time observations lacking over most of the Sahel [see Cowie *et al.*, 2014, for a critical discussion of the quality of the SYNOP data over northern Africa]. The observations must therefore be interpreted with caution.

2.1.3. Estimate of Dust-Generating Winds

Dust uplift depends on both atmospheric and soil controls. As the focus here is on the model representation of haboobs and not of dust sources, dust-generating winds are

D R A F T

January 14, 2016, 2:57pm

D R A F T

112 estimated with the dust uplift potential [DUP, *Marsham et al.*, 2011]:

$$113 \quad \text{DUP} = \nu U_{10}^3 \left(1 + \frac{U_t}{U_{10}} \right) \left(1 - \frac{U_t^2}{U_{10}^2} \right), \quad (1)$$

114 with ν the fraction of bare soil, U_{10} the 10-m wind speed, and U_t the threshold for dust
 115 uplift. DUP is based on the parameterization of *Martcorena and Bergametti* [1995] and
 116 isolates the atmospheric control, thus dust uplift over a uniform surface is expected to
 117 depend on DUP only. A station- and season-dependent threshold U_t taken from *Cowie*
 118 *et al.* [2014] is used for the observed winds, while a space- and time-uniform threshold
 119 $U_t = 7 \text{ m s}^{-1}$ taken from *Marsham et al.* [2011] is used for the modeled winds in the
 120 absence of gridded values to use in the model. Although this gives a small mis-match in
 121 the thresholds between observations and model, *Cowie et al.* [2014] shows that it is the
 122 seasonal cycle in winds, not in thresholds, that determines the seasonal cycle in DUP.

123 **2.1.4. Identification of Haboobs**

124 Haboobs are detected in EXPL to tune the parameterization of haboobs in the other
 125 runs. Following *Heinold et al.* [2013], the leading edge of cold pools is automatically
 126 identified by thresholds for rapid cooling and strong updrafts. As in PKMB15, these
 127 thresholds are defined as -1 K h^{-1} on the anomaly in temperature tendency with respect
 128 to the mean diurnal cycle and 0.5 m s^{-1} on the vertical velocity, respectively. The temper-
 129 ature tendency is taken on the 925-hPa pressure level rather than at 2-m height, because
 130 the stable layer can prevent cold pools from reaching the surface at night [*Heinold et al.*,
 131 2013]. The vertical velocity is taken on the 850-hPa pressure level, which shows a strong
 132 signal of updraft during cold pool propagation [e.g., *Knippertz et al.*, 2009; *Roberts and*
 133 *Knippertz*, 2014]. The surface wind is then attributed to a convective storm within 40
 134 km of the identified leading edge of the cold pool. Although this automated identification

D R A F T

January 14, 2016, 2:57pm

D R A F T

largely matches a manual identification, it exhibits sensitivity to the chosen thresholds when the cold pools weakly contrast with their environment [Heinold *et al.*, 2013]. The chosen thresholds are rather conservative and the identification therefore misses some of the haboobs. Sensitivity tests in PKMB15 suggests a relative uncertainty on the order of 30%.

2.2. Parameterization of Haboobs

2.2.1. Original Formulation

Haboobs are parameterized in the 0.44° and 0.22° runs following the conceptual model of PKMB15. The conceptual model is illustrated in Figure 2 and briefly described here. The downdraft mass flux from the convection scheme M_{dd} (kg s^{-1}) spreads out in a cylindrical cold pool that propagates radially with speed

$$C = \frac{M_{dd}}{2\pi R h \rho} \quad (2)$$

with R the radius, h the height, and ρ the density of the cold pool. Within the cold pool, the wind speed increases linearly with increasing radius up to the leading edge R (black arrows in Figure 2), then decreases exponentially with radial length scale R_0 beyond R (not shown). The wind speed also increases logarithmically with increasing height up to the “nose” of the cold pool z_{max} , with a rate depending on the roughness length z_0 , then decreases linearly above z_{max} until it vanishes at height h (black arrows in Figure 2). The cold pool is further steered with speed $C_{st} = 0.65U_{env}$, with U_{env} the environmental wind at the height where M_{dd} originates from. Within the cold pool, the steering wind (gray arrows in Figure 2) follows the vertical profile of the radial wind (black arrows). The total wind is finally obtained as the vector addition of the radial and steering winds. For

the sake of simplicity, the cold pool is considered static between two time steps. Here the parameterization of haboobs is applied offline to hourly model outputs, between which the cold pool is considered static. The conceptual model is thoroughly described in PKMB15.

The parameters of the conceptual model are tuned for the DUP from parameterized haboobs to match the DUP from haboobs identified in EXPL, on average over time and space. Based on an example of a developing cold pool in PKMB15, the parameters are set to $h = R/10$, $R_0 = R/3$, and $z_{max} = 100$ m. In the original formulation, the radius of cold pools R is taken as constant, thus Equation 2 becomes

$$C = \frac{5M_{dd}}{\pi R^2 \rho} \quad (3)$$

and R is the only free parameter. As in PKMB15, M_{dd} from the *Tiedtke* [1989] scheme is further scaled with an arbitrary factor of 10 to reach realistic values. ~~In contrast, M_{dd} from the ? scheme reaches higher values by one order of magnitude and thus does not need to be scaled.~~

2.2.2. Alternative Formulation

While the frequency of DUP from identified haboobs decreases quasi logarithmically (blue curve in Figure 3), the frequency of DUP from parameterized haboobs is skewed, with quicker decrease for low DUP and slower decrease for high DUP in CTRL-P and HIRES-P (solid red and orange curves in Figure 3). In particular, the frequency of extreme DUP is overestimated. ~~The skew is even stronger in BECH-P (solid green curve in Figure 3).~~ To reduce the skew, the surface area of the cold pool πR^2 is taken as proportional to the downdraft mass flux M_{dd} and the vertical velocity of downdrafts w_{dd} is taken as

D R A F T

January 14, 2016, 2:57pm

D R A F T

constant, i.e.,

$$M_{dd} = \pi R^2 \rho w_{dd}. \quad (4)$$

Equation 2 then becomes

$$C = 5w_{dd}, \quad (5)$$

thus the propagation speed is constant and w_{dd} is the only free parameter. Note that M_{dd} still controls the integrated DUP through the surface area of the cold pool πR^2 in Equation 4. The constant propagation speed of cold pools in the alternative formulation is typical of mesoscale convective systems [Houze, 2004], while the constant radius of cold pools in the original formulation is typical of downbursts [Fujita and Byers, 1977], both being observed sources of haboobs.

The alternative formulation successfully reduces the skew and the frequency of extreme DUP in CTRL-P (dashed red curve in Figure 3). However, the alternative formulation weakly impacts on the frequency of DUP in HIRES-P (dashed orange curve in Figure 3) ~~and the improvement is unclear in BECH-P (dashed green curve in Figure 3)~~. Both formulations are therefore retained and compared in the rest of the paper. The parameterized DUP is further limited to $10^4 \text{ m}^3 \text{ s}^{-3}$ with both formulations to prevent too extreme events linked to very intense M_{dd} .

2.2.3. Gust Formulation

Following Nakamura *et al.* [1996], the maximum possible 10-m wind speed from convective gusts $U_{10,conv}$ can be estimated from the downdraft convective available potential energy (DCAPE) and the horizontal momentum carried by a convective downdraft:

$$U_{10,conv} = \sqrt{\alpha \int_0^H 2g \frac{\theta_d - \theta}{\theta} dz + \beta U_H^2} \quad (6)$$

D R A F T

January 14, 2016, 2:57pm

D R A F T

with H the height at which the downdraft starts, g the acceleration due to gravity, θ_d and θ the potential temperature of the downdraft and the environment, respectively, U_H the horizontal wind speed at height H , and α and β two tuning parameters. Although this formulation was originally suggested by *Nakamura et al.* [1996] for convective gusts in the midlatitudes, a similar formulation was suggested by *Grandpeix and Lafore* [2010] to parameterize the propagation speed of subgrid cold pools over Africa.

A parameterization of convective gusts using Equation 6 is integrated in the *Tiedtke* [1989] scheme in COSMO, with the tuning parameter $\alpha = 0.2$ [*Schulz and Heise*, 2003]. The transport of horizontal momentum is not accounted for (i.e., $\beta = 0$) to avoid unrealistic strong gusts in cases of weak convection below a strong jet, and a threshold of 0.015 mm h^{-1} in convective precipitation is required to avoid too frequent gusts in light rain [*Heise*, 2006]. Here, $U_{10,conv}$ was output without any threshold in convective precipitation, because the precipitation can evaporate before reaching the ground in haboobs over the Sahara. DUP is computed from $U_{10,conv}$ using Equation 1 and scaled to match the DUP from identified haboobs on average over time and space. The scaling parameter σ represents the fractional surface of the grid cells over which convective gusts occur. The frequency of DUP with the gust formulation (dotted red and orange curves in Figure 3) matches that of identified dust storms at low DUP (blue curve in Figure 3) but drops at higher DUP and misses the tail of the distribution. ~~The gust formulation is not available for BECH-P, because it is not integrated in the ? scheme in COSMO.~~

3. Evaluation of the Model Runs

The model runs are compared and assessed against available observations for precipitation and wind. The evaluation is focused on the arid and semi-arid regions where

D R A F T

January 14, 2016, 2:57pm

D R A F T

haboobs occur. Six areas ~~of identical size~~ covering the same number of grid cells are defined and discussed in various parts of the paper (Figure 1): 27.5°N-35°N and 15°W-10°E (hereafter the Atlas, which also includes northern Algeria) or 10°E-35°E (hereafter the Mediterranean), 20°N-27.5°N and 15°W-10°E (hereafter the Sahara West) or 10°E-35°E (hereafter the Sahara East), and 12.5°N-20°N and 15°W-10°E (hereafter the Sahel West) or 10°E-25°E (hereafter the Sahel East). Although haboobs also occur over the Arabian Peninsula, the evaluation is restricted to northern Africa.

3.1. Precipitation

The observations exhibit three distinct regimes of precipitation (Figure 4a). First, the tropical regime controlled by the monsoon over the Sahel West and East. Second, the subtropical regime over the Atlas and Mediterranean, with precipitation concentrating on the mountains and on the sea. Third, the dry regime with very weak precipitation over the Sahara West and East. These regimes show different seasonal cycles. The precipitation reaches a strong peak in August over the Sahel West and East (black curves in Figure 5e,f) due to the maximal northward extension of the monsoon. The precipitation reaches a weaker peak in January over the Atlas and Mediterranean (black curves in Figure 5a,b) due to the maximal activity of midlatitude systems. The precipitation finally exhibits both peaks but with weaker amplitude over the Sahara West and East (black curves in Figure 5c,d).

The model runs differ in their representation of the monsoon. The EXPL run captures the northward extension (Figure 4b), as well as the timing but underestimates the amplitude compared to the observations (blue curves in Figure 5e,f). The CTRL-P and HIRES-P runs also capture the northward extension of the monsoon (Figure 4c, d) and better

D R A F T

January 14, 2016, 2:57pm

D R A F T

capture the amplitude but exhibit too early onset and too late retreat (red and orange curves in Figure 5e,f). ~~In contrast, the BECH-P run overestimates both the northward extension (Figure 4e) and the amplitude of the monsoon (green curves in Figure 5e,f).~~

The model runs agree better in the representation of the subtropical regime, as they all underestimate the observed precipitation in fall and winter over the Atlas and Mediterranean (Figure 5a,b). This suggests that the model resolution ~~and the convection scheme~~ play a minor role in the representation of the subtropical compared to the tropical regime. The model runs differ again in the representation of the dry regime over the Sahara West and East, where EXPL and HIRES-P lack any precipitation whereas CTRL-P exhibits tracks of individual systems ~~and BECH-P extends the monsoon far northward~~ (Figures ~~4b-e~~ b-d and 5c,d).

The observations exhibit a clear diurnal cycle of precipitation (black curve in Figure 6). They reach a peak in the afternoon when convection is triggered, then decrease slowly in the evening when organized convective systems propagate, and decrease quicker in the morning when the systems disaggregate. This diurnal cycle is mainly influenced by the tropical regime, since the diurnal cycle exhibits a smaller amplitude in the subtropical and dry regimes (see Figure S1 for the diurnal cycle of precipitation over each area). Note that the area-averaged diurnal cycle in Figure 6 is ~~not expected to be found at any single location~~ a composite of local diurnal cycles that strongly vary geographically, as organized convective systems tend to form over mountain ranges and propagate to the west [*Fink and Reiner, 2003; Laing et al., 2008*].

~~Apart from BECH-P, the model runs~~ The model runs strongly contrast with the observations and exhibit a surprisingly similar diurnal cycle of precipitation consider-

D R A F T

January 14, 2016, 2:57pm

D R A F T

ing their different representation of convection. The EXPL run exhibits a diurnal cycle of weak amplitude, where precipitation slowly increases in the afternoon and evening to peak at night (blue curve in Figure 6). ~~This~~ The delay compared to the observations (black curve in Figure 6) suggests that the lifetime of organized convective systems is overestimated in EXPL (V. Maurer, manuscript in preparation, ~~2015~~2016). The CTRL-P and HIRES-P runs peak at noon (red and orange curves in Figure 6), which is expected with parameterized convection. However, the precipitation also increases in the evening and at night. ~~Finally, BECH-P exhibits a primary peak at noon but also a secondary peak at night.~~ The modeled diurnal cycles in Figure 6 are also influenced by the tropical regime mainly but are found in the other regimes as well, albeit with smaller amplitude (see Figure S1 for the diurnal cycle of precipitation over each area).

3.2. Dust Uplift Potential

The density of the SYNOP network drops over arid zones, thus some single stations are crucial to capture the relevant processes for dust emission. In particular, the station of Faya in northern Chad exhibits the highest observed DUP (18°N, 19°E in Figure 7a). Faya is located in the Bodélé Depression, which is known as a major source of dust due to the strong low-level jet in winter and spring [Washington and Todd, 2005]. The station of Bordj Badji Mokhtar in southern Algeria also exhibits high observed DUP (21°N, 1°E in Figure 7a). Bordj Badji Mokhtar is located close to the center of the Saharan heat low in summer, which is also a major source of dust [Marsham et al., 2013a; Allen et al., 2013, 2015]. Further stations exhibit high DUP over northeastern Sudan and over central Algeria, as well as near the Atlantic and Mediterranean coasts. In contrast, the stations exhibit lower DUP over the western Sahel and over the Libyan Desert (Figure 7a).

D R A F T

January 14, 2016, 2:57pm

D R A F T

The model runs capture the observed pattern of DUP overall but differ regionally. They succeed in exhibiting highest DUP over the Bodélé Depression around Faya, high DUP over central Algeria and near the Atlantic and Mediterranean coasts, as well as low DUP over the Libyan Desert (Figure 7b-e). In contrast, the model runs locally fail in exhibiting high DUP, e.g., over the southern Sahara around Bordj Badji Mokhtar. The model runs furthermore overestimate DUP over the western Sahel, where the match between the sharp meridional gradient in modeled DUP and in roughness length (contours in Figure 1) suggests a too low roughness length in the model (see also Figure S2 for a scatter plot of DUP between observations and EXPL subsampled at SYNOP stations). Beyond the geographical pattern, the magnitude of DUP increases with increasing model resolution (Figure 7c,d), in particular over mountain ranges (contours), and decreases when convection is parameterized with the ? scheme instead of the Tiedtke [1989] scheme (Figure 7e).

The observed and modeled DUP are further compared with respect to their seasonal and diurnal cycles. To compensate for the varying density of SYNOP stations between the different areas, the observed DUP is first averaged between the stations of each area then between the areas. The observed DUP is scaled with the fraction of land over each area. The observed DUP is aggregated over each area and scaled with the fraction of land for comparison with the modeled DUP. Although the comparison is affected by the density of stations and the frequency of observations, results are consistent with subsampling the modeled wind to the location and time of observations (see Figure S3 for the correlation of seasonal and diurnal cycles of DUP between observations and EXPL subsampled at SYNOP stations). As dust uplift is unlikely on elevated ground, elevations over 800 m

D R A F T

January 14, 2016, 2:57pm

D R A F T

are excluded from the modeled DUP. They are, however, included in the observed DUP, because 4 SYNOP stations are concerned only. Among them is the crucial station of Bordj Badji Mokhtar, which is located at 816 m above sea level, but which elevation remains below 800 m in the model orography (contours in Figure 7b-e). ~~Although the comparison is biased by the density of stations and the frequency of observations, results are consistent with subsampling the modeled wind to the location and time of observations (see Figure S2 for the correlation of seasonal and diurnal cycles of cubed wind between SYNOP observations and EXPL run).~~ b-d).

The observed DUP reaches a strong seasonal peak in winter over the Sahel East (black curve in Figure 8f) due to the contribution of the strong low-level jet, in Faya in particular. It also reaches a seasonal peak in winter over the Atlas and Mediterranean (black curves in Figure 8a,b) due to midlatitude systems such as lee cyclones over the Atlas and Sharav cyclones [Alpert and Ziv, 1989] over the Mediterranean. In contrast, the observed DUP reaches a seasonal peak in summer over the Sahara West (black curve in Figure 8c), which matches the monsoon cycle (Figure 5c). ~~The observed DUP finally~~ Finally, the observed DUP exhibits a rather flat seasonal cycle over the Sahara East and Sahel West (Figure 8d,e). In the diurnal cycle, the observed DUP reaches a peak in the morning (black curve in Figure 9) due to the downbreak of the nocturnal low-level jet [Fiedler et al., 2013], then slowly decreases in the afternoon due to dry convection in the boundary layer [Parker et al., 2005] and remains low at night due to the stable layer inhibiting strong surface winds (see Figure ~~S3~~ S4 for the diurnal cycle of DUP over each area).

The model runs capture the observed morning peak and its slow decrease in the diurnal cycle of DUP, although delayed, and again with magnitude depending on the model

D R A F T

January 14, 2016, 2:57pm

D R A F T

334 resolution ~~and convection scheme~~ (Figure 9). However, the model runs lack the observed
335 winter peak in the seasonal cycle of DUP over the Sahel East (Figure 8f), which suggests
336 that they underestimate the contribution of the low-level jet [see *Fiedler et al.*, 2013, for a
337 discussion of the representation of the nocturnal low-level jet and its breakdown in models].
338 The model runs also lack the observed winter peak over the Atlas and Mediterranean
339 (Figure 8a,b), which suggests that they underestimate the contribution of midlatitude
340 systems to DUP. The model runs better match the observations over the Sahara West,
341 where they reach a seasonal peak in summer (Figure 8c). The model runs also reach a
342 seasonal peak in summer over the Sahel West (Figure 8e), which strongly overestimates
343 the observed DUP and again suggests a too low roughness length in the model (contours
344 in Figure 1).

3.3. Discussion

345 The strong circulation of the Saharan heat low, as well as monsoon surges, contribute
346 to the summer peak in DUP over the Sahara West (Figure 8c). In addition, further
347 processes also contribute to the summer peak in modeled DUP. Mesoscale convective
348 systems produce strong surface winds at the leading edge of cold pools (Figure 10a).
349 Although they are driven by moist convection, they generally do not produce surface
350 precipitation over the Sahara, where the evaporation is too strong. Mesoscale convective
351 systems are found in EXPL only, because their formation and propagation require the
352 explicit representation of convection [*Marshall et al.*, 2011; *Garcia-Carreras et al.*, 2013;
353 *Heinold et al.*, 2013; *Largerone et al.*, 2015; *Sodemann et al.*, 2015].

354 The parameterized runs also exhibit some organization of convection but mostly with
355 weak surface winds. However, cases of extreme surface winds created by deep cyclones

D R A F T

January 14, 2016, 2:57pm

D R A F T

are found in CTRL-P and HIRES-P (Figure 10b). The deep cyclones form in August and September over the Sahel and migrate westward then northwestward into the Sahara. The single case illustrated here contributes most of the September DUP over the Sahel West and Sahara West in CTRL-P. A few of such cyclones are also responsible for the precipitation over the Sahara West in CTRL-P (Figure 4c) and for the peak in September over the Sahel West in CTRL-P and HIRES-P (Figure 5e).

At first sight, the modeled deep cyclones match the concept of Soudano-Saharan depressions, whose exact definition and meteorological characteristics are somewhat unclear [Schepanski and Knippertz, 2011]. They also exhibit similarities with tropical cyclones, which can form in August and September from African easterly waves, but exclusively offshore [e.g., Berry and Thorncroft, 2005]. We therefore suggest that the deep cyclones are a model artifact and are due to the failure of the convective parameterization in releasing the atmospheric instability through mesoscale convective systems. ~~This is consistent with such cyclones not being found in BECH-P, which uses a different convective parameterization (Table 1).~~ The convective parameterization contributes little to the precipitation associated with the deep cyclones, which thus only weakly affect the parameterization of haboobs.

4. Haboobs in the Model Runs

The spatial distribution, seasonal and diurnal cycles of haboobs are given here for the different model runs. The identified haboobs are first discussed in the EXPL run and compared to those observed during field campaigns. The parameterized haboobs are then discussed for the ~~other~~ CTRL-P and HIRES-P runs, using the different formulations of the parameterization, and compared to those identified in EXPL.

D R A F T

January 14, 2016, 2:57pm

D R A F T

4.1. Explicit Haboobs

The EXPL run exhibits high DUP from haboobs in relation with both orographic convection and the monsoon flow. Highest DUP is found in the Atlas area, over the mountain range itself and over the southern foothills (Figure 11a). High DUP is also found over a wide region in the Sahel West area, over the Hoggar Mountains in the Sahara West, and over Sudan in the Sahel East area. In contrast, low DUP is found in the dry Sahara East and Mediterranean areas, as well as over the southern part of the Sahel West area. As in the DUP from the model's total wind (Figure 7), a sharp meridional gradient over the Sahel West (Figure 11a) matches that in roughness length (contours in Figure 1).

To some extent, the pattern of DUP from haboobs (Figure 11a) matches the pattern of total DUP (Figure 7b), with high DUP over the Atlas and the Sahel West, and low DUP over the Sahara East. The contribution of haboobs to the total DUP, however, contrasts between the areas and is generally higher where the total DUP is higher (~~white contours in Figure 11a~~[Figure 11f](#)). It reaches 28 % over the Sahel West but 9 % only over the Sahara East, and 18 % on average over all areas (Table 2). The contribution of haboobs is higher during the May-October period, when it reaches 24 % on average and up to 33 % over the Sahel West. As in the seasonal and diurnal cycles, elevations below 800 m only are considered here.

Haboobs exhibit a strong seasonal cycle in EXPL, with high activity in spring and summer in the different areas. In the Atlas area, DUP reaches a primary peak in May and a secondary peak in July (blue curve in Figure 12a). Haboobs in the area are related to upper-level troughs from the midlatitudes, which reduce the atmospheric stability and favor convection [*Knippertz et al.*, 2007]. The low DUP in the Mediterranean and Sahara

D R A F T

January 14, 2016, 2:57pm

D R A F T

East areas exhibits similar seasonal cycles but with much smaller amplitudes (blue curves in Figure 12b,d). Over the Sahel West and East and the Sahara West, the seasonal cycle is controlled by the monsoon. DUP in the Sahel West quickly increases in May to reach a primary peak in June during the monsoon onset, then reaches a secondary peak in August during the monsoon maximum before quickly decreasing in September during the monsoon retreat (blue curve in Figure 12e). The August peak has larger amplitude than the June peak in the Sahara West and Sahel East areas, where the monsoon flow arrives later in the season (blue curves in Figure 12c,f). The different areas exhibit similar diurnal cycles of DUP, which increases in the afternoon to reach a peak or a plateau in the evening, then decreases at night (blue curve in Figure 13; see Figure [S4-S5](#) for the diurnal cycle of haboobs over each area).

These results are consistent with the available observations of haboobs, although the modeled DUP and the observed frequency of storms are different diagnostics and thus can be compared qualitatively only. Several haboobs were observed in May-June 2006 over southern Morocco during the Saharan Mineral Dust Experiment (SAMUM) field campaign [*Knippertz et al.*, 2007]. Frequent cold pools from moist convection were further observed over the area in May-September during the 2002-2006 period [*Emmel et al.*, 2010] at surface stations of the Integrated Approach to the Efficient Management of Scarce Water Resources in West Africa (IMPETUS) project. The highest activity was observed in August and attributed to the midlevel transport of moisture from the Sahel [*Knippertz et al.*, 2003; *Knippertz*, 2003]. These results were confirmed when the study was extended to the 2002-2012 period and to northern Algeria and Tunisia [*Redl et al.*, 2015]. They validate the high DUP found over the Atlas in EXPL (Figure 11a). The relatively low

D R A F T

January 14, 2016, 2:57pm

D R A F T

modeled activity in August (blue curve in Figure 12a) may be due to a lack of moisture transport from the Sahel in the model or to a lower activity in August 2006 compared to other years.

Over the Sahel West, haboobs were observed in June 2006 during the African Monsoon Multidisciplinary Analysis (AMMA) field campaign [*Flamant et al.*, 2007; *Bou Karam et al.*, 2008]. Intense haboobs were further observed over the area from the end of May to the end of July during the 2006-2008 period at the AMMA Sahelian Dust Transect of 3 stations aligned around 14°N [*Marticorena et al.*, 2010]. The majority of the haboobs were observed in the evening, which is consistent with high evening DUP in EXPL (blue curve in Figure 13). These results also validate the primary peak in modeled DUP in June (blue curve in Figure 12e). The secondary peak in modeled DUP in August suggests a too weak seasonal cycle of roughness length in the model.

To the best of the authors' knowledge, haboobs were not documented over the other areas in 2006, thus the modeled DUP is assessed against observations from other years. Over the Sahara West, haboobs were observed at Bordj Badji Mokhtar in June 2011 and 2012, at night mostly [*Marsham et al.*, 2013a; *Allen et al.*, 2013, 2015]. This is consistent with the secondary peak in modeled DUP in June (blue curve in Figure 12c) and with the higher modeled DUP between 18 and 06 UTC (blue curve in Figure 13). In contrast with Bordj Badji Mokhtar, few haboobs were observed at Zouerate, northern Mauritania, in June 2011 [*Todd et al.*, 2013], which is also consistent with the lower modeled DUP over that region (Figure 11a). Over the Sahel East, the first climatology of haboobs reported cases over Khartoum between May and October and highest activity in June [*Sutton*, 1925]. This agrees with the modeled activity from May to September but

D R A F T

January 14, 2016, 2:57pm

D R A F T

contrasts with the modeled peak in August (blue curve in Figure 12f). This also suggests a too weak seasonal cycle of roughness length in the model, although the 1916-1923 period documented by *Sutton* [1925] may not be comparable to 2006. Finally, the low DUP over the Sahara East and the Mediterranean areas (blue curves in Figure 12b,d) is consistent with the extreme dryness of the Libyan Desert [e.g., *O'Hara et al.*, 2006] and thus the lack of moist convective storms.

The modeled DUP in EXPL can also be compared to the modeled DUP in the run with explicit convection used in PKMB15. This run was performed with the UK Met Office Unified Model [*Walters et al.*, 2011] using a 4-km grid spacing over the western Sahel and Sahara for the June-July 2006 period (hereafter the 4-km run). The EXPL and 4-km runs agree on the high DUP from haboobs over northern Mali, while high DUP over the Hoggar at Air Moutains is found in EXPL only (compare Figure 11a here with Figure 11a in PKMB15), which suggests stronger orographic convection in EXPL than in the 4-km run. The two runs differ in the location of the sharp meridional gradient in DUP, which is again closely related to the pattern of roughness length (compare the contours in Figure 1 with Figure 1c in PKMB15). Despite the differences in the spatial distribution, the two runs compare well in the contribution of haboobs to the total DUP, with 16 % in the 4-km run (PKMB15) and 22 % in EXPL over the same area and time period. The spatial distribution in EXPL is weakly impacted by considering the whole year instead of the June-July period only (compare Figure S5-S6 with Figure 11a).

However, the diurnal cycle differs markedly between the two runs, as the 4-km run exhibits a strong and narrow peak at 18 UTC (Figure 12 in PKMB15), while EXPL exhibits a weak and broad peak between 18 and 00 UTC (blue curve in Figure 13). A

D R A F T

January 14, 2016, 2:57pm

D R A F T

weak and broad peak at 00 UTC is also found in EXPL over the western Sahel and Sahara for the June-July period only as in PKMB15 (Figure S6S7). The difference in diurnal cycle of DUP is consistent with the difference in the diurnal cycle of precipitation, which exhibits a too strong and narrow peak in the 4-km run [Marsham et al., 2013b; Birch et al., 2014] and a too weak and broad peak in EXPL (blue curve in Figure 6) as compared to TRMM observations. This suggests that haboobs are too short-lived in the 4-km run and too long-lived in EXPL.

4.2. Parameterized Haboobs

The parameterization of haboobs in CTRL-P ~~and~~ HIRES-P ~~and BECH-P~~, is tuned to match the DUP averaged over the whole year 2006 and over all areas in EXPL, excluding elevations over 800 m. The root-mean-square error (RMSE) of the parameterization is also computed with respect to EXPL (Table 3). The spatial RMSE is first computed from the annual DUP interpolated on the 0.44° grid then averaged over all areas, while the seasonal RMSE is first computed from the monthly DUP over each area then averaged over all months and all areas.

The different runs require different tuning parameters. With the original formulation, the tuning parameter R approximately scales with the grid spacing between CTRL-P and HIRES-P (Table 3). In Equation 3, this compensates for M_{dd} approximately scaling with the grid surface area, i.e., the square of the grid spacing. With the alternative formulation, the tuning parameter w_{dd} weakly changes with the grid spacing between CTRL-P and HIRES-P (Table 3). This is due to C not depending on M_{dd} in Equation 5. ~~Between CTRL-P and BECH-P, the parameters R and w_{dd} decrease and increase, respectively (Table 3), which accounts for higher M_{dd} in CTRL-P after scaling with the~~

D R A F T

January 14, 2016, 2:57pm

D R A F T

~~arbitrary factor 10.~~ Finally, with the gust formulation ([Equation 6](#)), the tuning parameter σ increases between CTRL-P and HIRES-P (Table 3), which compensates for DCAPE decreasing with grid spacing.

The parameterization captures the geographical pattern of identified haboobs in EXPL (Figure 11a) but with some sensitivity to the model run and to the formulation. When applied to CTRL-P with the original formulation, the parameterization succeeds in exhibiting highest DUP over the Atlas area, high DUP over a wide region in the Sahel West area, and low DUP over the Sahara East (Figure 11b). The parameterization, however, misses local features of DUP and lacks the sharp meridional gradient in the southern part of the Sahel West area. Using the alternative formulation weakly affects the spatial distribution of parameterized DUP, with differences in local features only (Figure 11c). In contrast, using the gust formulation strongly impacts on the spatial distribution. The large region of high DUP is shifted from the Sahel West to the Sahara West and the region of low DUP is extended from the Sahara East to the Mediterranean (Figure 11d). This suggests that computing the DCAPE in the deep Saharan boundary layer overestimates the parameterized DUP. The northward shift in DUP increases the spatial RMSE as compared to the original and alternative formulations, which perform equally well (Table 3).

Applying the parameterization to HIRES-P instead of CTRL-P produces smaller-scale features, as expected from the higher resolution, but weakly affects the spatial distribution, either with the original formulation (Figure 11e), or with the alternative and the gust formulations (not shown). The spatial RMSE slightly increases in HIRES-P as compared to CTRL-P but the original and alternative formulations again per-

D R A F T

January 14, 2016, 2:57pm

D R A F T

form equally well, whereas the gust formulation exhibits higher spatial RMSE (Table 3). Applying the parameterization to BECH-P produces a scattered spatial distribution, with lower DUP over the Sahel West and higher DUP over the Sahara East (Figure 11f). This is consistent with the scattered and northward-extended precipitation in BECH-P (Figure 4e). Using the alternative instead of the original formulation slightly improves the spatial distribution (not shown), but both exhibit high spatial RMSE as compared to the CTRL-P and Hires-P runs (Table 3). This shows that, although the parameterization of haboobs can be tuned for different convection schemes, the resulting DUP depends on the representation of the monsoon, which in turn depends on the convection scheme [Marshall et al., 2013b; Birch et al., 2014].

The parameterization also succeeds in reproducing the seasonal cycle of haboobs related to the monsoon over the Sahel West and East and the Sahara West. With the original formulation applied to CTRL-P, the parameterization captures the primary peak in June over the Sahel West (solid red curve in Figure 12e) and in August over the Sahara West and the Sahel East (solid red curves in Figure 12c,f). The parameterization also captures the weaker seasonal cycle over the Mediterranean and Sahara East areas (solid red curves in Figure 12b,d). In contrast, the parameterization poorly captures the seasonal cycle over the Atlas, where it overestimates the weak peak in February and underestimates the stronger peaks in May and July (solid red curve in Figure 12a). This suggests that the parameterization produces too high DUP in the convection embedded in winter storms, and too low DUP in the convection favored by upper-level troughs in spring and summer. The parameterization also overestimates the weak peak in February over the Mediterranean, Sahara West, and Sahel West areas (solid red curves in Figure 12b,c,e). The

D R A F T

January 14, 2016, 2:57pm

D R A F T

~~parameterization, however, overall improves the seasonal cycle of DUP in the CTRL-P model run (dashed red curve in Figure 8).~~

As for the spatial distribution, applying the parameterization to HIRES-P instead of CTRL-P weakly impacts on the seasonal cycle, although the amplitude increases over the Sahel West and East (solid orange curves in Figure 12e,f). This is consistent with the higher amplitude of the monsoon cycle in HIRES-P (orange curves in Figure 5e,f). The higher amplitude of DUP increases the seasonal RMSE as compared to CTRL-P (Table 3). ~~Applying the parameterization to BECH-P shifts the seasonal cycle earlier over the Sahel West and East and the Sahara West, and increases its amplitude over the Sahara East (solid green curves in Figure 12e-f). This is consistent with the earlier and amplified monsoon cycle in BECH-P (green curves in Figure 5e-f), and also increases the seasonal RMSE as compared to CTRL-P (Table 3).~~ As for the spatial distribution again, using the alternative formulation weakly affects the seasonal cycle, although DUP slightly decreases in winter and increases in spring and summer (dashed curves in Figure 12). This improves the seasonal cycle and decreases the seasonal RMSE in CTRL-P and HIRES-P ~~, but exaggerates the seasonal cycle and further increases the seasonal RMSE in BECH-P~~ (Table 3).

In contrast with the alternative formulation, using the gust formulation strongly changes the seasonal cycle. After increasing during the monsoon onset, DUP stagnates over the Sahel East and even drops over the Sahel West (dotted curves in Figure 12e,f). This is due to the asymmetry in DCAPE between the monsoon onset and retreat, which matches the observed dust uplift over the Sahel and southern Sahara [Marsham *et al.*, 2008]. Over the Atlas area, the gust formulation reaches a peak in August (dotted curves in Figure

D R A F T

January 14, 2016, 2:57pm

D R A F T

12a), which also matches the observed frequency of haboobs [Emmel et al., 2010]. This however contrasts with the seasonal cycle of haboobs in EXPL (blue curves in Figure 12a,e,f), which therefore suggests that the match between the gust formulation and the observations is due to compensating errors. ~~The~~ Finally, the weak peak in February ~~finally~~ vanishes with the gust formulation (dotted curves in Figure 12), which improves the seasonal cycle. The gust formulation still shows the highest seasonal RMSE for both CTRL-P and HIRES-P (Table 3).

~~As expected from Figure 6, the~~ The parameterization does not succeed in capturing the diurnal cycle of haboobs. With all formulations and applied to all runs, the parameterized DUP increases quicker in the morning and reaches its peak earlier in the afternoon as compared to EXPL (Figure 13). This is consistent with the parameterized convection ~~being triggered too early~~ reaching its peak at noon (Figure 6), which is a known issue in the Tropics [e.g., Marsham et al., 2013b; Birch et al., 2014]. The amplitude increases but the diurnal cycle is weakly impacted when using the alternative formulation (dashed curves in Figure 13). In contrast, the amplitude of the diurnal cycle strongly increases with the gust formulation (dotted curves). This shows that the DCAPE exhibits a stronger diurnal cycle than the downdraft mass flux, which again suggests that computing the DCAPE in the deep Saharan boundary layer overestimates the parameterized DUP. The relative amplitude of the different formulations is consistent between the different areas (see Figure ~~S4~~ S5 for the diurnal cycle of haboobs over each area).

When added to the DUP from the resolved model wind, the parameterized DUP overall improves the seasonal cycle in CTRL-P and HIRES-P (dashed curves in Figure 8) as compared to EXPL. However, this total DUP still exhibits substantial biases, which can

D R A F T

January 14, 2016, 2:57pm

D R A F T

be explained by several factors. On the one hand, the parameterization itself exhibits biases as compared to EXPL, e.g. the underestimation of DUP from haboobs over the Atlas in spring and summer (Figure 12a). The tuning of the parameterization may also contribute to the underestimation, as it uses the rather conservative identification of haboobs in EXPL as a reference. On the other hand, the resolution is expected to affect the resolved winds independently of haboobs, e.g., over complex topography, or for specific processes such as the low-level jet. The resolution furthermore leads to the overestimation of DUP from resolved winds over the Sahel West in summer, where the representation of the monsoon is affected (Figure 5e) and deep cyclones develop (Figure 10b) in CTRL-P and HIRES-P. The parameterization therefore offers a solution for the important issue of lacking haboobs in the model runs with parameterized convection, but other biases need to be carefully investigated in these model runs. Finally, the parameterized DUP improves the diurnal cycle in CTRL-P and HIRES-P (dashed curves in Figure 9) as compared to EXPL, but through a general increase in DUP only.

5. Conclusion

Haboobs occur over most dust sources worldwide and contribute ~~to about~~ at least half of dust emissions over the central Sahara in summer [*Marsham et al., 2013a; Allen et al., 2013, 2015*]. However, they are absent from most large-scale weather and climate models, which do not explicitly represent convection and thus haboobs. Here, an unprecedented one-year-long run with explicit convection delivers the first full seasonal cycle of haboobs over the different arid regions of northern Africa. This computationally very expensive run further allows testing a simple parameterization based on the downdraft mass-flux of the

D R A F T

January 14, 2016, 2:57pm

D R A F T

603 convection scheme, originally developed in PKMB15, in a set of additional model runs
604 with parameterized convection.

605 The explicit run exhibits two contrasting regimes. Highest DUP (dust uplift potential,
606 i.e., dust-generating winds) from haboobs is found in the subtropical regime over the Atlas
607 and northern Algeria, where it reaches its peak in spring and summer due to midlatitude
608 troughs. High DUP from haboobs is also found in the tropical regime over the Sahel
609 and the western Sahara, where it reaches its peak in summer due to the monsoon flow.
610 The results are consistent with observations of haboobs during the few field campaigns
611 over these areas, as well as with an earlier explicit run restricted to the western Sahel
612 and Sahara, and to a shorter time period. Low DUP from haboobs is finally found over
613 the dry eastern Sahara. The contribution of haboobs to the total DUP reaches 18 % ~~on~~
614 ~~average annually~~ over northern Africa, 24 % between May and October, and up to 33 %
615 over the western Sahel during that period.

616 The parameterization succeeds in capturing the spatial pattern of DUP from haboobs as
617 compared to the explicit run. The parameterization also succeeds in capturing the seasonal
618 cycle due to the monsoon in the tropical regime, while it struggles with the seasonal cycle
619 due to midlatitude systems in the subtropical regime. The parameterization can be tuned
620 for the model resolution and for an alternative formulation with weak impact on the spatial
621 and temporal distributions. ~~However, the distributions depend on the representation of~~
622 ~~the monsoon. In particular~~In contrast, using a ~~different convection scheme extends the~~
623 ~~monsoon northward, which in turn~~formulation based on DCAPE shifts the parameterized
624 DUP northward and worsens the results. ~~Using a formulation based on DCAPE creates~~
625 ~~similar effects~~With the original and the alternative formulation, the parameterization

D R A F T

January 14, 2016, 2:57pm

D R A F T

improves the seasonal cycle of DUP, although the overall performance remains constrained by other limitations in the model runs.

The main limitations are common to both explicit and parameterized runs. The diurnal cycle of haboobs differs between parameterized and explicit DUP, but also between explicit DUP from two different models, which is consistent with differences in the diurnal cycle of precipitation and emphasizes the uncertainty in modeling convective organization. The seasonal cycle in the subtropical regime contrasts between parameterized and explicit DUP from haboobs, but also between explicit and observed DUP, which is again consistent with differences in the seasonal cycle of precipitation and suggests a model deficiency in this regime. Finally, the spatial distribution differs over the Sahel West between parameterized and explicit DUP from haboobs, but also between modelled and observed DUP, which shows the high sensitivity to the roughness length in this area.

The results are also subject to uncertainties in the spatial and seasonal distribution of haboobs. One part of the uncertainty lies in the identification of haboobs in the explicit run, which becomes ambiguous when the cold pools evolve into complex structures [Heinold *et al.*, 2013], the identification being rather conservative here. The other part of the uncertainty lies in the scarcity of surface observations, which lack both spatial and temporal sampling over northern Africa [Cowie *et al.*, 2014]. Furthermore, identifying haboobs is challenging and must often be done manually, even with high-resolution data [Engerer *et al.*, 2008; Provod *et al.*, 2015]. This raises the need for more observations over northern Africa, or for new algorithms to identify haboobs in available satellite and surface observations, as recently suggested by Redl *et al.* [2015].

D R A F T

January 14, 2016, 2:57pm

D R A F T

Despite the limitations discussed above, the results presented here show that the parameterization originally developed by PKMB15 is robust with respect to the model and its resolution, as well as to the formulation with constant radius or constant propagation speed of cold pools. The parameterization is simple and can be used online or offline, providing that the downdraft mass flux is stored, in large-scale weather and climate models with mass-flux convection schemes. It can thus be implemented in full dust models and the results be compared with extensive observations beyond the SYNOP winds considered here, as, e.g., aerosol optical depth (AOD) from satellites and AERONET stations. The parameterization [may in particular compensate for the too low AOD over summertime West Africa in large-scale dust models compared to observations \[e.g., Johnson et al., 2011; Ridley et al., 2012; Guirado et al., 2014; Cuevas et al., 2015\]](#). It has potential to solve a long-standing issue in simulating dust storms.

Acknowledgments. The authors thank Vera Maurer for valuable discussions about the COSMO-CLM simulations and Sophie Cowie for guidance to use SYNOP observations, [as well as two anonymous reviewers for constructive comments that helped improving the manuscript](#). The authors gratefully acknowledge the computing time granted by the John von Neumann Institute for Computing (NIC) and provided on the supercomputer JUROPA at Jülich Supercomputing Centre (JSC). For access to the model data please contact ingeborg.bischoff-gauss@kit.edu. The TRMM data was obtained through the NASA Goddard Earth Sciences (GES) Data and Information Services Center (DISC). The SYNOP data was obtained through the Met Office Integrated Data Archive System (MIDAS). The code for parameterizing haboobs is available from the corresponding author

D R A F T

January 14, 2016, 2:57pm

D R A F T

upon request. This work was funded by the European Research Council (ERC) grant
257543 “Desert Storms”.

References

Allen, C. J., R. Washington, and S. Engelstaedter (2013), Dust emission and transport mechanisms in the central Sahara: Fennec ground-based observations from Bordj Badji Mokhtar, June 2011, *J. Geophys. Res. Atmos.*, *118*(12), 6212–6232, doi:10.1002/jgrd.50534.

Allen, C. J. T., R. Washington, and A. Saci (2015), Dust detection from ground-based observations in the summer global dust maximum: Results from Fennec 2011 and 2012 and implications for modeling and field observations, *J. Geophys. Res. Atmos.*, *120*(3), 897–916, doi:10.1002/2014JD022655.

Alpert, P., and B. Ziv (1989), The Sharav Cyclone: Observations and some theoretical considerations, *J. Geophys. Res. Atmos.*, *94*(D15), 18,495–18,514, doi:10.1029/JD094iD15p18495.

Baldauf, M., A. Seifert, J. Förstner, D. Majewski, M. Raschendorfer, and T. Reinhardt (2011), Operational Convective-Scale Numerical Weather Prediction with the COSMO Model: Description and Sensitivities, *Mon. Wea. Rev.*, *139*(12), 3887–3905, doi:10.1175/MWR-D-10-05013.1.

~~Bechtold, P., M. Khler, T. Jung, F. Doblas-Reyes, M. Leutbecher, M. J. Rodwell, F. Vitart, and G. Balsamo (2008), Advances in simulating atmospheric variability with the ECMWF model: From synoptic to decadal time scales, *Quart. J. Roy. Meteor. Soc.*, *1337–1351*, .~~

D R A F T

January 14, 2016, 2:57pm

D R A F T

- 691 Berry, G., and C. Thorncroft (2005), Case study of an intense African easterly wave, *Mon.*
692 *Wea. Rev.*, *133*(4), 752–766, doi:10.1175/MWR2884.1.
- 693 Birch, C. E., D. J. Parker, J. H. Marsham, D. Copsey, and L. Garcia-Carreras (2014),
694 A seamless assessment of the role of convection in the water cycle of the West African
695 Monsoon, *J. Geophys. Res. Atmos.*, *119*(6), 2890–2912, doi:10.1002/2013JD020887.
- 696 Bou Karam, D., C. Flamant, P. Knippertz, O. Reitebuch, J. Pelon, M. Chong, and
697 A. Dabas (2008), Dust emissions over the Sahel associated with the West African mon-
698 soon intertropical discontinuity region: A representative case-study, *Quart. J. Roy.*
699 *Meteor. Soc.*, *134*(632), 621–634, doi:10.1002/qj.244.
- 700 Cowie, S. M., P. Knippertz, and J. H. Marsham (2014), A climatology of dust emission
701 events from northern Africa using long-term surface observations, *Atmos. Chem. Phys.*,
702 *14*(16), 8579–8597, doi:10.5194/acp-14-8579-2014.
- 703 [Cuevas, E., C. Camino, A. Benedetti, S. Basart, E. Terradellas, J. M. Baldasano,](#)
704 [J. J. Morcrette, B. Marticorena, P. Goloub, A. Mortier, A. Berjón, Y. Hernández,](#)
705 [M. Gil-Ojeda, and M. Schulz \(2015\), The MACC-II 2007–2008 reanalysis: atmospheric](#)
706 [dust evaluation and characterization over northern Africa and the Middle East, *Atmos.*](#)
707 [*Chem. Phys.*, *15*\(8\), 3991–4024, doi:10.5194/acp-15-3991-2015.](#)
- 708 Dee, D. P., S. M. Uppala, A. J. Simmons, P. Berrisford, P. Poli, S. Kobayashi, U. Andrae,
709 M. A. Balmaseda, G. Balsamo, P. Bauer, P. Bechtold, A. C. M. Beljaars, L. van de Berg,
710 J. Bidlot, N. Bormann, C. Delsol, R. Dragani, M. Fuentes, A. J. Geer, L. Haimberger,
711 S. B. Healy, H. Hersbach, E. V. Hólm, L. Isaksen, P. Kållberg, M. Köhler, M. Ma-
712 tricardi, A. P. McNally, B. M. Monge-Sanz, J.-J. Morcrette, B.-K. Park, C. Peubey,
713 P. de Rosnay, C. Tavalato, J.-N. Thépaut, and F. Vitart (2011), The ERA-Interim re-

D R A F T

January 14, 2016, 2:57pm

D R A F T

analysis: configuration and performance of the data assimilation system, *Quart. J. Roy. Meteor. Soc.*, *137*(656), 553–597, doi:10.1002/qj.828.

Emmel, C., P. Knippertz, and O. Schulz (2010), Climatology of convective density currents in the southern foothills of the Atlas Mountains, *J. Geophys. Res. Atmos. (1984–2012)*, *115*(D11), doi:10.1029/2009JD012863.

Engerer, N. A., D. J. Stensrud, and M. C. Coniglio (2008), Surface Characteristics of Observed Cold Pools, *Mon. Wea. Rev.*, *136*(12), 4839–4849, doi:10.1175/2008MWR2528.1, ~~doi:10.1175/2008MWR2528.1.~~

Fiedler, S., K. Schepanski, B. Heinold, P. Knippertz, and I. Tegen (2013), Climatology of nocturnal low-level jets over North Africa and implications for modeling mineral dust emission, *J. Geophys. Res. Atmos.*, *118*(12), 6100–6121, doi:10.1002/jgrd.50394.

Fink, A. H., and A. Reiner (2003), Spatiotemporal variability of the relation between African Easterly Waves and West African Squall Lines in 1998 and 1999, *J. Geophys. Res. Atmos.*, *108*(D11), n/a–n/a, doi:10.1029/2002JD002816.

Flamant, C., J.-P. Chaboureaud, D. J. Parker, C. M. Taylor, J.-P. Cammas, O. Bock, F. Timouk, and J. Pelon (2007), Airborne observations of the impact of a convective system on the planetary boundary layer thermodynamics and aerosol distribution in the inter-tropical discontinuity region of the West African Monsoon, *Quart. J. Roy. Meteor. Soc.*, *133*(626), 1175–1189, doi:10.1002/qj.97.

Fujita, T., and H. Byers (1977), Spearhead Echo and Downburst in Crash of an Airliner, *Mon. Wea. Rev.*, *105*(2), 129–146, doi:10.1175/1520-0493(1977)105<0129:SEADIT>2.0.CO;2.

D R A F T

January 14, 2016, 2:57pm

D R A F T

- Gantner, L., and N. Kalthoff (2010), Sensitivity of a modelled life cycle of a mesoscale convective system to soil conditions over West Africa, *Quart. J. Roy. Meteor. Soc.*, *136*(S1), 471–482, doi:10.1002/qj.425.
- Garcia-Carreras, L., J. Marsham, D. Parker, C. Bain, S. Milton, A. Saci, M. Salah-Ferroudj, B. Ouchene, and R. Washington (2013), The impact of convective cold pool outflows on model biases in the Sahara, *Geophys. Res. Lett.*, *40*(8), 1647–1652, doi:10.1002/grl.50239.
- Grandpeix, J.-Y., and J.-P. Lafore (2010), A density current parameterization coupled with Emanuel’s convection scheme. Part I: The models, *J. Atmos. Sci.*, *67*(4), 881–897, doi:10.1175/2009JAS3044.1.
- [Guirado, C., E. Cuevas, V. E. Cachorro, C. Toledano, S. Alonso-Pérez, J. J. Bustos, S. Basart, P. M. Romero, C. Camino, M. Mimouni, L. Zeudmi, P. Goloub, J. M. Baldasano, and A. M. de Frutos \(2014\), Aerosol characterization at the Saharan AERONET site Tamanrasset, *Atmos. Chem. Phys.*, *14*\(21\), 11,753–11,773, doi:10.5194/acp-14-11753-2014.](#)
- Heinold, B., P. Knippertz, J. Marsham, S. Fiedler, N. Dixon, K. Schepanski, B. Laurent, and I. Tegen (2013), The role of deep convection and nocturnal low-level jets for dust emission in summertime West Africa: Estimates from convection-permitting simulations, *J. Geophys. Res. Atmos.*, *118*(10), 4385–4400, doi:10.1002/jgrd.50402.
- Heise, E. (2006), Improved diagnosis of convective and turbulent gusts: test results of new gust parameterization, *COSMO Newsletter*, *6*, 103–114.
- Houze, R. A. (2004), Mesoscale convective systems, *Rev. Geophys.*, *42*(4), n/a–n/a, doi:10.1029/2004RG000150.

D R A F T

January 14, 2016, 2:57pm

D R A F T

- Huffman, G. J., D. T. Bolvin, E. J. Nelkin, D. B. Wolff, R. F. Adler, G. Gu, Y. Hong, K. P. Bowman, and E. F. Stocker (2007), The TRMM Multisatellite Precipitation Analysis (TMPA): Quasi-Global, Multiyear, Combined-Sensor Precipitation Estimates at Fine Scales, *Journal of Hydrometeorology*, 8(1), 38–55, doi:10.1175/JHM560.1.
- [Johnson, B. T., M. E. Brooks, D. Walters, S. Woodward, S. Christopher, and K. Schepanski \(2011\), Assessment of the Met Office dust forecast model using observations from the GERBILS campaign, *Quart. J. Roy. Meteor. Soc.*, 137\(658\), 1131–1148, doi:10.1002/qj.736.](#)
- Knippertz, P. (2003), Tropical–Extratropical Interactions Causing Precipitation in Northwest Africa: Statistical Analysis and Seasonal Variations, *Mon. Wea. Rev.*, 131(12), 3069–3076, doi:10.1175/1520-0493(2003)131;3069:TICPIN;2.0.CO;2, ~~doi:10.1175/1520-0493(2003)131;3069:TICPIN;2.0.CO;2.~~
- Knippertz, P. (2014), Meteorological Aspects of Dust Storms, in *Mineral Dust*, edited by P. Knippertz and J.-B. W. Stuut, pp. 121–147, Springer Netherlands, doi:10.1007/978-94-017-8978-3.
- Knippertz, P., A. H. Fink, A. Reiner, and P. Speth (2003), Three Late Summer/Early Autumn Cases of Tropical–Extratropical Interactions Causing Precipitation in Northwest Africa, *Mon. Wea. Rev.*, 131(1), 116–135, doi:10.1175/1520-0493(2003)131;0116:TLSEAC;2.0.CO;2, ~~doi:10.1175/1520-0493(2003)131;0116:TLSEAC;2.0.CO;2.~~
- Knippertz, P., C. Deutscher, K. Kandler, T. Müller, O. Schulz, and L. Schütz (2007), Dust mobilization due to density currents in the Atlas region: Observations from the Saharan Mineral Dust Experiment 2006 field campaign, *J. Geophys. Res. Atmos.* (1984–2012),

D R A F T

January 14, 2016, 2:57pm

D R A F T

112(D21), doi:10.1029/2007JD008774.

Knippertz, P., J. Trentmann, and A. Seifert (2009), High-resolution simulations of convective cold pools over the northwestern Sahara, *J. Geophys. Res. Atmos.* (1984–2012), 114(D8), doi:10.1029/2008JD011271.

Kocha, C., P. Tulet, J.-P. Lafore, and C. Flamant (2013), The importance of the diurnal cycle of Aerosol Optical Depth in West Africa, *Geophys. Res. Lett.*, 40(4), 785–790, doi:10.1002/grl.50143.

Laing, A. G., R. Carbone, V. Levizzani, and J. Tuttle (2008), The propagation and diurnal cycles of deep convection in northern tropical Africa, *Quart. J. Roy. Meteor. Soc.*, 134(630), 93–109, doi:10.1002/qj.194.

Largerón, Y., F. Guichard, D. Bouniol, F. Couvreux, L. Kergoat, and B. Marticorena (2015), Can we use surface wind fields from meteorological reanalyses for Sahelian dust emission simulations?, *Geophys. Res. Lett.*, 42(7), 2490–2499, doi:10.1002/2014GL062938, 2014GL062938.

Marsham, J. H., D. J. Parker, C. M. Grams, C. M. Taylor, and J. M. Haywood (2008), Uplift of Saharan dust south of the intertropical discontinuity, *J. Geophys. Res. Atmos.*, 113(D21), n/a–n/a, doi:10.1029/2008JD009844.

Marsham, J. H., C. M. Grams, and B. Mühr (2009), Photographs of dust uplift from small-scale atmospheric features, *Weather*, 64(7), 180–181, doi:10.1002/wea.390.

Marsham, J. H., P. Knippertz, N. S. Dixon, D. J. Parker, and G. M. S. Lister (2011), The importance of the representation of deep convection for modeled dust-generating winds over West Africa during summer, *Geophys. Res. Lett.*, 38(16), n/a–n/a, doi:10.1029/2011GL048368.

D R A F T

January 14, 2016, 2:57pm

D R A F T

- Marshall, J. H., M. Hobby, C. Allen, J. Banks, M. Bart, B. Brooks, C. Cavazos-Guerra,
S. Engelstaedter, M. Gascoyne, A. Lima, et al. (2013a), Meteorology and dust in the cen-
tral Sahara: Observations from Fennec supersite-1 during the June 2011 Intensive Ob-
servation Period, *J. Geophys. Res. Atmos.*, *118*(10), 4069–4089, doi:10.1002/jgrd.50211.
- Marshall, J. H., N. S. Dixon, L. Garcia-Carreras, G. Lister, D. J. Parker, P. Knippertz,
and C. E. Birch (2013b), The role of moist convection in the West African monsoon
system: Insights from continental-scale convection-permitting simulations, *Geophys.*
Res. Lett., *40*(9), 1843–1849, doi:10.1002/grl.50347.
- Marticorena, B., and G. Bergametti (1995), Modeling the atmospheric dust cycle: 1. De-
sign of a soil-derived dust emission scheme, *J. Geophys. Res. Atmos.*, *100*(D8), 16,415–
16,430, doi:10.1029/95JD00690.
- Marticorena, B., B. Chatenet, J.-L. Rajot, S. Traoré, M. Coulibaly, A. Diallo, I. Koné,
A. Maman, T. NDiaye, and A. Zakou (2010), Temporal variability of mineral dust
concentrations over West Africa: analyses of a pluriannual monitoring from the AMMA
Sahelian Dust Transect, *Atmos. Chem. Phys.*, *10*(18), 8899–8915, doi:10.5194/acp-10-
8899-2010.
- Nakamura, K., R. Kershaw, and N. Gait (1996), Prediction of near-surface gusts generated
by deep convection, *Meteorol. Appl.*, *3*(2), 157–167, doi:10.1002/met.5060030206.
- O’Hara, S. L., M. L. Clarke, and M. S. Elatrash (2006), Field measurements
of desert dust deposition in Libya , *Atm. Env.*, *40*(21), 3881–3897, doi:
10.1016/j.atmosenv.2006.02.020.
- Panitz, H.-J., A. Dosio, M. Büchner, D. Lüthi, and K. Keuler (2014), COSMO-CLM
(CCLM) climate simulations over CORDEX-Africa domain: analysis of the ERA-

D R A F T

January 14, 2016, 2:57pm

D R A F T

- Interim driven simulations at 0.44° and 0.22° resolution, *Clim. Dyn.*, *42*(11-12), 3015–3038, doi:10.1007/s00382-013-1834-5.
- Pantillon, F., P. Knippertz, J. H. Marsham, and C. E. Birch (2015), A Parameterization of Convective Dust Storms for Models with Mass-Flux Convection Schemes, *J. Atmos. Sci.*, *72*(6), 2545–2561, doi:10.1175/JAS-D-14-0341.1.
- Parker, D., R. Burton, A. Diongue-Niang, R. Ellis, M. Felton, C. Taylor, C. Thorncroft, P. Bessemoulin, and A. Tompkins (2005), The diurnal cycle of the West African monsoon circulation, *Quart. J. Roy. Meteor. Soc.*, *131*(611, A), 2839–2860, doi:10.1256/qj.04.52.
- Provod, M., J. Marsham, D. Parker, and C. Birch (2015), A characterization of cold pools in the West African Sahel, *Mon. Wea. Rev.*, doi:10.1175/MWR-D-15-0023.1.
- Redl, R., A. H. Fink, and P. Knippertz (2015), An objective detection method for convective cold pool events and its application to northern Africa, *Mon. Wea. Rev.*, *143*(12), 5055–5072, doi:10.1175/MWR-D-15-0223.1.
- Ridley, D. A., C. L. Heald, and B. Ford (2012), North African dust export and deposition: A satellite and model perspective, doi:10.1175/J. Geophys. Res. Atmos., *117*(D2), n/MWR-D-15-0223.1a-n/a, doi:10.1029/2011JD016794, d02202.
- Ridley, D. A., C. L. Heald, J. Pierce, and M. Evans (2013), Toward resolution-independent dust emissions in global models: Impacts on the seasonal and spatial distribution of dust, *Geophys. Res. Lett.*, *40*(11), 2873–2877, doi:10.1002/grl.50409.
- Roberts, A. J., and P. Knippertz (2014), The formation of a large summertime Saharan dust plume: Convective and synoptic-scale analysis, *J. Geophys. Res. Atmos.*, *119*(4), 1766–1785, doi:10.1002/2013JD020667.

D R A F T

January 14, 2016, 2:57pm

D R A F T

- Schepanski, K., and P. Knippertz (2011), Soudano-Saharan depressions and their importance for precipitation and dust: a new perspective on a classical synoptic concept, *Quart. J. Roy. Meteor. Soc.*, *137*(659), 1431–1445, doi:10.1002/qj.850.
- Schulz, J.-P., and E. Heise (2003), A new scheme for diagnosing near-surface convective gusts, *COSMO Newsletter*, *3*, 221–225.
- Sodemann, H., T. M. Lai, F. Marengo, C. L. Ryder, C. Flamant, P. Knippertz, P. Rosenberg, M. Bart, and J. B. McQuaid (2015), Lagrangian dust model simulations for a case of moist convective dust emission and transport in the western Sahara region during Fennec/LADUNEX, *J. Geophys. Res. Atmos.*, *120*(12), 6117–6144, doi:10.1002/2015JD023283, 2015JD023283.
- Sutton, L. J. (1925), Haboobs, *Quart. J. Roy. Meteor. Soc.*, *51*(213), 25–30, doi:10.1002/qj.49705121305.
- Tiedtke, M. (1989), A Comprehensive Mass Flux Scheme for Cumulus Parameterization in Large-Scale Models, doi:10.1175/1520-0493(1989)117<1779:ACMFSF>2.0.CO;2.
- Todd, M., C. T. Allen, M. Bart, M. Bechir, J. Bentefouet, B. Brooks, C. Cavazos-Guerra, T. Clovis, S. Deyane, M. Dieh, et al. (2013), Meteorological and dust aerosol conditions over the western Saharan region observed at Fennec Supersite-2 during the intensive observation period in June 2011, *J. Geophys. Res. Atmos.*, *118*(15), 8426–8447, doi:10.1002/jgrd.50470.
- Walters, D. N., M. J. Best, A. C. Bushell, D. Copsey, J. M. Edwards, P. D. Falloon, C. M. Harris, A. P. Lock, J. C. Manners, C. J. Morcrette, M. J. Roberts, R. A. Stratton, S. Webster, J. M. Wilkinson, M. R. Willett, I. A. Boutle, P. D. Earnshaw, P. G. Hill, C. MacLachlan, G. M. Martin, W. Moufouma-Okia, M. D. Palmer, J. C. Petch, G. G.

D R A F T

January 14, 2016, 2:57pm

D R A F T

Rooney, A. A. Scaife, and K. D. Williams (2011), The Met Office Unified Model Global Atmosphere 3.0/3.1 and JULES Global Land 3.0/3.1 configurations, *Geosci. Model Dev.*, 4(4), 919–941, doi:10.5194/gmd-4-919-2011.

Washington, R., and M. C. Todd (2005), Atmospheric controls on mineral dust emission from the Bodélé Depression, Chad: The role of the low level jet, *Geophys. Res. Lett.*, 32(17), n/a–n/a, doi:10.1029/2005GL023597.

D R A F T

January 14, 2016, 2:57pm

D R A F T

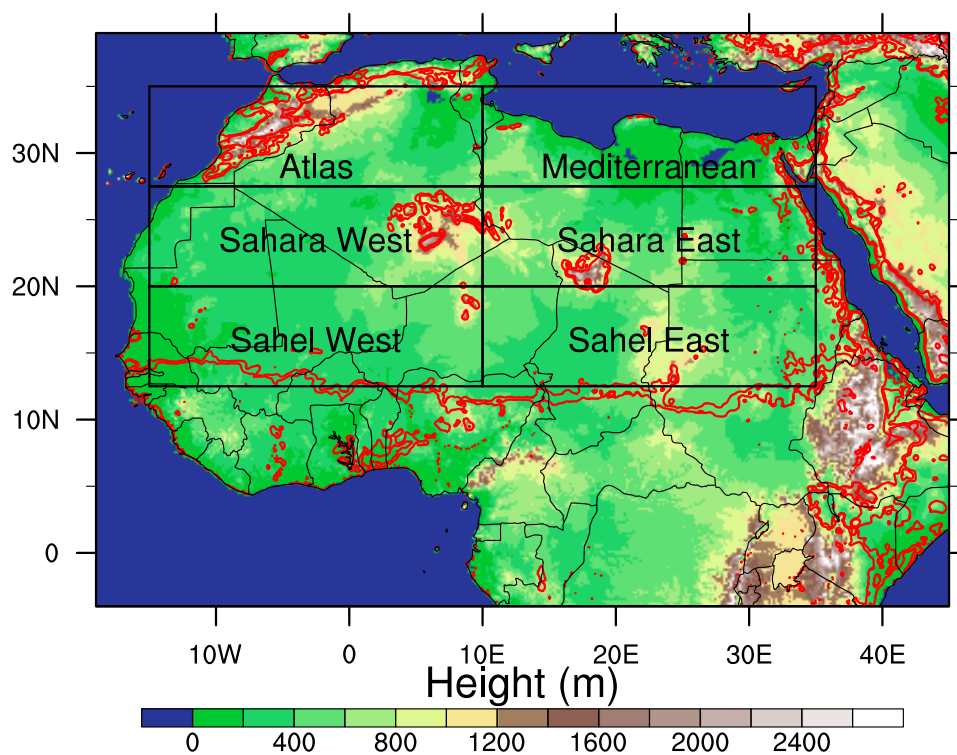


Figure 1. Domain and orography in the EXPL model run. ~~Contours~~ Red contours show the roughness length at typical values of 0.05 and 0.1 m to mark the border between arid and vegetated areas. The areas defined in Section 3 are marked by boxes and labelled.

D R A F T

January 14, 2016, 2:57pm

D R A F T

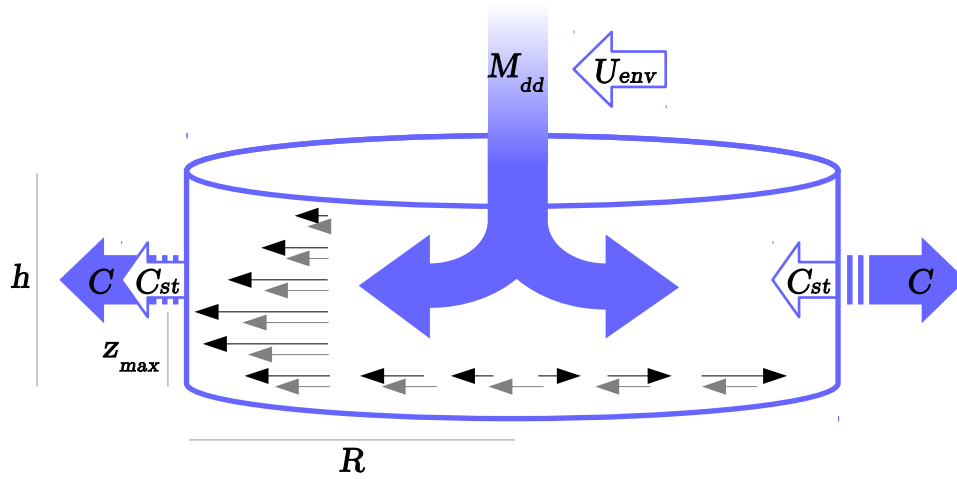


Figure 2. Schematic of the conceptual model, with M_{dd} the downdraft mass flux, U_{env} the environmental steering wind, C and C_{st} the propagation and steering speeds of the cold pool, respectively, h and R the height and radius of the cold pool, respectively, and z_{max} the height of maximum wind. Thin black and gray arrows illustrate the radial and the steering wind within the cold pool, respectively. From *Pantillon et al.* [2015]. ©American Meteorological Society. Used with permission.

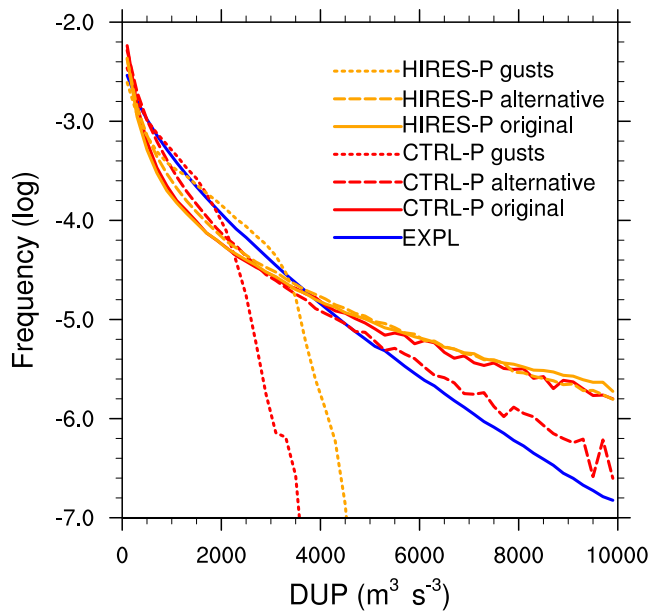


Figure 3. Probability distribution function of DUP computed over the year 2006 and over all domains displayed in Figure 11 from haboobs identified in EXPL and parameterized in CTRL-P, ~~HIRE-P~~, and ~~BECH-P~~ HIRE-P with the original, the alternative, and the gust formulation (Table 3).

D R A F T

January 14, 2016, 2:57pm

D R A F T

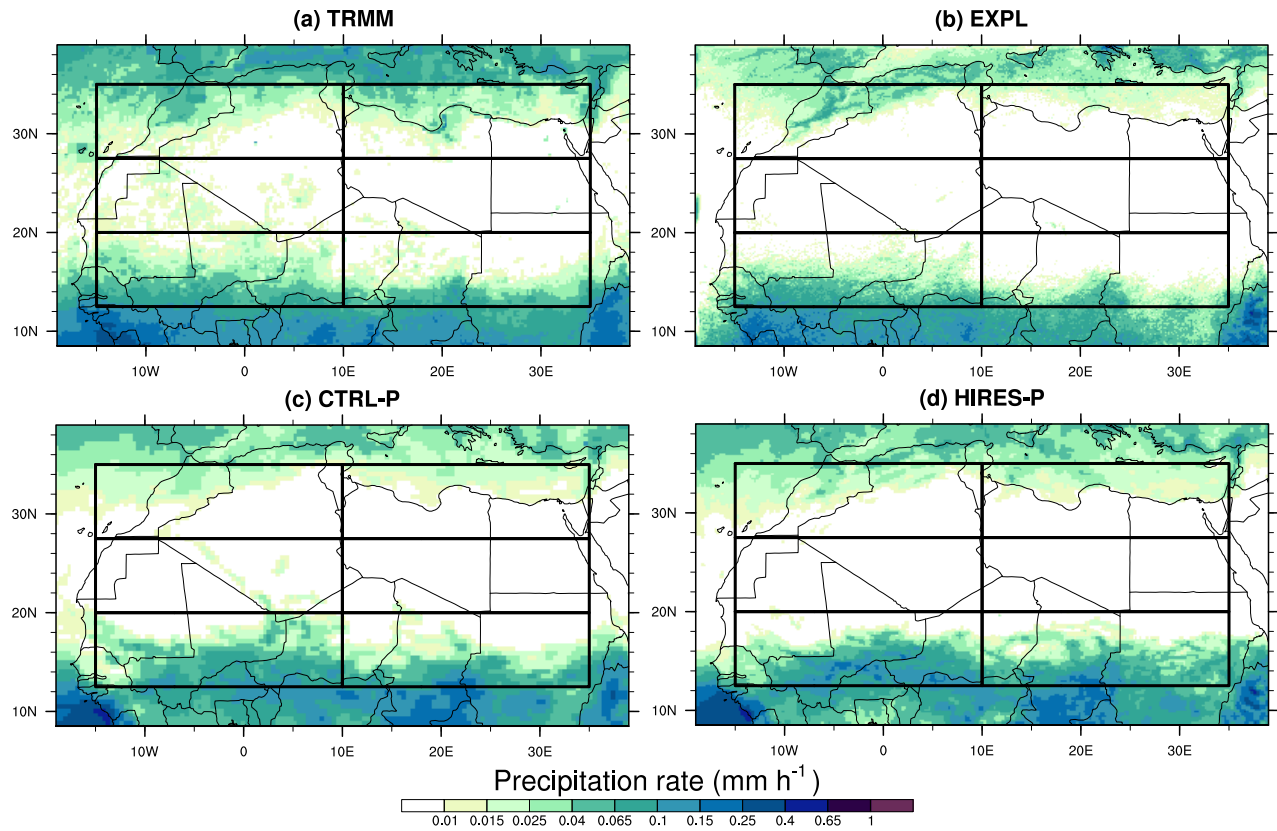


Figure 4. Spatial distribution of precipitation rate averaged over the year 2006 in the TRMM-3B42 observation product (a) and in the EXPL (b), CTRL-P (c), and HIRES-P (d) ~~and BECH-P (e)~~-model runs (Table 1). The boxes mark the areas defined in Section 3.

D R A F T

January 14, 2016, 2:57pm

D R A F T

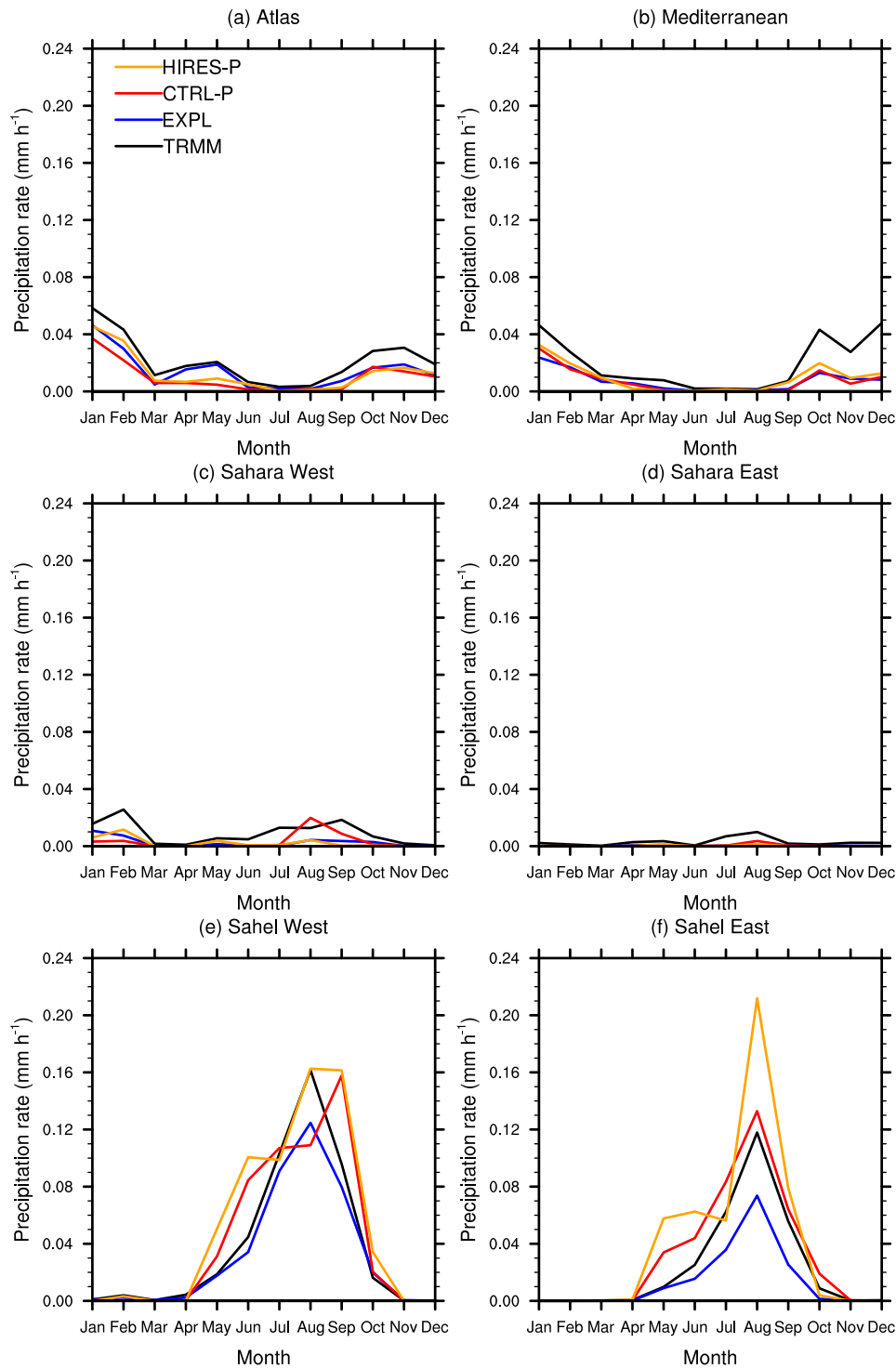


Figure 5. Seasonal cycle in precipitation rate averaged over each area marked by a box in Figure 4 in the TRMM-3B42 observation product and in the EXPL, CTRL-P, ~~HIRES-P~~, and ~~BECH-P~~ HIRES-P model runs (Table 1).

D R A F T

January 14, 2016, 2:57pm

D R A F T

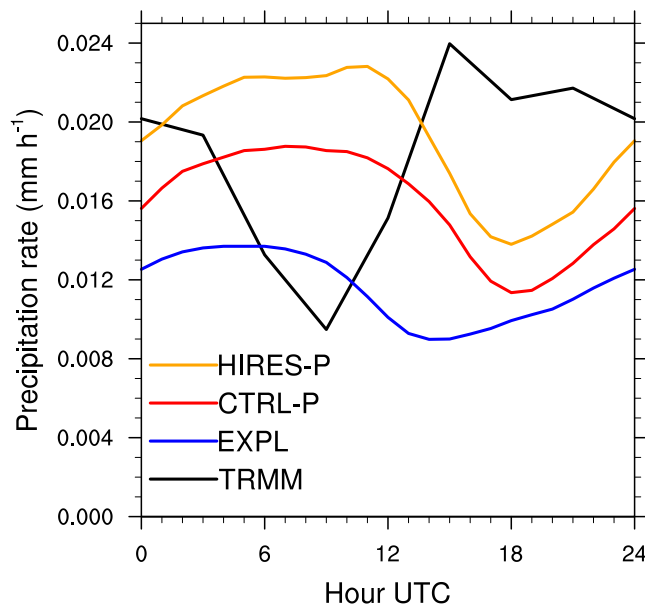


Figure 6. Diurnal cycle in precipitation rate averaged over the year 2006 and over all areas marked by boxes in Figure 4 in the TRMM-3B42 observation product and in the EXPL, CTRL-P, ~~HIRES-P~~, and ~~BECH-P~~ HIRES-P model runs (Table 1).

D R A F T

January 14, 2016, 2:57pm

D R A F T

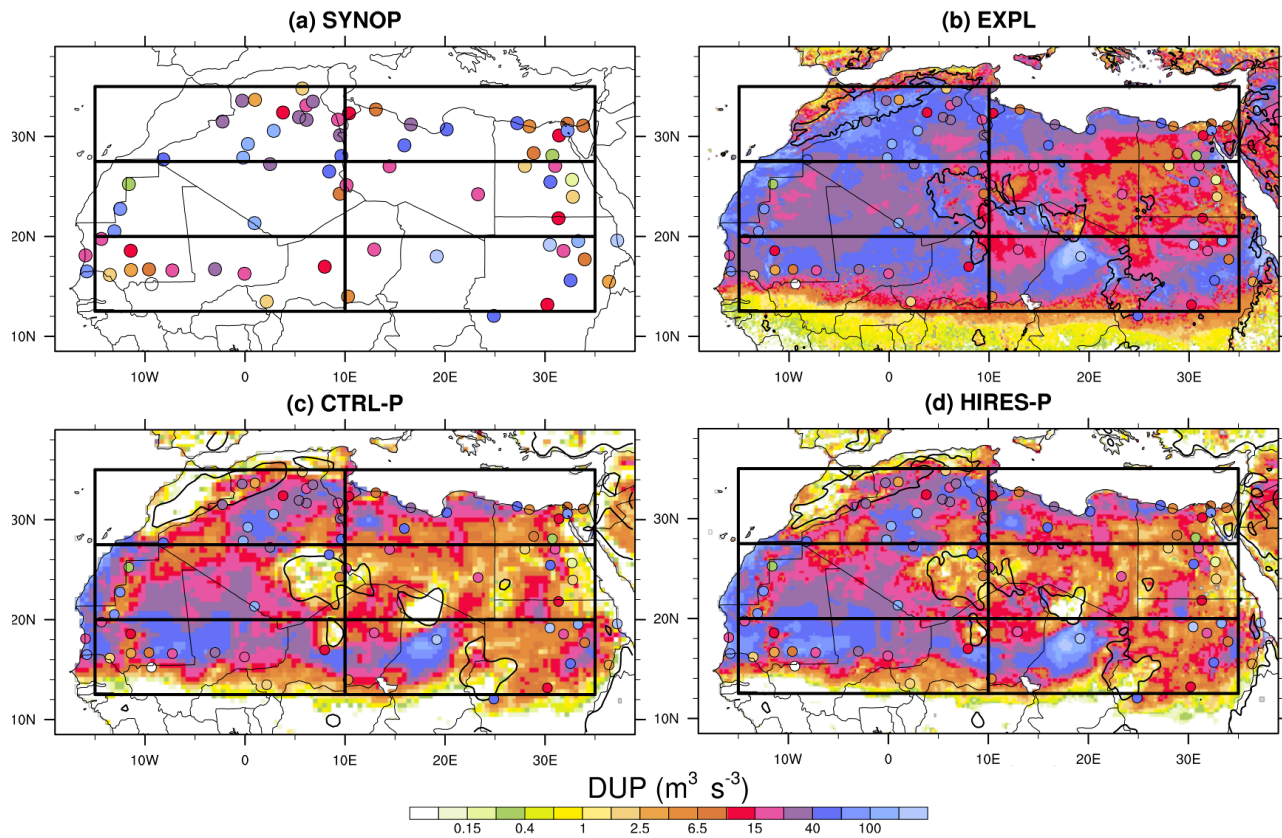


Figure 7. Spatial distribution of DUP averaged over the year 2006 from the observed wind at SYNOP stations (a) and from the resolved model wind in the EXPL (b), CTRL-P (c), and HIRES-P (d) ~~and BECH-P (e)~~ model runs (Table 1). The DUP in (a) is overplotted in (b-e) for comparison. The contours in (b-e) show the 800-m elevation in the model runs. The boxes mark the areas defined in Section 3.

D R A F T

January 14, 2016, 2:57pm

D R A F T

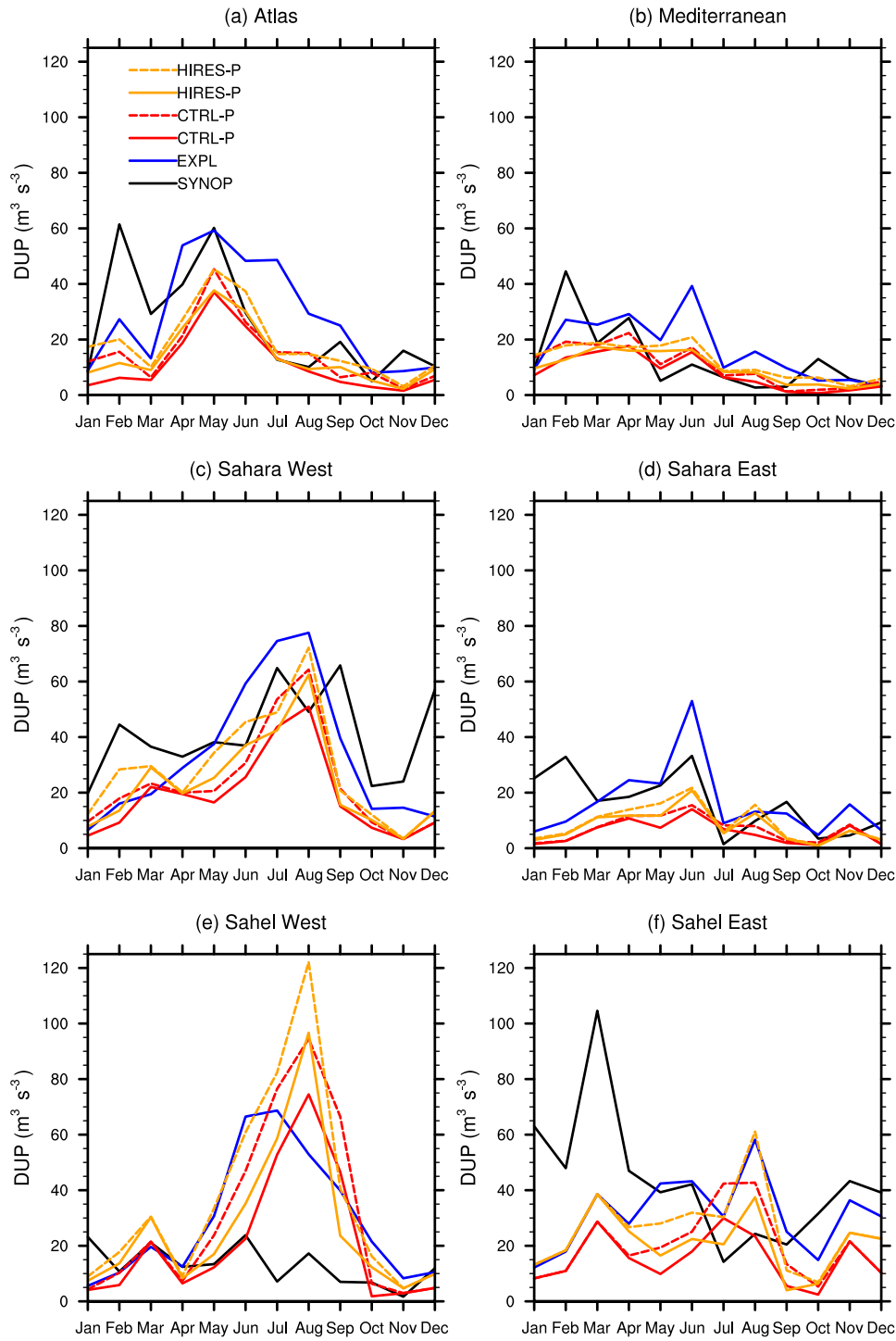


Figure 8. Seasonal cycle in DUP averaged over each area marked by a box in Figure 7 from the observed wind at SYNOP stations and from the resolved model wind in the EXPL, CTRL-P, ~~HIRES-P~~, and ~~BECH-P~~ HIRES-P model runs (Table 1). The dashed ~~curve~~ curves show the total DUP from the resolved model wind and the haboobs parameterized with the original formulation.

D R A F T

January 14, 2016, 2:57pm

D R A F T

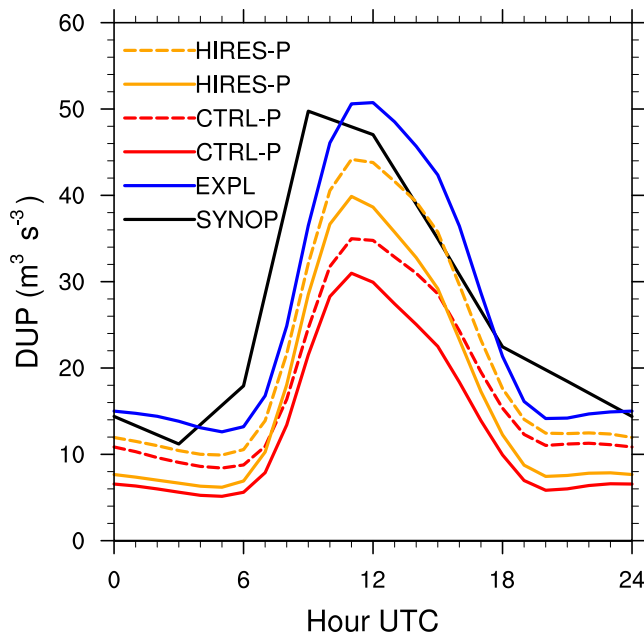


Figure 9. Diurnal cycle in DUP averaged over the year 2006 and over all areas marked by boxes in Figure 7 from the observed wind at SYNOP stations and from the resolved model wind in the EXPL, CTRL-P, ~~HIRES-P~~, and ~~BECH-P~~ HIRES-P model runs (Table 1). The dashed curves show the total DUP from the resolved model wind and the haboobs parameterized with the original formulation.

D R A F T

January 14, 2016, 2:57pm

D R A F T

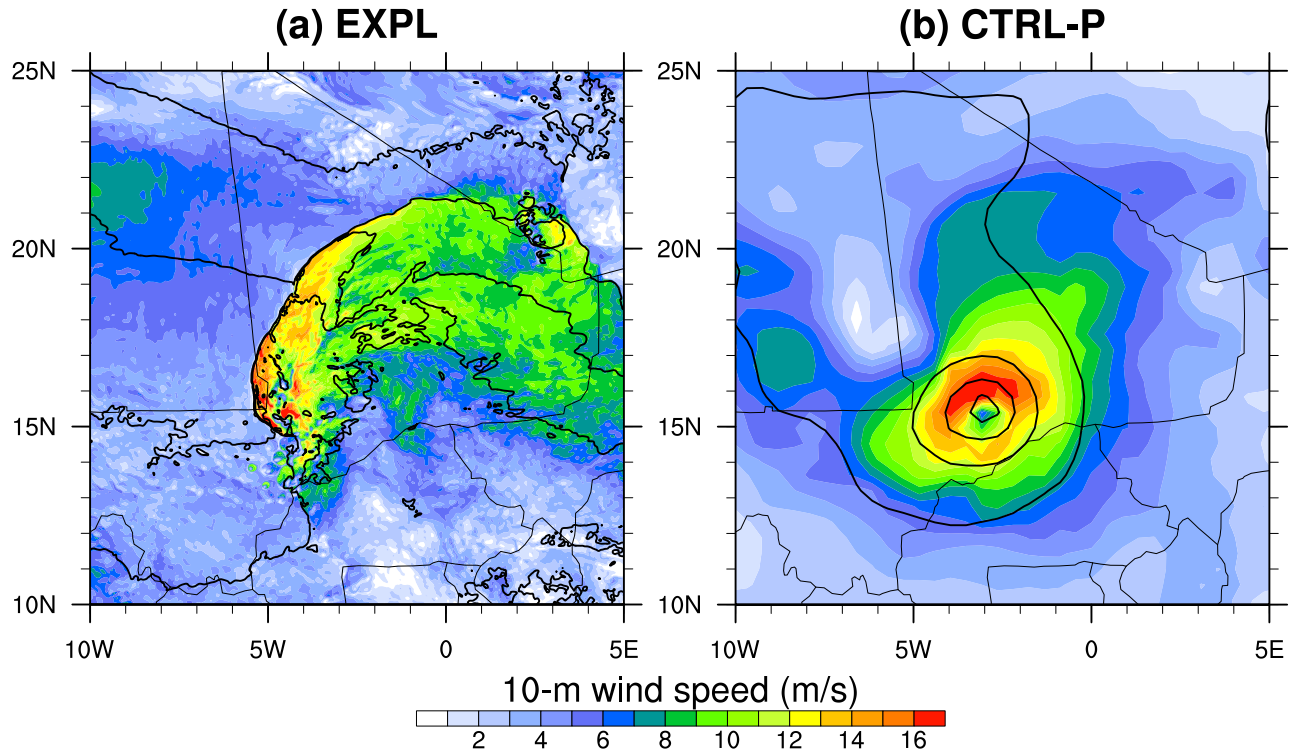


Figure 10. Examples of storms in the model runs: mesoscale convective system at 1800 UTC 03 August 2006 in EXPL (a) and deep cyclone at 0600 UTC 10 September 2006 in CTRL-P (b). Contours show the 925-hPa temperature every 5 K in (a) and the mean-sea-level pressure every 5 hPa in (b).

D R A F T

January 14, 2016, 2:57pm

D R A F T

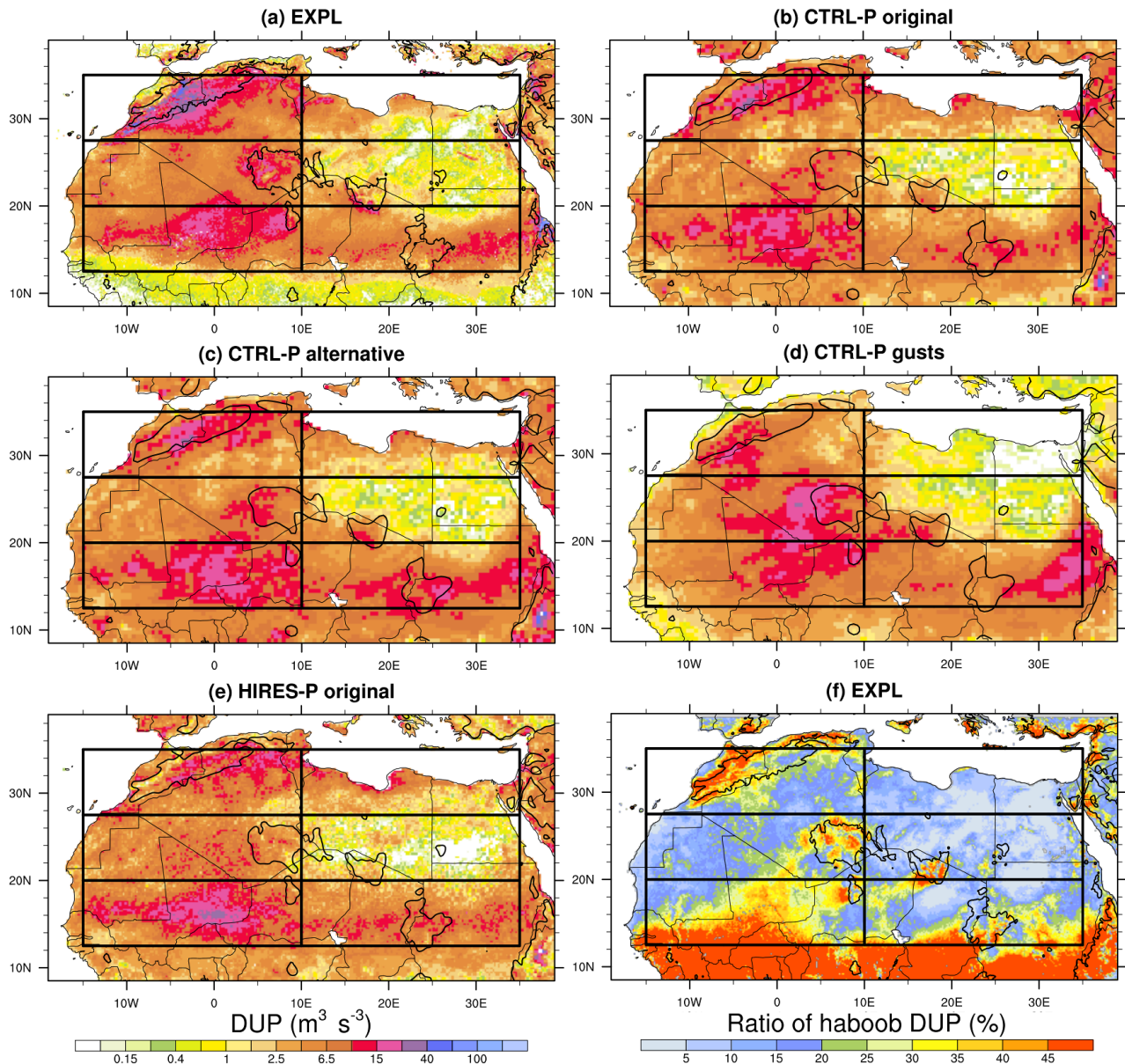


Figure 11. Spatial distribution of DUP averaged over the year 2006 from haboobs identified in EXPL (a), parameterized in CTRL-P with the original formulation (b), the alternative formulation (c), and the gust formulation (d), and parameterized in HIRES-P (e) and BECH-P (f) with the original formulation. The white contours in (a) show where the identified haboobs contribute more than 25 % of the DUP from the total model wind. The black contours show the 800-m elevation. The boxes mark the areas defined in Section 3.

D R A F T

January 14, 2016, 2:57pm

D R A F T

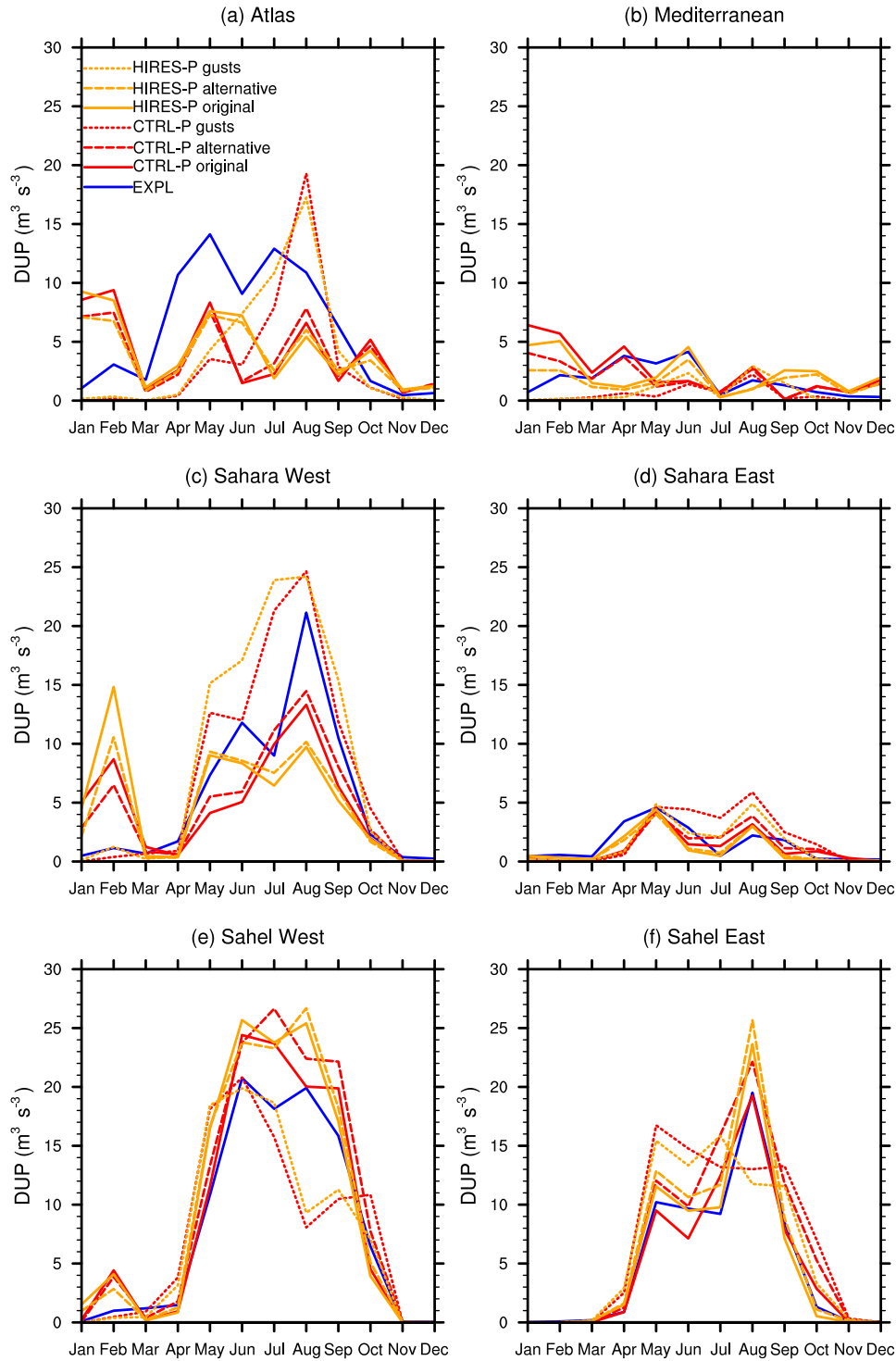


Figure 12. Seasonal cycle in DUP averaged over each area marked by a box in Figure 11 from haboobs identified in EXPL and parameterized in CTRL-P, HIRES-P, and BECH-P-HIRES-P with the original, the alternative, and the gust formulation (Table 3).

D R A F T

January 14, 2016, 2:57pm

D R A F T

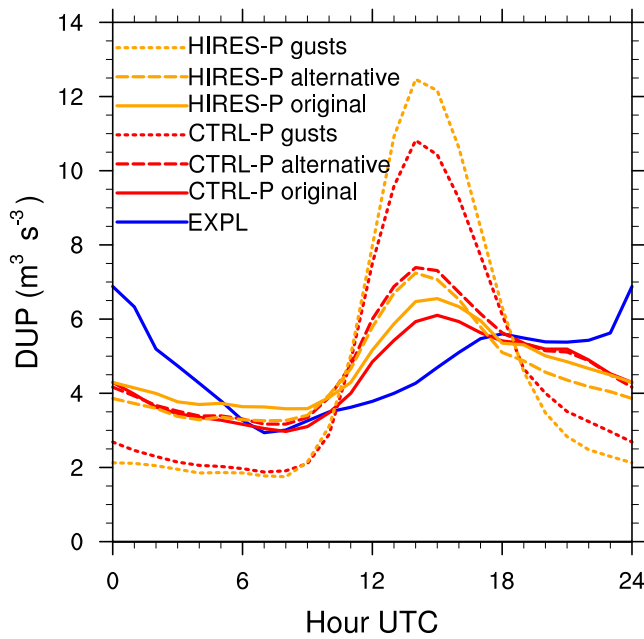


Figure 13. Diurnal cycle in DUP averaged over the year 2006 and over all areas marked by boxes in Figure 11 from haboobs identified in EXPL and parameterized in CTRL-P, ~~HIREP-P~~, and ~~BECH-P~~-HIREP-P with the original, the alternative, and the gust formulation (Table 3).

D R A F T

January 14, 2016, 2:57pm

D R A F T

Table 1. List of model runs with principal characteristics of their configuration.

Name	Grid spacing	Vertical levels	Moist convection
CTRL-P	0.44° (50 km)	35	Tiedtke [1989] Parameterization
HIRES-P	0.22° (25 km)	35	Tiedtke [1989] Parameterization
BECH-P 0.44° (50 km) 35 ? Africa EXPL	0.025° (2.8 km)	50	Explicit

Table 2. DUP attributed to haboobs in the explicit run, averaged over the whole year 2006

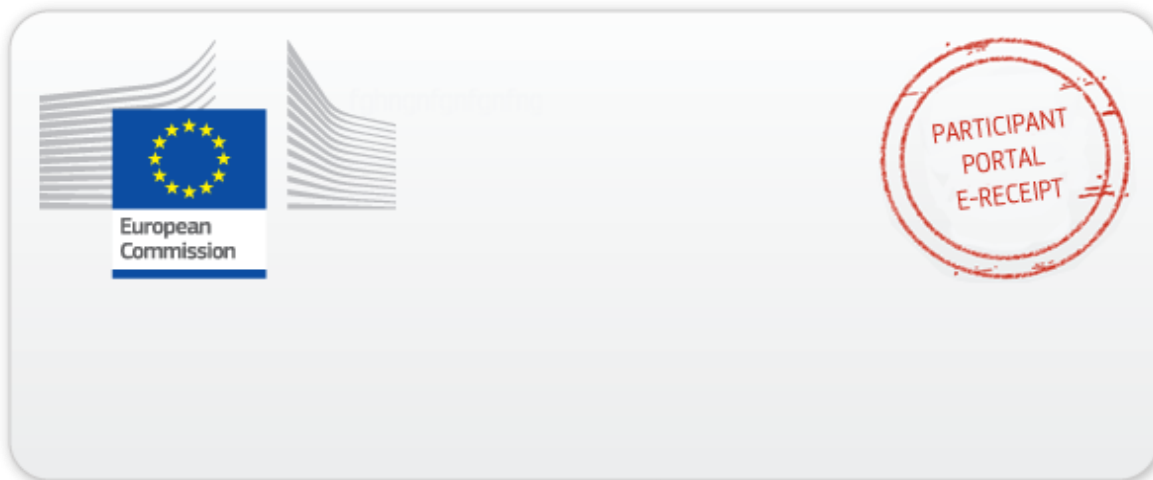
and over the May-October period only, in $\text{m}^3 \text{s}^{-3}$ and as fraction of the total DUP in brackets.

	Atlas	Mediterranean	Sahara West	Sahara East	Sahel West	Sahel East	All
Whole year	6.1 (21%)	1.7 (10%)	5.6 (17%)	1.5 (9%)	8.0 (28%)	5.0 (16%)	4.6 (18%)
May-Oct	9.2 (25%)	1.9 (12%)	10.3 (21%)	2.0 (11%)	15.3 (33%)	9.7 (27%)	8.1 (24%)

Table 3. Tuning of the parameterization for each run and formulation, and spatial and

seasonal root-mean-square error (RMSE) of DUP (in $\text{m}^3 \text{s}^{-3}$) with respect to EXPL.

Run	Formulation
CTRL-P	Original
CTRL-P	Alternative
CTRL-P	Gustav
HIRES-P	Original
HIRES-P	Alternative
HIRES-P	Gustav
BECH-P Original $R = 4.0 \text{ km}$ 3.97 3.60 BECH-P Alternative $w_{dd} = 7.0 \text{ m s}^{-1}$ 3.95 4.06 height	



This electronic receipt is a digitally signed version of the document submitted by your organisation. Both the content of the document and a set of metadata have been digitally sealed.

This digital signature mechanism, using a public-private key pair mechanism, uniquely binds this eReceipt to the modules of the Participant Portal of the European Commission, to the transaction for which it was generated and ensures its full integrity. Therefore a complete digitally signed trail of the transaction is available both for your organisation and for the issuer of the eReceipt.

Any attempt to modify the content will lead to a break of the integrity of the electronic signature, which can be verified at any time by clicking on the eReceipt validation symbol.

More info about eReceipts can be found in the FAQ page of the Participant Portal. (<http://ec.europa.eu/research/participants/portal/page/faq>)